2018

THE DEVELOPMENT OF MICROFLUIDIC DEVICES FOR THE PRODUCTION OF SAFE AND EFFECTIVE NON-VIRAL GENE DELIVERY VECTORS

Jason Matthew Absher
University of Kentucky, jason.absher@uky.edu
Digital Object Identifier: https://doi.org/10.13023/etd.2018.307

STUDENT AGREEMENT:

I represent that my thesis or dissertation and abstract are my original work. Proper attribution has been given to all outside sources. I understand that I am solely responsible for obtaining any needed copyright permissions. I have obtained needed written permission statement(s) from the owner(s) of each third-party copyrighted matter to be included in my work, allowing electronic distribution (if such use is not permitted by the fair use doctrine) which will be submitted to UKnowledge as Additional File.

I hereby grant to The University of Kentucky and its agents the irrevocable, non-exclusive, and royalty-free license to archive and make accessible my work in whole or in part in all forms of media, now or hereafter known. I agree that the document mentioned above may be made available immediately for worldwide access unless an embargo applies.

I retain all other ownership rights to the copyright of my work. I also retain the right to use in future works (such as articles or books) all or part of my work. I understand that I am free to register the copyright to my work.

REVIEW, APPROVAL AND ACCEPTANCE

The document mentioned above has been reviewed and accepted by the student's advisor, on behalf of the advisory committee, and by the Director of Graduate Studies (DGS), on behalf of the program; we verify that this is the final, approved version of the student's thesis including all changes required by the advisory committee. The undersigned agree to abide by the statements above.

Jason Matthew Absher, Student

Dr. Daniel W. Pack, Major Professor

Dr. Tom Dziubla, Director of Graduate Studies

THE DEVELOPMENT OF MICROFLUIDIC DEVICES FOR THE PRODUCTION OF SAFE AND EFFECTIVE NON-VIRAL GENE DELIVERY VECTORS

Dissertation

A dissertation submitted in partial fulfillment of the
requirements for the degree of Doctor of Philosophy in the
College of Engineering
at the University of Kentucky

By

Jason Matthew Absher

Lexington, KY

Director: Dr. Daniel W. Pack, Professor of Chemical Engineering

Lexington, KY

ABSTRACT OF DISSERTATION

THE DEVELOPMENT OF MICROFLUIDIC DEVICES FOR THE PRODUCTION OF SAFE AND EFFECTIVE NON-VIRAL GENE DELIVERY VECTORS

Including inherited genetic diseases, like lipoprotein lipase deficiency, and acquired diseases, such as cancer and HIV, gene therapy has the potential to treat or cure afflicted people by driving an affected cell to produce a therapeutic protein. Using primarily viral vectors, gene therapies are involved in a number of ongoing clinical trials and have already been approved by multiple international regulatory drug administrations for several diseases. However, viral vectors suffer from serious disadvantages including poor transduction of many cell types, immunogenicity, direct tissue toxicity and lack of targetability. Non-viral polymeric gene delivery vectors (polyplexes) provide an alternative solution but are limited by poor transfection efficiency and cytotoxicity. Microfluidic (MF) nano-precipitation is an emerging field in which researchers seek to tune the physicochemical properties of nanoparticles by controlling the flow regime during synthesis. Using this approach, several groups have demonstrated the successful production of enhanced polymeric gene delivery vectors. It has been shown that polyplexes created in the diffusive flow environment have a higher transfection efficiency and lower cytotoxicity. Other groups have demonstrated that charge-stabilizing polyplexes by sequentially adding polymers of alternating charges improves transfection efficiency and serum stability, also addressing major challenges to the clinical implementation of non-viral gene delivery vectors.

To advance non-viral gene delivery towards clinical relevance, we have developed a microfluidic platform (MS) that produces conventional polyplexes with increased transfection efficiency and decreased toxicity and then extended this platform for the production of ternary polyplexes. This work involves first designing microfluidic devices using computational fluid dynamics (CFD), fabricating the devices, and validating the devices using fluorescence flow characterization and absorbance measurements of the resulting products. With an integrated separation mechanism, excess polyethylenimine (PEI) is removed from the outer regions of the stream leaving purified polyplexes that can go on to be used directly in transfections or be charge stabilized by addition of polyanions such as polyglutamic acid (PGA) for the creation of ternary polyplexes. Following the design portion of the research, the device was used to produce binary particle characterization was carried out and particle sizes, polydispersity and zeta

potential of both conventional and MS polyplexes was compared. MS-produced polyplexes exhibited up to a 75% reduction in particle size compared to BM-produced polyplexes, while exhibiting little difference in zeta potential and polydispersity. A variety of standard biological assays were carried out to test the effects of the vectors on a variety of cell lines – and in this case the MS polyplexes proved to be both less toxic and have higher transfection efficiency in most cell lines. HeLa cells demonstrated the highest increase in transgene expression with a 150-fold increase when comparing to conventional bulk mixed polyplexes at the optimum formulation. A similar set of experiments were carried out with ternary polyplexes produced by the separation device. In this case it was shown that there were statistically significant increases in transfection efficiency for the MS-produced ternary polyplexes compared to BM-produced poyplexes, with a 23-fold increase in transfection activity at the optimum PEI/DNA ratio in MDA-MB-231 cells. These MS-produced ternary polyplexes exhibited higher cell viability in many instances, a result that may be explained but the reduction in both free polymer and ghost particles.

KEYWORDS: Gene Delivery, Non-Viral Gene Delivery Vectors, Microfluidics, Ternary Polyplex, Lab-On-A-Chip

Jason Absher
Student Signature

May 21, 2018
Date

THE DEVELOPMENT OF MICROFLUIDIC DEVICES FOR THE PRODUCTION OF SAFE AND EFFECTIVE NON-VIRAL GENE DELIVERY VECTORS

BY

Jason Matthew Absher

Dr. Daniel Pack
Director of Dissertation

Dr. Tom Dziubla
Director of Graduate Studies

May 21, 2018
Date

DEDICATION

To My Family and Friends

ACKNOWLEDGEMENTS

The following dissertation has been greatly benefited from the insights of a variety people from my advisor, to my peers, to my family and to my friends. First, I would like to acknowledge Dr. Pack for his guidance and insights without which this project wouldn't exist. I also wish to thank my complete dissertation committee, as well as any outside readers: Dr. Tom Dziubla, Dr. Brad Berron and Dr. Jason DeRouchey. Each of these individuals has provided guidance without which this research may not have been possible or, if completed, would have been greatly diminished.

In addition to the technical support provided by my predecessors, I have received abundant technical support from my lab mates and other researchers outside of my lab. In lieu of this I would like to thank: Landon Mott, Robert Wensing, Logan Warriner, Huy Ngo, Kai Su, Steve Rheiner, Matt Mckerlin, Angela Gutierrez, Jacob Lilly, Carolyn Jordan and many others.

Finally, I would like to thank my friends and family for the emotional support and encouragement that they have provided throughout my time as a graduate student. Without this group of people, I am sure my experience would have been much less fun and possibly the acquisition of my degree may have been impossible. I would like to thank the following people specifically: Lisa Willinger, David Absher, Delbretta Absher, Brandon Absher, Amanda Absher, Ken Anderson, Henrietta Anderson, Delbert Anderson, Derek Bocard, Matt Smith, Josh Spencer, Daniel Fletcher, Jeff Harman, Ashley Jackson, Nathan Poynter, Zach Selby, Hannah Selby, Will Mack, John Hoben, and many others.

Table of Contents

List of Figures

Chapter 1: Introduction

In the early years of gene therapy, recombinant viruses were most often used as gene delivery vectors, but after a number of setbacks associated with immunogenicity, new delivery techniques have been explored. In 1995, Boussif et al. showed that the commercially available polymer, polyethylenimine (PEI), demonstrates gene delivery activity when complexed with DNA [1]. PEI and similar polymers exhibit weak or no immunogenicity, making them safer gene delivery vectors. Due to the comparatively low delivery efficiency, high cytotoxicity and aggregation in the presence of serum, however, conventional polymer vectors are not typically clinically viable. Many different polymers have been produced specifically for the purpose of gene delivery [2–8], but none have made polymer-based gene delivery a viable treatment option.

A recent method developed by a number of groups to improve polymer-based gene delivery is to use ternary polyplexes comprising DNA and two different types of polymers [2,9–13]. With this technique, polycation/DNA polyplexes are formed by mixing of the constituents, as in conventional polymer based gene delivery, but subsequently the polyplexes are exposed to a second anionic polymer. The anionic polymer forms a complex with the cationic binary polyplex, resulting in a ternary polyanion/polycation/DNA polyplex. For example, Wang et al. demonstrated that multiple ternary polyplexes exhibited increased gene delivery efficiency and reduced cytotoxicity in comparison to binary PEI/DNA complexes [14]. Two of the polyanions used were polyglutamic acid (PGA) and polyaspartic acid (PASP). It was shown that the ternary polyplexes aggregated much less in solutions containing serum than did the binary complexes, and that this enhanced the delivery efficiency of the vectors. The

ability to deliver genes in serum is very attractive as it more accurately models in vivo conditions. A problem with this approach, as with conventional polycation/DNA complexes, is that the assembly process is poorly controlled leading to relatively large particles with broad size distributions. We propose that better control of the complex assembly will provide more reproducible, smaller, more uniform and more efficient polyplexes.

Polymeric vectors are most commonly produced through bulk mixing of the components in which a polymer solution is added to a solution of plasmid DNA followed by mechanical mixing (i.e., shaking or vortexing). This method most often produces particles between 200-500 nm in diameter [15]. Sizes can be controlled to some extent by varying the polymer:DNA ratio, but the resulting size distributions are heterogeneous. Several recent publications have reported the assembly of gene delivery vectors in microfluidic (MF) devices [16–18]. Koh et al. demonstrated a MF device that was capable of producing smaller and more uniform PEI/DNA complexes [16]. This device passes a plasmid DNA (pDNA) stream through a central channel that is flanked on either side by streams of PEI. Due to the laminar flow environment, characteristic of MF channels, the polymer can reach the DNA by diffusion only. This controlled environment is ideal for the assembly of small monodisperse particles. It was demonstrated that polyplexes produced this way exhibit higher gene delivery efficiency than those produced by bulk mixing [16]. Neither their MF system nor, to our knowledge, any yet reported provides for layer-by-layer assembly of ternary polyplexes, however.

Polymer-based gene delivery demonstrates great potential for the treatment of a variety of diseases. Since this method does not involve viral components, it bypasses the

negative immune responses associated with viral gene delivery. Through a multidisciplinary approach combining microfluidics and drug design, the proposed research project seeks to address major barriers hindering polymer-based gene delivery from entering the clinic. We suggest that the controlled mixing environment provided by the MF device combined with the functionality of ternary polyplexes will result in layer-by-layer (LbL) assembly of particles capable of increased delivery efficiency, reduced cytotoxicity and functionality approaching that of a virus.

1.1 Specific Objectives

The primary objective of this work was to design microfluidic devices for the removal of free PEI and the production of ternary polyplexes. The specific objectives of the three experimental chapters are shown below.

1.1.1 Literature Review of Ternary Polyplexes

In order to fulfill the primary objective of this work, a thorough literature review of ternary polyplex examples is necessary. Here I show how ternary polyplexes fit in to the gene delivery environment and give specific mechanisms by which the addition of anionic polymers aid in gene delivery. I then describe key categories of polymers that have been explored, examine which cellular barriers to delivery the polyplexes were designed to overcome, and highlight points in which research could be expanded. The goal of this review is to give insight into TP design and formulation for further application in microfluidics.

1.1.2 Literature Review of Microfluidic Device for the Production of Polyplexes

Similarly, a thorough literature review of microfluidic devices designed to produce polyplexes was carried out to aid in the realization of the primary objective. In this section I provide a brief review of the broader context in which microfluidics fits and then discuss devices that have been designed specifically for the production of polyplexes. Two categories of devices are defined, specific examples of the results from experiments carried out in devices from both categories are explored, and areas in which I believe research could be expanded are highlighted. The goal of this review is to gain understanding about specific designs and polymer systems that have been employed for polyplex generation.

1.1.3 Design, Development, and Validation of a Microfluidic Separator Device for the Production of Polyplexes

After gaining understanding of previous MF designs that have been employed for the production polyplexes, computational fluid dynamic models of novel device designs were created. Important parameters highlighted in the literature were explored using the model to aid in the design of a microfluidic separator (MS) device. After determining the appropriate geometry of the device, I fabricated the device using photolithographic techniques described in more detail below. The device was then validated for flow performance using fluorescence flow characterization. The physicochemical properties of the MS-produced polyplexes were determined and compared to conventional BM-produced polyplexes. Finally, I carried out transfections in three human cell lines and

compared gene expression and toxicity for bulk-mixed and MS-produced binary polyplexes.

1.1.4 Comparing Different Mixing Methods and Molecular Weights for the Production of Ternary Polyplexes

Having designed and validated a device for the production of PEI/DNA polyplexes, I then explore the effects of different mixing methods, based on previous techniques from literature, on gene expression in human cells. A key advantage of TPs is their ability to maintain higher gene expression levels in media containing serum, so I compare transfections from the TPs in both serum-free and serum-containing media. Simultaneous experiments looking at the effect of PGA molecular weight on transfection efficiency were carried out and helped to establish an optimized molecular weight for transfection. This leads to the use of the material in future microfluidic formulations.

1.1.5 Microfluidic Production of Ternary Polyplexes and Comparison of Different Production Methods

A sequential MF mixer was then designed for comparison with BM and MS methods for the production of TPs. The physicochemical properties of the TPs produced by each method were then compared. Transfections were then carried out to probe the gene expression and toxicity of TPs produced by each method on three different human cell lines. Additional transfections were carried out to explore the cellular uptake through flow cytometry experiments on the HeLa cell line. The final sample composition was then assessed to determine the amount of free PEI and potential for ghost particles.

1.1.6 Concluding Remarks

Conclusions drawn from the research are given and future directions of the research, as understood by the author, are given.

Chapter 2: Literature Review of Ternary Polyplexes

2.1 Introduction

Gene therapy is the treatment of diseases through the use of genetic material which codes for proteins that, when produced by a target cell, produce therapeutic effects by replacing a disease-causing gene, making a disease-causing gene inactive, or introducing a novel gene into the body to help treat a disease. Genetic diseases are obvious targets of for this type of therapy since the replacement of faulty genes with "normal" genes may cure the disease. An example of one such disease is lipoprotein lipase deficiency, for which a gene therapy drug has already been approved in Europe [19]. Other genetically inherited diseases that have been targeted by gene therapy researchers include hemophilia [20], severe combined immune defficiency [21], adrenoleukodystrophy [22], Leber congenital amaurosis [23], and others [24–26]. In addition to inherited genetic disorders, gene therapy has also been used to treat diseases that are acquired such as cancer. Cancer treatment makes up the bulk of gene therapy research [27], and a variety strategies have been employed such as suicide gene therapy [28], oncolytic viral therapy [29], antiangiogenisis [30] and immunotherapies [31]. Other acquired diseases for which gene therapies have been studied include neurodegenerative diseases such as Parkinson's disease [32] and Huntington's disease [33], and also infectious diseases like HIV [34] and hepatitis [35].

With such broad applicability and high potential for treating or curing diseases, gene therapy has gained a lot of attention among health science researchers and the general media. Generally, there are two primary methods of delivering genetic material:

viral vectors or synthetic vectors. In most cases the vector used to deliver the genetic material is a modified virus such as adeno-associated viral (AAV) vectors [36], lentiviral vectors [37], and retroviral vectors [38]. While these viral vectors have had some success, there are safety concerns associated with their use such as oncogenisis [39], immunogenicity [40], limited cell specificity [41], as well as safety concerns and complications associated with the large-scale production of viruses [42].

In comparison to viral vectors, synthetic vectors offer a potentially safer alternative by sidestepping many of the issues highlighted above [43] [44]. These non-viral vectors include polymers [45], cationic lipids [46], metallic nanoparticles [47], and hybrids of all of these. In general, these materials are weakly or non-immunogenic; often contain easily modifiable chemistries, which make them amenable to cell-specific targeting; and are easily adapted to common chemical processing. In spite of these advantages over their viral counterparts, synthetic vectors have had little clinical success. This is due to their comparatively low gene delivery efficiency, which is a result of their inability to overcome delivery barriers including the need for stability in serum and protection of their genetic cargo, cell-specific targeting, cellular internalization (often through endocytosis), endosomal escape, and transcription.

Ternary polyplexes (TPs) offer a potential solution to the problems presented by both viral and traditional synthetic vectors. TPs comprise nucleic acids, ionic polymers, lipids or metallic nanoparticles, which form nano-sized complexes through entropic interactions that are capable of gene delivery [Fig. 2.1]. These vectors are capable of addressing multiple delivery barriers, while often doing so in sequence allowing for

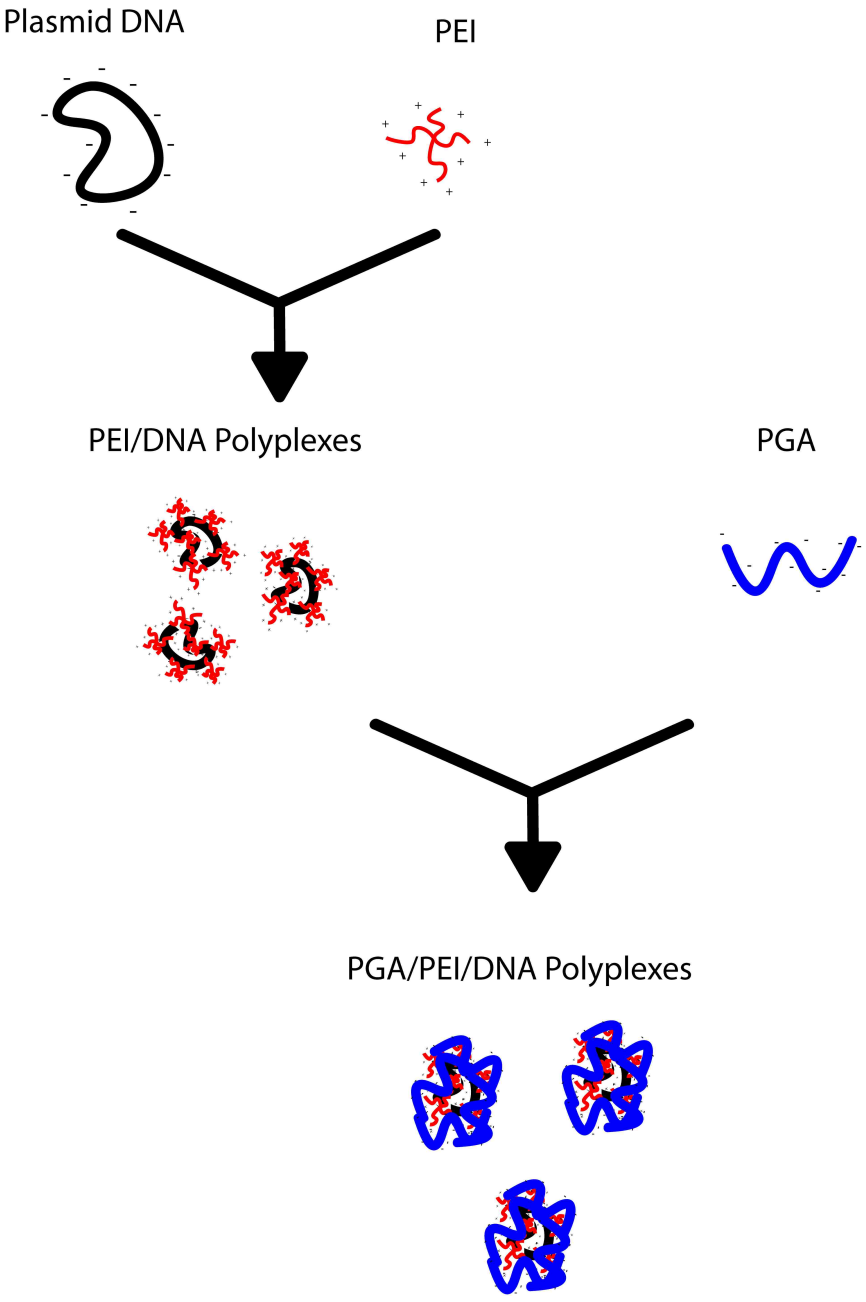

Figure 2.1: Schematic of a typical ternary polyplex bulk mixing method where binary polycation/DNA polyplexes are formed and then coated with polyanions.

programmed gene delivery. In this review, we will look at a variety of TPs that have been explored and compare the ways in which researchers are attempting to solve the problems of low delivery efficiency and toxicity associated with synthetic vectors. Here we will identify five broad categories of ternary polyplexes and summarize some important examples and their findings. There will be some overlap between categories, for example many peptide and synthetic polymer containing TPs are targeting, but we have made every attempt to categorize them into the most pertinent categories.

2.2 Types of Ternary Polyplexes

2.2.1 Ternary Polyplexes Generated Using Conventional Gene Delivery Materials

Off-the-shelf TPs where the constituent polymers are used without any further chemical modification or purification. The advantage with this type of polyplex is that it is simple to use and should translate easily to an industrial production environment. Due to these attributes, off the shelf TPs represent one of the more economically and industrially viable types of TP.

For example, Kurosaki et al. investigated a variety of off the shelf polynucleic acid- and polyamino acid-coated PEI/DNA polyplexes for uptake, gene delivery efficiency and toxicity [48]. The polyanions included polyadenylic acid (polyA), polyinosinic-polycytidylic acid (polyIC), α-polyaspartic acid (α-PAA), α-polyglutamic acid (α-PGA) and γ-polyglutamic acid (γ-PGA). Of all the tested polyanions, γ-PGA showed the most promise, demonstrating transgene efficiencies similar to that of binary PEI/DNA polyplexes, while exhibiting much less toxicity than the control in B16-F10

cells. Though only γ-PGA was shown to be effective at delivering DNA, all polyanion-coated polyplexes were shown to be much less toxic than the binary polyplexes. These results, along with dynamic light scattering and zeta potential measurements showing that the outside of the particle is coated and negatively charged, suggest that neutralization of the positively charged amine groups associated with the PEI is essential for decreasing the toxicity of polycation based synthetic vectors. In fact, in a follow up paper by the same group, γ-PGA was also shown to decrease the toxicity of a variety of cationic lipids and polymers [polypeptides poly-L-arginine hydrochloride (PLA) and poly-L-lysine hydrobromide (PLL), and the liposomes N-[1-(2, 3-dioleyloxy) propyl]-N, N, N-trimethylammonium chloride (DOTMA)-cholesterol (Chol) and DOTMA-dioleylphosphatidylethanolamine (DOPE)], demonstrating that anionic coatings can help reduce the toxicity in multiple types of cationic complexes [15]. Since γ-PGA demonstrated significantly greater gene expression and cellular uptake of polyplexes compared to the other polyanions, the authors suggest that polyplexes coated with γ-PGA may be internalized through a receptor-specific mechanism. Through inhibition studies involving hypothermia, excess γ-PGA, or the combination of both, the authors conclude that the γ-PGA polyplexes are taken up by an energy-dependent process and a γ-PGA specific receptor mediated pathway. However, additional uptake studies need to be carried out to identify the specific uptake pathway.

Wang et al. also explored some off-the-shelf polyanions to create TPs with PEI and DNA, and demonstrated similar results showing increased transfection efficiencies and decreased toxicity in HeLa cells [13]. Here the researchers used off the shelf anionic polysaccharides alginic acid (ALG) and heparin (HEP), as well as α-PAA of molecular

weight 10 kDa (α-PAA10) and α-PGA of molecular weight 7 kDa (α-PGA7). A primary outcome of this research is the demonstration of advantages that TPs have in serum-containing media. The group carried out transfections in both serum-free media and media containing 10% fetal bovine serum (FBS) and demonstrated a maximum of ~15% increase in gene delivery in both conditions when compared to either PEI/DNA polyplexes or Lipofectamine 2000. Demonstrating increased transfection activity in serum-containing media is an important step towards making non-viral gene delivery clinically viable, since the environment mimics that of *in vivo* administration. Isothermal titration calorimetry (ITC) showed that the TPs have a decreased binding affinity with serum proteins, which provides an explanation for the increased transfection efficiency in the presence of serum. Since serum proteins are less likely to adsorb on the polyplex surface, the authors conclude that the vectors undergo less aggregation and are less likely to experience interference from the proteins during uptake. The researchers further demonstrated that loosening of the compact DNA/PEI polyplexes occurs with the introduction of polyanions, which is due to competition between the anionic phosphate groups associated with the DNA and cationic groups associated with the polyanion. They went on to show that there was a pK_a-dependent critical value of Acid/Amine ratio over which DNA dissociates completely from the TPs. There is a discrepancy between the work of the two groups in that Kuorsaki et al. showed no transfection activity for α-PGA and α-PAA while Wang et al. showed dramatically increased transfection activities in either case when compared to PEI/DNA polyplexes. Additionally, there are large differences between the particle sizes reported in the two papers for TPs comprising similar constituent polymers. Either of these discrepancies could be due to differences in

molecular weight of the polyanions (the molecular weights of the polyanions are not given by Kurosaki et al.). Wang et al. investigated a range of polyanion/DNA ratios whereas Kurosaki et al. reported only one ratio, which may not be the optimal ratio. Another possible reason for the difference in transfection activities is that different cell lines were employed in these two studies.

Urtti et al. demonstrated the use of hyaluronan (HA) of a variety of molecular weights to coat PEI/DNA polyplexes and shield the positive charge of the polyplex without affecting the transfection efficiency and increasing the complex stability [49]. Interestingly, the HA facilitated uptake by the CD44 receptor, which is prevalent on the ocular surface. In this case the researchers were focused on ocular delivery as the eye provides the advantage of cell-specific targets, and it is an immune-privileged area. Transfections of human corneal epithelial (HCE) cells with HA/PEI/DNA TPs demonstrated increased transfection activities when the HA molecular weight was less than 10 kDa, in comparison to DOTAP/DOPE lipoplexes and PEI/DNA polyplexes. Uptake studies carried out using flow cytometry indicate that the low molecular weight HAs facilitate CD44 receptor-mediated uptake, though further exploration is needed to determine the optimum molecular weight for maximum CD44 binding affinity.

Human serum albumin (HSA) has also been employed as an off-the-shelf polyanion for the production of TPs [50]. In this case, Nicoli et al. used HSA to coat PEI/siRNA complexes to demonstrate knockdown of TurboGFP in MDA-MB-231 and human primary pulmonary microvascular endothelial cells (HPMEC) cells. These HSA-coated TPs demonstrated enhanced gene silencing in comparison to PEI/DNA polyplexes and comparable transfection efficiency to that of Lipofectamine 2000. Similar to other

papers, the researchers demonstrated negative zeta potentials for the TPs suggesting that the polyplexes would have charge-shielding potential and enhanced stability in circulation. TP sizes were determined through DLS and shown to be similar to that of other TPs. TP cellular internalization was shown to be facilitated by caveolin-mediated endocytosis, which provides an explanation for the role of HSA in the internalization of the polyplexes. TPs containing bovine serum albumin in place of HSA exhibited a similar particle size but exhibited a significant decrease in transfection efficiency. This result suggests that HSA offers some specificity in the uptake of the cell lines investigated, though further investigation is required.

2.2.2 Ternary Polyplexes Comprised of Synthetically Modified Polypeptides (SPP)

TPs may be generated in which one or both of the polyanion and polycation are synthetic polypeptides. A major advantage of the use of polypeptides is that, in the context of the cellular barriers to delivery, they maintain the advantages of off-the-shelf polyanions while providing additional functions for overcoming important barriers to efficient gene delivery. However, polypeptides are generally more difficult and expensive to synthesize compared to most synthetic polymers and are likely more immunogenic than synthetic polymers.

Chen and co-workers developed polyethylenimine-poly(L-lysine)-poly(L-glutamic acid) (PELG) and OEI-poly(benzyl-L-aspartate)-poly(benzyloxycarbonyl-L-lysine) (OEI-PBLA-PLys(Z)) (OEAL) as zwitterionic polymers for use in TP formulations [51,52]. PELG and OEAL were shown to be pH responsive polymers that, when used in TP formulations and exposed to a mildly acidic environment, demonstrate

charge conversional behavior changing from negative to positive surface charge. When binary PEI/DNA polyplexes were coated with PELG or OEAL at physiological pH, the surface charge of the TPs is negative. As is the case with the TP systems mentioned above, this negative surface allows for less aggregation due to decreased association with serum proteins. However, when these zwitterionic coated TPs enter an acidic environment such as that of a tumor, the surface charge of the TPs rapidly changes to positive. For example, the zeta potential changed from ~-20 mV at pH of 7.4 to 25 mV and pH 6.8. Since the pH of tumors is lower than that of normal tissues, these pH responsive systems offer a way in which to target cancerous growths using a non-viral vector by activating the TP when in the proximity of tumors. Transfections at pH 7.4 and 6.8 were carried out to mimic either the normal cellular environment or tumor environment, respectively. The PELG and OEAL TPs demonstrated a more than 10-fold increase in transfection activity at the lower pH, showing both the advantage of positive polyplex surface charge in transfection and that of negative polyplex surface charge in charge-shielding *in vitro*. Since a primary justification for the necessity of charge shielding with TPs is aggregation with serum proteins, the researchers went on to investigate the *in vivo* efficacy of the TPs. BALB/C nude mice with HeLa xenograft tumors were given intratumoral injections of TPs carrying a gene coding for *rev-casp-3*, which was engineered by the same group to have high apoptotic activity [53]. The tumor mass was monitored over a period of 20 days and both PELG and OEAL TPs demonstrated higher inhibition of tumor growth than the positive controls with tumors treated by PELG TPs having a reduction in volume of ~30% in comparison to tumors in

untreated mice and those treated with OEAL TPs having ~70% smaller tumor size than tumors in untreated mice.

Another example of a modified polypeptide used for gene delivery is carboxymethyl poly(L-histidine) (CM-PLH) [54]. Asayama et al. first reported the synthesis of the carboxymethyl-modified polypeptide and demonstrated the pH responsive capabilities of the molecule [55]. Including an imidazole containing polypeptide group in the TP formulation allowed for improved solubility in aqueous solutions at pH above 6.0 and enhanced membrane disruptive abilities at lysosomal pH. The addition of the carboxymethyl groups allowed for charge shielding effects similar to other polyanions, while the imidazole group allowed for enhanced buffering capacity leading to endosomal membrane disruption and escape. The researchers went on to use the novel anionic polypeptide to coat binary PEI/DNA polyplexes to create CM-PLH/PEI/DNA ternary polyplexes. They went on to show that the surface charge, determined through zeta potential measurements, was close to neutral demonstrating the coating of the PEI/DNA polyplexes with CM-PLH. These ternary polyplexes exhibited a 300-fold increase in gene expression over PEI/DNA polyplexes as demonstrated by transfections with the luciferase gene and subsequent luciferase assay.

2.2.3 Ternary Polyplexes Based on Synthetic Polymers

Like SPP constituents, synthetic polymers offer more complex molecular structures that address cellular barriers to delivery, often in a programmed sequential manner. In this case, the constituent polymers of the TP require significant chemical modification and purification steps, similar to synthetically modified polypeptides.

One important type of synthetic polymer based TP involves the engineering of micelles imparting a range of functionality for overcoming cellular barriers to delivery [56–58]. For example, Li et al. developed a temperature-responsive TP micelle system consisting of two block co-polymer hybrid shells complexed with DNA [56]. The polymers synthesized for delivering genetic material in this case were polyethylene glycol (PEG) based polymer PEG-b-poly{N'-[N-(2-aminoethyl)-2-aminoethyl]aspartamide} (PEG-b-PAsp(DET)) and poly(N-isopropylacrylamide)-b-PAsp(DET) (PNIPAM-b-PAsp(DET)). These TPs are formed by first mixing the two copolymers together at 25 °C followed by addition of DNA at the same temperature, forming TPs with PNIPAM and PEG polymer segments on the surface. After the formation of the polyplexes the solution was heated to 37 °C, which is above the critical solution temperature for PNIPAM, which upon condensation forms a hydrophobic layer between the DNA core and PEG regions. This thermo-responsive formulation allows for more compact DNA complexation, while the hydrophobic region acts as barrier further shielding the DNA from nucleases in the extracellular environment, which enables longer circulation time for systemic delivery. These TPs demonstrated higher in vitro transfections in HeLa cells compared to binary polyplex micelles (BPM's) consisting of DNA and PEG-b-PAsp(DET) and comparable transfection compared to Lipofectamine. Uptake studies were also carried out using flow cytometry and showed higher uptake of the TP vectors compared to binary polyplex micelles of PEG-b-PAsp(DET). The authors show that the enhancement of cellular uptake is due to enhanced protection in the extracellular environment, association of the TP with the cellular membrane due to the presence of the hydrophobic region, and enhanced endosome membrane disruption due to

the presence of free PNIPAM segments as evidenced by confocal microscopy studies and fluorescently labeled constituents. Since a primary goal of this research was to increase circulation time of the vectors and yield a TP capable of effective systemic delivery, in vivo experiments were also carried out by injection of the vectors into the tail vein of tumor-bearing mice. Blood circulation, tumor accumulation and antitumor activity of the TPs was probed, and in all instances the TPs demonstrated enhanced in vivo properties in comparison to BPMs. Most notably, the TPs efficiently delivered sFlt-1 pDNA to tumor-bearing mice, eliciting strong antitumor activity. The TP micelles were administered to the mice for 12 days and at the end of the period the relative volume of the tumors was half of that of tumors from mice treated in the same manner with BPMs.

Another interesting example of a ternary polyplex micelle system is the development of a photosensitive vector by Nomoto et al. [57]. In this case a triblock copolymer PEG-b-PAsp(DET), modified further to include poly(L-lysine) (PEG-b-PAsp(DET)-PLys), was developed as the DNA-condensing polymer. The PLys segment complexes with the DNA forming a stable core compartment, the PAsp forms an intermediate compartment for incorporation of a photosensitizer and the PEG segment of the polymer forms an outer shell. Finally, the light-responsive dendrimeric phthalocyanine derivative (DPc) was incorporated into the intermediate PAsp compartment through electrostatic interactions. Keeping the DNA and DPc segregated into different compartments is essential to prevent inactivation of the DNA by the DPc through the formation of reactive oxygen species (ROS). The group demonstrated enhanced physicochemical properties of the TP in comparison to the BPM via TEM, FRET and DLS analysis. Notably, the inclusion of the DPc resulted in smaller average

particle sizes at a DPc/Asp(DET) ratio of 1:1. FRET analysis showed a decrease in FRET efficiency, defined as the ratio of fluorescein intensity to Cy3 fluorescence intensity, for two control samples. The control samples in this case are a randomly mixed sample of pDNA, DPc and PEG-PAsp(DET)-PLys and a sample without the intermediate compartment, which was prepared by adding DPc to a pDNA/PEG-PLys polyplex micelle. The results indicated that the DPc TP formed a three-layer system where DNA preferentially associates with the PLys layer. In vitro experiments with the DPc-based TPs was carried out in both HeLa and HUVEC cell lines, checking for cellular localization, cell viability and protein expression. Localization studies indicated that TPs that did not undergo photo irradiation showed little escape of the DNA from endolysosomes, while photoirradiated TPs demonstrated a high degree of DNA escape from the region. Viability studies demonstrated that TPs containing higher levels of DPc caused a greater degree of cytotoxicity upon irradiation, presumably due to ROS interactions with the cellular membrane and organelles. The DPc based TPs demonstrated fluence dependent protein expression with DPc/Asp(DET) ratios of one and two, demonstrating significant increases in expression after irradiation and performing about the same for either ratio. As with most cases performance in vivo after systemic administration is a key concern, and the group carried out in vivo studies in mice with subcutaneous HeLa and HCT 116 tumors by transfecting the Venus (yellow fluorescent protein) reporter gene. Photoirradiation was carried out with a semiconductor laser and photoirradiated tumors demonstrated nearly a 5-fold increase in fluorescence, proving photoresponsive materials can be a viable way to initiate endosomal escape at a specific place and time during the transfection process.

Finally, Lai et al. have developed a PEG-b-PAsp(DET) ternary polyplex system with a unique bioreducible coating polymer with cleavable disulfide linkages similar to polymers mentioned previously [51,58,59]. The engineered bioreducible polymer used in this instance is poly(ethylene oxide)-b-poly(propylene oxide)-b-poly(ethylene oxide)-b-PAsp(DET) (P(EPE)-b-PAsp(DET)) that was further modified to include a disulfide linkage yielding P(EPE)-SS-PAsp(DET). The P(EPE) segment allows further membrane disruption through amphiphilic association and subsequent disruption of the endosomal membrane in synergy with the membrane disruption properties associated with the PAsp(DET) segments. With a predetermined W:W value, particle characterization using DLS was carried out and demonstrated comparable particle sizes to other polyplexes, ~70 nm. As expected, the increasing addition of PEG-b-PAsp(DET) resulted in increasingly negative zeta potentials for the polyplexes. The addition of 10 mM DTT reducing agent resulted in positive surface charge over time which is attributed to the cleavage of the disulfide linkages, showing that the TPs would be responsive in reducing environments such as the endosome. Stability of the P(EPE)-SS-PAsp(DET) TPs was comparable to other PAsp(DET)-based TPs at physiological salt concentrations, as indicated by DLS analysis of the TPs over a period of 60 min where particle sizes were static at below 100 nm. In vitro transfections with the P(EPE)-SS-PAsp(DET) TPs were compared to P(EPE)-b-PAsp(DET) TPs of similar composition in MDA-MB-231 and A549 cell lines. The inclusion of the disulfide linkage resulted in as much as 2- and 9-fold higher transgene expression for disulfide-linked TPs when compared to those not containing the reducible bond, in MDA-MB-231 and A549 cell lines, respectively. Cytotoxicity differences between the two types of TPs was negligible and much less than PEI/DNA

polyplexes in both cases. It was also demonstrated that disulfide containing TPs were internalized much more efficiently than other TPs, though differences became marginal as PEG-b-PAsp(DET) percentages increased above 50%.

A system described by Sanjoh et al., which includes a synthetically modified PEG backbone like many other examples, demonstrates a dual pH-responsive behavior overcoming multiple cellular barriers in sequence [60]. Thiolated poly(L-lysine) was used as the complexing cation to form the binary polyplex core. An important distinction between this TP example and others is that in this instance the thiol groups in the core become crosslinked via pH-responsive disulfide bonds. The binary crosslinked polyplex is then coated with PEG-b-PAsp(DET) that has been modified with anionic cis-aconitic groups, PEG-b-PAsp(DET-Aco), to create a ternary cross-linked polyplex (PEG-CCP). As the cellular endosome begins to acidify, the PEG-CCP coating destabilizes and dissociates from the core, as demonstrated by monitoring zeta potentials of TPs over time at pH 5.5 and 7.4. It was demonstrated that the TPs exposed to the lower pH underwent a zeta potential change from -20 mV to 30 mV, while there was no change for TPs at the higher pH. The authors argue that the change in surface charge demonstrates that at endosomal pH the anionic cis-aconitic groups have been removed and PEG-b-PAsp(DET) dissociates from the TP leaving the more positively charged surface. This dissociated PEG-b-PAsp(DET) then begins to destabilize the endosome/lysosome membrane, similar to other PEG based polymers mentioned above, allowing for the escape of the cross-linked core into the cytoplasm. To investigate the stability and decomplexation of the TPs, polyanion exchange experiments were carried out in both reducing and non-reducing environments with dextran sulfate. Both the binary cores and

the TPs were investigated and compared to non-crosslinked binary cores and TPs with a . poly[N-(N'-uccinyl-2-aminoethyl)aspartamide] PAsp(EDA-Suc), a coating that doesn't have charge conversional functionality. In non-reductive conditions, the crosslinked cores and TPs demonstrated a significant increase in stabilization in comparison to their non-crosslinked counterparts. The crosslinked cores and TPs also released DNA in reducing environments through the cleavage of the disulfide bonds in the core. Further experiments demonstrated enhanced transgene expression with the TPs when transfecting HuH-7 and HUVEC cell lines in vitro and comparing to transfections with the PAsp(EDA-Suc) TPs coated and polyplexes formed by only non-crosslinked cores. Cell viability experiments demonstrated low cytotoxicity of the TPs and the same controls, and importantly demonstrated that coating the binary cores with PEGylated polyanions significantly reduces poplyplex toxicity. Using fluorescently labeled DNA and LysoTracker Green stain, the researchers were able to demonstrate that less DNA was associated with the endosomes and lysosomes with the TPs in comparison to controls, which further demonstrates the ability of the TPs to efficiently escape endosomes. This increase in endosome escape was attributed to the charge-conversional PEG-b-PAsp(DET-Aco) coating.

Another synthetic polymer engineered for overcoming cellular barriers to gene delivery as a TP component has been introduced by Wang et al. [14]. This TP also exhibits targeting, charge conversion, membrane disruption and self-dissociation functions. In this case the DNA core consists of the common PEI/DNA polyplex, and lauric acid-polyethylenimine-cyclohexanedicarboxylic anhydride-folic acid (LPHF) was synthesized as a charge conversional coating. Endosome escape in this case is mediated

by the proton sponge effect, as with other PEI-containing polyplexes. LPHF coated TPs demonstrated a larger particle size of ~300 nm at LPHF/PEI weight ratios 0 – 2, but upon further addition of LPHF the particle sized decreased to ~100 μm, similar to the size of PEI/DNA particles. Zeta potential measurements mirror those of off-the-shelf TPs, starting at ~25 mV for PEI/DNA and becoming increasingly negative with the addition of the LPHF, achieving a minimum surface charge of ~-35 mV. Since the TPs were expected to dissociate and release the PEI/DNA core in acidic conditions, particle size and zeta potential at different pH was investigated. Particle sizes and zeta potentials of the TPs were shown to be constant over a period of 12 hours at physiological pH. Over that same period at pH 6 or 5, both particle size and zeta potential increased, indicating pH-dependent dissociation of the LPHF from the PEI/DNA core. The LPHF polymer exhibited little cytotoxicity, with HeLa and A549 cell lines exhibiting similar viabilities to untreated controls both in media containing serum and serum-free media. Additionally, TPs exhibited less toxicity than PEI/DNA polyplexes, further demonstrating the ameliorating effect of charge shielding on cellular toxicity. Flow cytometry experiments probing cellular uptake of the LPHF TPs were carried out by transfecting folate positive HeLa and folate negative A549 cell lines, and additionally adding excess folate in some circumstances to probe inhibition. It was shown that transfections of the HeLa cell lines yielded a two-fold increase in fluorescence over the A549 cells when transfected with the TPs while the same cell lines transfected with PEI/DNA polyplexes yielded about the same fluorescence signal. Similarly, the folate inhibition assay showed ~ 45% reduction in fluorescence signal when excess folate was present in HeLa cells transfected by the TPs, both experiments providing strong evidence indicating folate-mediated endocytosis.

EGFP reporter gene transfections further indicated that LPHF TPs were more efficient gene delivery vectors than PEI/DNA polyplexes, exhibiting nearly a 3-fold increase in transfection efficiency in both HeLa and A549 cell lines. Another interesting finding is that while PEI/DNA polyplexes showed higher cellular uptake in comparison to LPHF TPs, the LPHF TPs demonstrated higher gene expression. This result demonstrates the importance of the dissociation of the coating polymer from the binary polyplex core. Cellular trafficking studies, carried out by labeling the PEI with FITC, staining the cells with Lysotracker and observing them at different time points, revealed that PEI/DNA polyplexes remained trapped in the endosome much longer than the LPHF TPs providing further validation of the inclusion of multiple functional entities to overcome cellular barriers to delivery. In vivo studies were also performed using nude mice with HeLa tumor xenografts and near-infrared fluorescence imaging at the tumor site. Results suggested that systemic delivery of the polymers was effective at both targeting tumors and decreasing tumor size. LPHF TPs also showed less noticeable effects on the body weight of the mice suggesting less drug associated toxicity on the mice.

2.2.4 Ternary Polyplexes Involving Metallic Nanoparticles (NPs)

TPs have been constructed using metallic NPs that are, in most cases, coated to allow polyelectrolyte complexation with the surface of the particle. Since metallic NPs generally are very monodisperse with well-defined geometries, they can be used as scaffolding onto which encourage enhanced TP size and uniformity and, in many instances, metallic NP based TPs allow for functions beyond gene delivery.

Elbakry et al. demonstrated the use of gold NPs (AuNPs) in TP formulations [61]. AuNPs were chosen for their high biocompatibility, easy synthesis, simple surface modification, narrow size distribution and availability in a variety of sizes. To form the TPs, AuNPs coated in 11-mercaptoundecanoic acid (MUA) were added to a PEI solution where the PEI coated the AuNP due to electrostatic interactions with the MUA coating. The PEI-coated AuNPs were then added to an siRNA solution, and the NPs were placed back in a PEI solution to form a PEI outer shell yielding PEI/siRNA/PEI-AuNPs. Surface charge reversal between each step, as evidence by zeta potential measurements, indicated that the TP synthesis progressed as expected. DLS measurements further demonstrated that the addition of the PEI and siRNA layers led to an increase in NP size from ~18 to ~27 nm, which is still much smaller than TPs described previously. Additional DLS experiments were carried out to probe aggregation of the PEI/siRNA/PEI-AuNPs in serum-containing media. While the TPs did aggregate, the size increased by only ~2.5-fold, and the final TP size is still much smaller than traditional polyplexes. Interestingly, the zeta potential of the TPs was found to be negative after incubation with serum containing media. This result, along with UV-vis analysis of the TPs post serum incubation, indicated that serum proteins coated the surface of the TPs and helped prevent aggregation. While more siRNA/PEI-AuNPs, lacking the outer PEI shell, were taken up by CHO-K1 cells, these polyplexes tended to undergo significant aggregation within endosomes. In contrast, the PEI/siRNA/PEI-AuNPs showed minimal intracellular aggregation, which may be due to the surface interactions of the TP with negatively charged serum proteins. Knockdown studies carried out in a CHO-K1 cell line stably expressing EGFP demonstrated concentration-dependent gene silencing with a 28%

reduction in EGFP production at the highest initial AuNP concentration of 0.37 nM. However, when the PEI/siRNA/PEI-AuNP polyplexes were compared to the traditional PEI/DNA polyplexes, the former required a higher concentration of both PEI and siRNA to achieve similar knockdown. The authors hypothesized that stronger binding interactions and the lack of free PEI in the PEI/siRNA/PEI-AuNPs formulation resulted in the decreased knockdown efficiency.

Although not strictly a TP since it involves the use of more than three constituents, Guo et al. built upon the previously mentioned AuNP work by including cis-aconitic anhydride-functionalized poly(allylamine) (PAH-Cit) in the layer-by-layer process to form polyplexes with charge conversional properties [62] similar to others previously mentioned. In this case, the PAH-Cit acts as pH-sensitive charge conversional moiety allowing for the release of genetic material, and overcoming strong binding interactions associated with PEI/AuNPs. The charge reversal process was confirmed by gel electrophoresis to determine the amount of siRNA that is released from the polyplexes at pH 5. Both DNA transfection efficiency and siRNA knockdown efficiency were measured in vitro with HeLa cells at a variety of Au/DNA w/w's. In the case of DNA transfection, luciferase expression was shown to have a more than 3-fold increase in transfection efficiency at the optimum w/w of 7.5 compared to both PEI and Lipofectamine at an N/P of 10. In comparison, siRNA knockdown was shown to be most effective at a w/w of 10 by demonstration of inhibition lamin A/C expression using western blot techniques. Additional transfections were carried out with cy5-siRNA/PEI/PAH-Cit/PEI/MUA-AuNPs to probe the cellular internalization and distribution of the polyplexes. When comparing to PEI or Lipofectamine as positive

controls, the fluorescently labeled polyplexes were shown to be more equally distributed around the cytoplasm using confocal microscopy. The positive controls, however, were found to be clustered together. The authors attributed the broader distribution of fluorescence throughout the cell, in the case of the NPs, to the siRNA being more easily released from the polyplex and the enhanced endosomal escape, both of which are a result of the charge conversional PAH-Cit.

Another interesting TP of this type relies on the use of superparamagnetic iron oxide (SPIO) NPs to allow for simultaneous gene delivery and magnetic resonance imaging [63]. Deferoxamine-coated Fe_3O_4 SPIO NPs with diameters of 8–10 nm were complexed with plasmids and PEI 25 kDa to create the TPs. DNA packaging of the polyplex system was established using agarose gel electrophoresis and the results demonstrated the ability of the system to effectively complex with plasmid DNA. Transfections were carried out on HCC HepG2 cells using the pEGP-C1 plasmid. Internalization was measured by colorimetric assays using the absorbance of the SPIO NPs and it was shown that the amount of NPs inside the cell increased with increasing doses of the TPs. Additionally, GFP protein production was observed visually by fluorescence microscopy after transfections were carried out and the uptake efficiency of the TPs was found to be significantly lower than that of either PEI-based polyplexes or Lipofectamine. The TPs were considerably less toxic than either of the positive controls mentioned above. Although the transfection efficiency is lower than standard transfection agents, the ability to include magnetic resonance imaging as a therapeutic component is highly attractive. Perhaps a more complex TP including a charge conversional moiety would increase the transfection efficiency and maintain the low toxicities.

2.2.5 Ternary Polyplexes Designed Specifically for Targeting

TPs have been designed to include targeting ligands or other components that target specific cell surface receptors. By allowing the vectors to overcome multiple barriers to delivery at the same time, targeting shows great promise for aiding the development of clinically relevant non-viral gene delivery agents. In most cases, however, the specific component developed for targeting requires considerable synthesis effort and resources, making them potentially expensive in an industrial setting.

One such targeted TP, developed by Zhang et al., involves the use of folate (FA) to target cancer cells [64]. Many cancerous cell types over express FA receptors, while healthy cells exhibit limited expression, so these TPs can be used to target some tumors [65]. Minicircle DNA (mcDNA), a super-coiled plasmid lacking extraneous plasmid sequences, was employed for its advantages over conventional plasmids including prolonged gene expression and increased transfection efficiency. PEI was complexed with mcDNA to create PEI/mcDNA cores. A secondary cationic polymer, Folate-containing PEGylated PEI (FA-PEG)$_m$-PEI (FPP), was developed to coat the core and provide targeting. An interesting difference between this TP system and others mentioned throughout the review is that the additional FPP component contains PEI allowing for cellular uptake and endosomal escape, while containing the folate for targeting and PEG for biocompatibility. These TPs have a moderately positive surface charge, as evidenced by zeta potential measurements, to which the authors attribute their enhanced transfection efficiency in comparison to FPP/DNA binary polyplexes. The FPP/PEI/mcDNA TPs showed specific targeting capabilities and enhanced transgene expression levels in comparison to conventional polyplexes using a folic acid competition assay, with the TPs

exhibiting ~ 10-fold reduction in expression of luciferin at a folic acid concentration of 1 mg/mL versus in no folic aicd treatment. In comparison at the same folic acid concentration there was no significant change in luciferin expression over this range of folic acid concentrations. TP internalization was also explored using confocal microscopy and FITC-labeled polyplexes. It was shown that the FPP/PEI/mcDNA TPs were efficiently internalized into cells and that many of the TPs were able to escape the endosome prior to lysosomal degradation. Further cellular trafficking studies showed that that the mcDNA was released from the TPs within the nucleus, showing that the TP's have some ability to release the DNA. This capability may enhance gene expression and is attributed to the reduced electrostatic interactions between the polycation and mcDNA in comparison to plasmids. In vivo transfections of tumor-bearing mice further demonstrated the ability of the folate to target tumors overexpressing the receptor and enhance protein expression in comparison to conventional PEI/DNA polyplexes. While including folate ligands in polyplex constituents may provide an avenue for targeting tumor cells and the additional PEG component allows for enhanced biocompatibility, perhaps a polyanion modified to exhibit these properties would be more beneficial than PEI. As others have demonstrated, the use of anionic coatings has many benefits and in many cases enhances transfection– a trend that is especially pronounced in serum-containing media.

A very interesting class of targeted TP that includes single strand oligonucleotides (ssONs) for particle surface-charge reversal and targeting was developed by Chung et al. [66]. The specific oligonucleotide found to assist in receptor-mediated uptake was 5'-$C_{10}A_{20}$-3' and was coated on histidine-conjugated polyallylamine (PAL-His)/DNA

polyplex cores. PAL, which contains a high concentration of amine groups, exhibits some of the same positive attributes as other polycations mentioned, though PAL exhibits high toxicity and low endosomal escape. However, when modified with imidazole-containing histidine, PAL is able to buffer in acidic environments. Further, similar to PEI, this polycation exhibits the proton sponge effect allowing for endosomal escape. The inclusion of the ssONs as a complexed anionic coating allows for ameliorated toxicity and enhanced transfection activity in serum-containing media. Particle sizes ranged from 150 – 750 nm, with smaller particle sizes observed at higher ssONs/PAL-His ratios. Also, at these higher ratios the surface of the particles was negatively charged with a zeta potential around -30 mV. TPs formed at these higher ratios also demonstrated higher transfection activity than binary (PAL-His)/DNA cores and similar expression to ExGEN 500 used as a positive control, as assessed by EGFP and luciferase expression in HeLa cells. HEK-293, HepG2 and Hs68 cell lines were also evaluated for amenability to transfection with the novel TPs via luciferase expression, and it was found that much higher transfection activities were noted in the HEK-293 and HepG2 cell lines in comparison to the Hs68 cell line, which the authors attribute to differences in the fibroblasts of the cells. When compared to PAL-His/DNA polyplexes, the TPs demonstrated a 2-, 30- and 40-fold increase in transfection activity in HEK-293, HepG2 and Hs68 cell lines, respectively. Cellular uptake studies were also carried out in HeLa cells using YOYO-1 labeled plasmid along with confocal microscopy. It was shown that in all instances of molar ratios of ssONs/PAL-His explored, the plasmid was localized in the cytoplasm. To see whether dissociation ssONs occurred prior to cellular uptake, an additional experiment using Nulight (537)-5'-$C_{10}T_{20}$-3' ssONs was carried out.

Fluorescence confocal images revealed that the YOYO-1 labeled plasmid and Nulight ssONs were colocalized in the HeLa cells. The researchers also compared a different ssONs, 5'-$C_{10}T_{20}$-3', to the 5'-$C_{10}A_{20}$-3' as a polyplex coating. It was found that the T-containing ssONs demonstrated a 1000-fold decrease in transfection activity in HeLa cells, while having the same surface charge. These results seem to indicate that the 5'-$C_{10}A_{20}$-3' ssONs interacts with the cell surface to allow for polyplex delivery, but further experiments need to be carried out to fully understand the interaction.

A similar system developed by Zhang et al. involves the use of synthetic and natural amino acids to for the production of a family oligoaminoamides (OAA) with a high concentration of amine groups to allow for the proton sponge effect, and thus endosomal escape [67]. The synthetic amines used for construction of the OAAs are glutaroyl triethylene tetramine (Gtt), succinoyl pentaethylene hexamine (Sph) or succinoyl teraethylene pentamine (Stp), which along with natural amino acids, comprise low molecular weight sequence-defined polymers produced via solid phase-assisted synthesis. In addition to the cationic OAAs, transferrin (Tf)-conjugates were synthesized to target cells overexpressing the transferrin receptor (TfR), which is a characteristic of a number of cancers. Tf-conjugates that were explored include Tf-PLL, Tf-PEG-25PEI and Tf-PEG-linear PEI (lPEI). Three different mixing sequences were explored, and the method that resulted in the most efficient vectors was to mix the DNA and cationic oligomers first, followed by mixing the resulting complexes with the Tf-conjugate of interest. Transfection activity was greatly increased in a number of these TPs in comparison to previously reported polyplexes that did not contain the membrane-disruptive OAAs. Specifically, TPs consisting of Tf-PEG-PEI, histidine-rich 4-arm

OAAs and DNA exhibited a 100-fold increase in expression as evidenced by luciferase assay in the TfR over-expressing K562 cell line. By introducing large amounts of free Tf during transfections, the researchers showed a 600-fold decrease in gene expression, suggesting that the vectors were specifically targeted to TfR on the cell surface, and that the vectors undergo TfR-mediated uptake. Cell viability experiments indicated that the vectors exhibited low toxicity. Given their targetability, high transfection activity and endosomal escape capability, these vectors represent a potential step towards clinical relevancy for TPs. However, the components to the vectors still require complex and involved synthesis that could be expensive on an industrial scale.

In an example of a more specific targeting scheme, Oliveira et al. have worked to develop a non-viral gene therapy to address peripheral nervous system disease [68]. Focusing on tetanus toxin for its ability to target neuronal cells following minimally invasive intra-muscular injection, the group developed a TP system consisting of a thiolated PEI (PEISH), 5 kDa PEG-modified tetanus toxin fragment (HC) and plasmid DNA. The PEI was decorated with the thiol moieties to lessen intervention of the positively charged PEI, which is known to disrupt cell specific targeting [69]. The PEG was included as a spacer and to enhance complex stability in the aqueous environment and increase the exposure of the HC to the surface of the TP. TP size was determined to be 60 – 90 nm, with higher molar ratios of PEG-HC achieving smaller particle sizes. Zeta potential was +20–30 mV over the range of PEG-HC molar ratios explored. Binding specificity was investigated in ND7/23 sensorial neuron cells and NIH 3T3 cells as a control. As the amount of PEG-HC increased, cellular internalization decreased in NIH 3T3 and high levels of cellular internalization in the neurons, indicating that the

polyplexes were capable of receptor-specific targeting. Additionally, competition by free HC moieties inhibited internalization of the polyplexes by the sensorial neuron cell line ND7/23 and including the moieties triggers specific internalization of the complexes. At the highest transfection and cellular internalization formulations there were signs of toxicity. The authors conclude that this toxicity is associated with the overexpression of GFP. However it seems the negative effects could be associated with free or bound PEI in addition to GFP overexpression since this is a known cause of cytotoxicity [70]. Transfections were also carried out in a dorsal root ganglion (DRG) primary cell culture, and both transfection efficiency and gene expression activity were assessed. Expression, evaluated by luciferase assay, showed significantly less gene expression for the targeted TPs versus conventional polyplexes, while cellular uptake was shown to be about the same for both vectors. However, when looking at neuron versus non-neuron cells, a significant increase in the proportion of transfected neuron cells was observed in comparison to non-neuronal cells. These results suggest that the TPs effectively target neuronal cells, but that some issue is present with addressing the cellular barriers to delivery after endocytosis. Perhaps in this case including charge conversional moieties would be beneficial to enhance endosomal escape and lessen the DNA/PEI binding interactions allowing for easier transcription of the genetic material.

Zhang et al. developed a targeted TP system consisting of plasmid DNA, Polyamidoamine (PAMAM) as the DNA condensing polycation, and polyanioninc heparin-modified to contain biotin ligands as the cell-targeting component [71]. Biotin receptors are known to be overexpressed on cancer cell surfaces, and so present an opportunity for targeting. The size of the TPs was about the same as PAMAM/DNA

polyplexes from 100 – 150 nm with slight variations when changing ratios of the polymers. Zeta potentials, as would be expected, are lower for the TPs in comparison to their binary counter parts, with the TPs showing a minimum of about 3 mV and the binary vectors having zeta potentials ranging from 20 to 40 mV. No significant differences were observed in the toxicities of the TPs and their binary counterparts. The biotin-containing TPs demonstrated statistically significant increases in transfection activities in HeLa cells over both binary PAMAM/DNA polyplexes and heparin/PAMAM/DNA TPs with maximum increases of 100-fold for the heparin-biotin/PAMAM/DNA TPs over the others at a heparin-biotin/DNA weight ratio of 1 and optimal PAMAM/DNA weight ratio of 20. After fluorescently labeling the TPs and staining the cell nucleus, the cells were transfected and confocal images were taken after an incubation period. Comparing the images, it appears that a large number of vectors were located within the cells, especially around the nucleus, for the TPs in comparison to binary controls.

Gu et al. employed HA to target CD44 receptors which are overexpressed in some cancerous cell lines [72,73]. The TP system consists of a reducible poly(amino amide) (RHB) and plasmid DNA core that is coated with HA through electrostatic interactions. The inclusion of disulfide linkages throughout the hyper-branched polymer allows for degradation of the novel RHB polymer in the lysosomal environment. Particle sizes and zeta potentials ranged from 160 to 190 nm and -1 to -10 mV, respectively, over a range of w/w ratios of HA/RHB/pDNA. The TP formulations exhibited low toxicity, especially in formulations containing higher amounts of HA. Additionally, the HA appeared to ameliorate the toxic effects of the amine containing RHB polymer with binary

RHB/DNA vectors showing lower cell viability. Erythrocyte agglutination was assessed for RHB/DNA and HA/RHB/DNA polyplexes. Obvious agglutination was observed with the RHB/DNA vectors, and very little agglutination was seen in cells treated with higher amounts of HA in HA/RHB/DNA complexes. When the HA/RHB/DNA weight ratio was 5:5:1, no agglutination was observed, which provides an explanation for the higher cell viability seen with this formulation since erythrocyte agglutination is associated with adverse effects. Cellular uptake and protein expression were assessed in CD44-positive B16F10 cells and CD44-negative NIH3T3 cells by transfecting with plasmid coding for GFP and observing fluorescence with confocal microscope or flow cytometry. Both protein expression and the percent of transfected cells for the B16F10 cell line was much higher than those of the NIH3T3 cell line. These results provide strong evidence for the targeting ability of the TP system. Serum resistance of the TP system was also probed by transfecting B16F10 with the vectors at increasing serum concentrations and carrying out the same flow cytometry and confocal assays. When comparing to RHB/DNA and Lipofectamine 2000, the TPs showed increasing enhancement of both gene expression and transfection efficiency with increasing serum concentration, which further demonstrates the ability of polyanionic coatings to improve serum stability for non-viral vectors. Intracellular distribution and colocalization studies were also carried out by tagging the DNA with YOYO-1 and lysosomes with Lyso-Tracker Red. Investigation of the TPs using confocal microscopy revealed that the TPs were primarily localized around the cell surface after two hours, and after 12 h a significant fraction was found within lysosomes. After 24 h, a large amount of green fluorescence was observed in and around the nucleus, indicating that the YOYO-1 stained DNA had escaped from degradative

lysosomal compartments. Inhibition studies revealed that translocation of the DNA was dependent on microtubules and cytoplasmic dynein, but that kinesin did not play a role in TP internalization. In vivo studies to asses CD44 targeting after systemic administration of the TPs were carried out in C57BL/6 mice bearing pulmonary tumors. Much higher localization was seen in the TP formulations than that of either the RHB/DNA or naked plasmid. Comparing healthy Balb/c mice with tumor-bearing Balb/c mice, gene transfection was higher for the TPs in comparison to either naked plasmid or RHB/DNA polyplexes and, importantly, the lung tissue was effectively targeted as it displayed the highest gene expression in tumor-bearing mice. Taken together, these results suggest that using HA to both stabilize TP formulations for systemic administration and for targeting CD44-overexpressing tissues is a promising technique for advancing non-viral gene delivery.

In an effort to advance the work on HA TP systems, Liang et al. developed a similar system but with HA-green tea catechin complexes (HA-EGCG) as the anionic coating [74]. The EGCG complex is known for its ability to inhibit enzymes like nucleases, hyaluronidase and collagenase, which the authors intended to enhance systemic delivery of the TPs [75–77]. In contrast to Gu et al., the authors in this case employed PEI as the DNA-condensing polycation. The TPs were created by first bulk mixing the PEI and DNA to create the polyplex core and then mixing the HA-EGCG to provide the stabilizing anionic coating. Particle sizes of the HA-EGCG/PEI/DNA complexes were similar to that of both conventional PEI/DNA complexes and HA/PEI/DNA TPs. Zeta potential, as would be expected, decreased with increasing amounts of either HA or HA-EGCG to the TP formulations. Stabilization of the plasmid

by the TP was explored using agarose gel electrophoresis, and it was shown that HA/PEI/DNA polyplexes were unstable when treated with heparin. In comparison, the HA-EGCG/PEI/DNA TPs remained stable even at very high concentrations of the polyanion. The in vitro transfection efficiency was evaluated using CD44-positive HCT-116 cells and CD44-negative HEK293 cells to determine the ability of the TP to target CD44 receptors. Greater transfection efficiency was noted for the HA-EGCG/PEI/DNA TPs in the HCT-116 cells in comparison to PEI/DNA polyplexes, but not in the case of the CD44-negative HEK 293 cells. These results, along with inhibition studies, suggest the ability of HA to target CD44 receptors, in agreement with previously mentioned results from others [49,72]. When comparing transfection efficiencies between HA/PEI/DNA and HA-EGCG/PEI/DNA TPs, much higher transfection efficiency was noted for the former as assessed via flow cytometry. The authors attribute this enhancement to the improved stabilization of the HA-EGCG/PEI/DNA TPs since the experiments were carried out in serum-containing media. In vivo experiments involving the systemic administration of both HA/PEI/DNA and HA-EGCG/PEI/DNA TPs to HCT-116 tumor-bearing mice further demonstrated the ability of the former TP formulation to enhance transfection for the HA-containing TP systems. These results further bolster the argument that the inclusion of ECGC in the system helps to stabilize the TP system and protect against enzymatic degradation.

A simpler approach to targeting was developed by Jing et al. to target metastatic tumors by exploiting the overexpression of metalloproteinases (MMPs) in these cells [78]. The system used PEI to form the TP core and then coated the particles with gelatin B (GPD-B), which is anionic. Since gelatin is produced by the hydrolysis of collagen, the

researchers reasoned that MMPs would degrade the anionic TP coating when close to cancerous cells, allowing for the positively charged PEI/DNA core to associate with and transfect the cells. C3 cells, which express a high amount of MMP, and HeLa cells, which express a relatively low amount of MMP, were both transfected with the TPs. It was shown that the GPD-B coating decreased transfection activity in the HeLa cells while maintaining relatively constant levels of protein expression in the C3 cell line compared to PEI/DNA polyplexes. This result suggests that the addition of the GPD-B allows for the targeting of MMP overexpressing cells by activating when they are near such cells. Experiments carried out to further show that the presence of MMPs degraded the surface coating of the TPs were undertaken. For example, by exposing the TPs to MMP for 6 h and comparing the zeta potentials between the treated and an untreated control, the researchers observed a modest increase in zeta potential as determined by electrophoretic light scattering (ELS). The zeta potential increase was attributed to the degradation of the GPD-B coating by the MMPs. Erythrocyte aggregation assays were carried out to demonstrate the charge shielding capacity of the TP system. When compared to standard PEI/DNA polyplexes the TP-treated erythrocytes demonstrated significantly less aggregation. Interestingly, when the TPs were first exposed to MMPs and then introduced to the erythrocytes, similar aggregation to that of the PEI/DNA polyplexes occurred. This result further suggests that the GPD-B coating is degraded in the presence of MMPs and releases the standard PEI/DNA polyplex core.

2.3 Future Directions

Recent advances in the development of non-viral gene delivery vectors show great promise in advancing the vectors towards clinical relevance. With the ability to incorporate a variety of functions to address cellular barriers to delivery, TPs show great promise in leading the way to the clinic. However, there are still many obstacles that need to be overcome before non-viral components are the standard for gene delivery.

TP systems discussed in this review and elsewhere still suffer from relatively low gene delivery efficiency in comparison to viruses. Through stabilization of the polyplexes, charge conversion, degradable coatings and membrane disruption, the variety of polymers developed address nearly all cellular barriers to delivery, but all the necessary functions have not been included in a single vector since no vector to our knowledge includes a mechanism to address entrance into the nuclear membrane. To compete with viral vectors, TPs need to address the barriers in concert with minimal byproducts and, ideally, produced through simple and safe chemical processes. This is clearly a tall order, however the use of simple chemical modifications to already established polyplex systems may allow for the inclusion of endogenous chemical moieties that can address cellular barriers to delivery. These TPs could then be assembled in a sequential manner allowing for fully programmed delivery of genetic material, while maintaining biocompatibility.

One obstacle that is recurrent throughout the literature is the absence of standard practices on which to base interpretation of experimental results. For example, in many cases researchers seeking to advance on the work of others use different cell lines or modify a constituent polymer in follow up experiments. In order to more clearly

understand the enhancements of a particular system, transfections of the same cell lines would be ideal. Additionally, being consistent with the polyplex core would also be helpful since it would allow for a clear understanding that the modification in question is responsible for the observed influence.

In line with the above observation, standard methods for assembly of ternary polyplexes would also be helpful in understanding the influences of particular systems. It is well known throughout the field that different mixing methods can influence transfection results. Presumably through changing the micro mixing environment, the current mixing practices result in variable polyplex physicochemical properties from researcher to researcher and experiment-to-experiment. New developments in microfluidic mixing or flash nanoprecipitation may help to overcome this issue by providing uniform and predictable mixing environments, which lead to uniform and predictable products. Thus, producing TPs through one of these mixing methods may prove to be a useful tool for advancing the field.

Chapter 3: Literature Review of Microfluidics for the Production of Polyplexes

3.1 Introduction

Microfluidic (MF) devices have gained much attention for allowing researchers the ability to control mixing regimes and tune physicochemical properties of synthesized nanoparticles [79]. In addition to their applications in nanoprecipitation, MF devices have applicability in sensing [80], chemical analysis [81], cell sorting [82], and as components in many sensitive chemical instruments [83–85]. Defined by their micron and sub-micron scales, these devices necessarily deal with very small volumes of fluids, ranging from microliters down to femtoliters [86]. Geometrically confining the fluids to these small flow regimes results in laminar flow within the device, which means diffusion, rather than convection, is the dominant force controlling mixing. The common method to predict if a particular fluid flow is either laminar or turbulent is by calculating the Reynold's number (Re) for a fluid, geometry and flow rate [Eqn. 1] [87].

$$Re = \frac{\rho V L}{\mu} \qquad (1)$$

Where ρ is the fluid density at the relevant temperature and pressure, V is the average velocity of the fluid within the channel, L is the width of the channel and μ is the viscosity. Re less than 2000 is generally considered to characterize laminar flow, and Re is typically much lower than 100 and often lower than 1.0 in the case of MF devices.

Confining the mixing to diffusion allows for the unique applications of MF devices whether those applications are for lab-on-a-chip chemical analysis [88], nanoparticle synthesis [89], or heat exchange [90]. These microreactors also provide for large surface to volume ratios allowing for enhanced heat and mass transfer. Although

there are many interesting applications, here we will focus on nanoparticle synthesis and specifically on MF devices for the production of polymeric gene delivery vectors.

By allowing for the precise control of the volumes of reactants and products, microreactors significantly enhance the control researchers have over chemical reactions leading to the formation of NPs [89]. This is desired since conventional bulk mixing (BM) strategies can lead to polydisperse NPs, and MF approaches can help isolate specific processes, such as nucleation and agglomeration that occur as NPs form in solution. Generally, there are two microfluidic strategies for the production of NPs, with much variation within each category depending on the desired product. The first utilizes special geometries and immiscible solvents to form droplets in which products mix, effectively resulting in very small batch reactors [Fig. 3.1B]. The other is continuous flow microfluidics, which typically leads to higher NP production rates and allows for more control and homogeneity of NPs [Fig. 3.1A].

Polymer-based gene delivery vectors are a significant type of NP with exciting potential to be used as clinically relevant non-viral gene delivery vectors [91]. In spite of their comparatively low gene delivery efficiency and potential cytotoxicity, these vectors typically contain chemically modifiable moieties that allow researchers to address their shortcomings [8,56]. Additionally, these types of polyplexes have the ability to overcome many of the safety and processing concerns associated with the administration and production of viral vectors. Chemical modification, complexation with additional polymers [63,92], and the use of biocompatible constituents [93] are some of the important techniques employed to address the many cellular barriers to delivery. Some

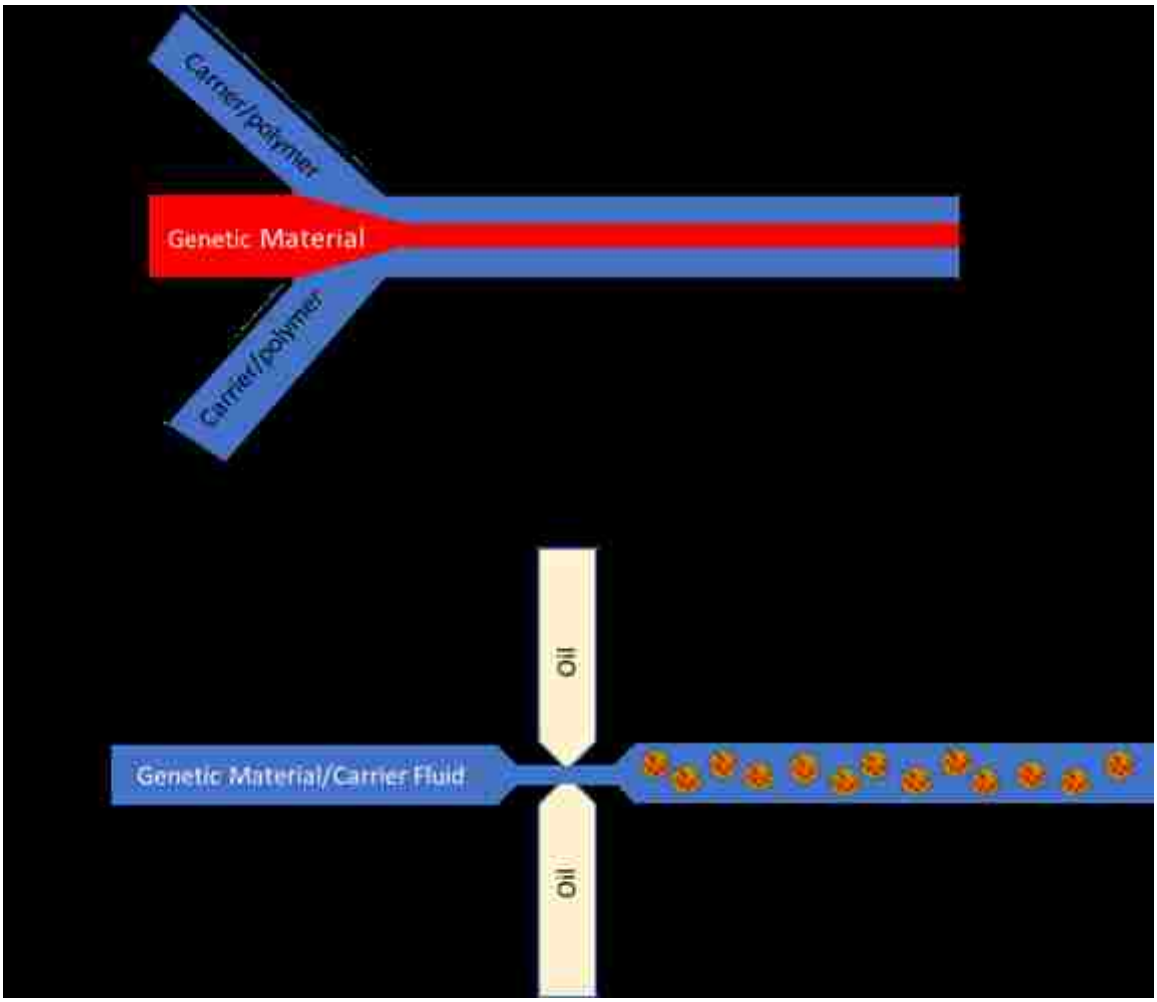

Figure 3.1: Schematics of A) a continuous hydrodynamic flow focusing microfluidic reactor and B) a microdroplet reactor.

significant strategies addressed in more detail elsewhere in the manuscript, involve the use of cationic polymers for their ability to condense genetic material and buffer the acidification of the endosome and the use of additional anionic coatings to prevent serum aggregation and allow for cell targeting.

The following is a review of microfluidic strategies that have been developed for the production of non-viral gene delivery vectors, specifically focusing on vectors involving the use of polymers. Additional microfluidic strategies for generally advancing the field of gene therapy involve the development of devices for enhancing gene delivery to cells within the device. These strategies involve techniques ranging from electroporation [94] to the use of hydrodynamic force [95] and are outside of the scope of this review. For more details regarding these approaches a complete review can be found elsewhere [96].

3.2 Microfluidic Approaches for the Production of Polyplexes

3.2.1 Continuous Microfluidic Production of Non-Viral Gene Delivery Vectors

Strategies in this section involve the development of devices that allow for the production of polyplexes on a continuous basis. These devices involve the mixing of two or more solutions within a device and take advantage of the laminar flow regime to create an interface or interfaces, depending on the specific channel geometry, through which genetic material and polymers mix to create polyplexes in a controlled and continuous manner.

Koh et al. created a MF system for the production of PEI/DNA polyplexes using hydrodynamic flow focusing to create two interfaces on either side of a DNA stream through which the constituent polymers could diffuse [16]. The device geometry consisted of a 254 x 70 μm^2 cross section and 5 cm channel length in which diffusion of polymer into the DNA-containing stream occurs. They formed polyplexes at N/P ratios of 3.3 and 6.7 to demonstrate that MF polyplex fabrication could result in polyethylenimine (PEI)/DNA polyplexes with a lesser amount of the toxic cation while maintaining or improving gene expression, when compared to conventional BM-produced polyplexes. First, the researchers explored the effectiveness of both BM and MF for condensing DNA by PEI. Atomic force microscopy (AFM) was used to visualize the resulting particles from either method, and it was observed that MF-produced polyplexes appeared to have a smaller size and a similar size distribution when compared to those produced by BM. Additional particle characterization experiments were carried out using DLS and it was shown that particles produced by MF were roughly half the size of those produced by BM with a particle size of 494 nm at the N/P ratio of 3.3. Transfection efficacy as assessed by GFP expression in NIH 3T3 cells was 1.2- and 1.7-fold higher for the polyplexes produced by MF when compared to BM polyplexes at the higher 6.7 N/P ratio at 2 and 4 days post-transfection respectively. Polyplexes produced by both methods were also tested for toxicity in NIH 3T3 cells and it was observed that MF produced polyplexes were slightly less toxic than conventional polyplexes as assess by MTT assay. The MF polyplexes showed 16% and 5% higher cell viability for the 3.3 and 6.7 N/P ratios respectively. Employing confocal laser microscopy (CLM) the researchers explored the cellular uptake and distribution by fluorescently labeling the DNA and PEI.

It was observed that more of the polyplexes produced by the MF device were located around the nucleus than those produced by BM two days post-transfection. Additionally, after four days fewer condensed polyplexes were observed indicating the likely dissociation of the DNA from the PEI by that time.

Advancing on the previous work, Debus et al. explored a variety of microfluidic channel geometries and modified PEI's for the production of polyplexes [17]. In this case however, Y-shaped channel designs were employed rather than hydrodynamic flow focusing resulting in a single diffusion interface in contrast to the two interfaces that are employed in previous work. Channel diffusion lengths were varied from 2 mm to 500 mm to explore the effect of channel length on the physicochemical properties of various cationic polymers relevant to gene delivery. Using dyes to visualize the flow, the researchers observed less complete mixing in channels with shorter diffusion lengths, while liquids containing the dyes appeared to show some mixing in the longer channels. The cationic polymers that were explored were PEI, PEI 5 kDa (5PEI) and transferrin-conjugated PEI (Tf-PEI). The researchers found that the largest impact on polyplex size seemed to be the ratio of polymer to DNA and that changing other parameters, such as the flow ratio (FR), defined throughout this thesis as the ratio of the DNA stream flow rate to the total flow rate, had minimal impact on polyplex size. The polydispersity index (PdI) of the resulting polyplexes seemed to vary with respect to flow rate in the channels with shorter lengths, however in the longest channel explored, 200 mm, differences in PdI were almost unnoticeable. PdI's of polyplexes produced by the microfluidic device were generally lower than that of BM polyplexes, and fractionating PEI into low molecular weight fractions yielded smaller particles than other cationic polymers

explored. The Tf-PEI yielded the smallest particle sizes in both BM and MF preparations and also demonstrated significant decreases in size when micromixed. In addition to DNA, both siRNA and mRNA polyplexes were formed by the MF devices. Generally, they exhibited similar physicochemical property relationships to the DNA polyplexes, however there were significant differences in the physicochemical properties depending on which genetic material was used.

Another type of continuous production method for polyplexes is a three-dimensional hydrodynamic focusing (3DHF) device that was developed by Ho et al. and used to produce Turbofect®/DNA polyplexes [97]. In an effort to combat transverse diffusive broadening, a setback to 2D devices such as the ones mentioned above [98], the group developed a device capable of providing 3DHF yielding a laminar flow pattern of a center cylindrical flow sheathed around the circumference. Seeking to enhance mixing and thus quality of the polyplexes, the researchers developed a "hydrodynamic drifting" technique that is easily implementable on a planar MF device. The technique involves introducing a DNA stream and buffer stream side-by-side immediately before a 180º bend in the channel. The buffer stream is on the outer side of the bend and the centrifugal force induces Dean's vortexing. Subsequently, two polymer inlets are introduced on either side of the DNA/buffer stream and hydrodynamically focus it producing a cylindrical inner DNA stream surrounded by the buffer and polymer rich sheath stream. Mixing is enhanced in this case since a larger surface area is produced through which diffusive mixing can occur. The physicochemical properties of the 3DHF-produced polyplexes were interrogated by DLS. A 40% reduction in average particle size was observed with the device versus the conventional BM method with a particle size of 262

nm. Polyplex size at increasing flowrates was also investigated and, in this case, it was found that higher flowrates lead to smaller particles over the range of flow rates and particle compositions tested. Particle size distribution was also shown to be much smaller in the case of the 3DHF device in comparison to that of BM-produced polyplexes. Aggregation tendencies of the polyplex produced by either method were also explored, and it was seen that over a period of 400 min the 3DHF polyplexes demonstrated much less aggregation, with no significant increase in particle sizes in the case of 3DHF and nearly doubling in the case of conventional BM. Transfections were carried out in HEK 293 cells using plasmid coding for GFP for both BM and 3DHF polyplexes and visualized using confocal microscopy. Qualitatively, there was no difference in transfection efficiency, which at least demonstrates that shear stress imparted by the device does not negatively impact the functioning of the genetic material. Transfection efficiency was measured via flow cytometry, and a 15% increase in transfected cells was observed in the case of the 3DHF device with about ~75% of cells being transfected. Luciferase assays were also carried out, and a 2-fold increase in luminescence was observed suggesting a significant increase in gene expression for the 3DHF device.

In a more recent example, Wilson et al. employed the same 3DHF technique for the production of poly(beta-aminoester) (PBAE)/DNA NPs [99]. In addition to exploring the physicochemical properties and common transfection endpoints of the polyplexes produced by the device, the group also carried out nanoparticle tracking analysis and looked at stability of the polyplexes after lyophylization. Particle size, as determined by DLS, was not observed to be statistically different between BM and 3DHF methods for this polycation/DNA system. The authors suggest that the difference in particle size

enhancement in this case may be due to PBAE being amphiphilic and of higher charge density than PEI, which has been the most explored polycation for MF methods. Transfections of GB319, B16 and MDA-MB-231 cell lines were carried out and transfection efficiency, gene expression and cell viability were assessed. It was shown that freshly produced 3DHF polyplexes performed about the same as BM particles in efficacy, expression and toxicity in all three cell lines. In contrast, BM polyplexes that were lyophilized demonstrated a significant drop in transfection efficiency, while freeze-dried 3DHF-produced polyplexes showed little change. An additional experiment was carried out to assess the long-term storage potential of the freeze-dried particles, and it was shown that after two months of being stored at -80 °C there was no significant decrease in transfection efficacy. The group also developed a nanoparticle tracking analysis (NTA) method to assess concentration of NPs and plasmids contained per NP. Results for the PBAE/DNA NPs produced in this case led to estimations of about 20 plasmids per NP.

3.2.2 Droplet Microfluidics

In this case, strategies for improving polyplex formulation methods involve the use of a MF device capable of creating droplets in which NP complexation to form polyplexes occurs. Each drop produced by the device is considered to be a microreactor that allows for enhanced transport of chemical species due to the short diffusion distances and results in more stable and uniform NP formation. In the cases discussed, there is an aqueous phase and oil phase, and the immiscibility forces the creation of aqueous droplets.

Grigsby et al. developed a MF droplet system for the production of polyplexes using either plasmid DNA or RNA and poly(amido amine) poly(CBA-ABOL) [18]. The cationic and bioreducible block copolymer has previously been show to possess high gene delivery efficiency, low toxicity, and the ability to deliver multiple types of nucleic acids. After establishing optimum formulations, polyplexes were formed at polymer/DNA and polymer/RNA ratios of 45:1 and 60:1 (w:w), respectively. Comparing BM and MF droplet methods by DLS revealed particle sizes that were 40–50% smaller for the microfluidic device with particles averaging close to 100 nm. The size distribution was also considerably narrower for the MF polyplexes compared to those produced by the conventional method. Polyplexes produced by MF and BM demonstrated PdI's of 0.152 and 0.342, respectively. In addition, it was shown that the particles were stable over a period of 240 min by demonstrating consistent particle sizes over the time period by DLS. In comparison, particles produced by BM nearly doubled in size over the same period, which is a strong indication of aggregation. Free cationic polymer is often present in BM polyplex formulations and is generally considered to be a problem due to its potential toxicity. Using PicoGreen and RiboGreen assays, it was show that using microfluidics in formulation of either DNA or RNA polyplexes resulted in less free polymer in the final product. Primary mouse embryonic fibroblast (PMEF), human mesenchymal stem cells (hMSC), HepG2 human hepatocellular carcinoma cells and HEK293 human embryonic kidney cells were chosen to assess transfection and cellular uptake. With gains ranging from 6 to 31%, flow cytometry revealed that a larger fraction of cells was transfected by MF-produced polyplexes compared to conventional polyplexes. Total gene expression was measured by luciferase assay, and the same trend

was seen with 1.9- to 6.8-fold increases for the MF polyplexes compared to the conventional polyplexes. Additional flow cytometry experiments were carried out to assess the cellular uptake and trafficking of the polyplexes within the cells. By combining QD-FRET analysis and flow cytometry, the researchers observed that the MF-produced polyplexes stayed intact much longer than the readily unpacking BM polyplexes. They suggest that prolonged stability within the cell of polyplexes in the MF formulations could result in greater protection from degradation prior to endosomal escape.

3.3 Conclusions

Microfluidic devices have branched out of the realm of being used solely for sensing and analysis applications, and new applications in nanoprecipitation are being explored. Polymeric non-viral gene therapies are well-suited for these advanced nanoprecipitation devices due to day-to-day and experiment-to-experiment variations that are known issues for bulk-mixed polyplexes [45]. Employing the two primary MF mixing strategies of continuous hydrodynamic flow focusing and droplet generation, researchers have demonstrated the many advantages of using a lab-on-a-chip device for the production of polymeric gene delivery vectors. These advantages include the production of particles with narrower size distributions, lower cytotoxicity and higher transfection efficiencies. Additionally, the technique operates in a continuous fashion, which is a known advantage within the pharmaceutical field since the production of drugs can be easily standardized and the quality of the resulting product is more consistent [100].

Moving forward, MF devices have the potential for advancing the field of non-viral gene delivery employing the techniques mentioned above. However, there are still

issues with the use of the devices and room for advancement. For example, all of the previously mentioned examples produce relatively simple polyplex nanoparticles that may not provide enough functionality to overcome all of the cellular barriers to delivery. These particles, therefore, may fall short of required cellular uptake and gene expression levels necessary to compete with viral vectors. One innovation that may allow for the advancements necessary to get closer to these positive attributes of viral vectors is the design of chips to produce more complicated non-viral vectors such as ternary polyplexes.

Chapter 4: Microfluidic Production of PEI/DNA Polyplexes with Separation of Free Polymer

Polymeric gene delivery vectors offer a safer alternative to viral gene delivery. However, transfection efficiency remains low, and many polymers exhibit dose-limiting cytotoxicity. Conventional preparation of polyplexes by bulk mixing (BM) of polymers and DNA is a relatively uncontrolled process that leads to polydispersity of polyplex size and poor reproducibility. Alternatively, polyplexes may be prepared in microfluidic channels wherein polymers and DNA are brought into contact by diffusion, allowing better control of the process and leading to smaller and more uniform polyplexes. We have designed a microfluidic (MF) device for polyplex fabrication that has the capability of separating free polymer from the assembled particles, referred to as a microfluidic separator (MS). The transfection efficiency and cytotoxicity of BM and MS polyplexes comprising polyethylenimine (PEI) were compared in three model human cell lines: HeLa, U-87 MG and MDA-MB-231. MS polyplexes at 0.6:1 (w:w) PEI:DNA exhibited approximately 150-, 2.5-, and 7-fold increase in transgene expression compared to BM polyplexes in the three cell lines, respectively. MS polyplexes also exhibited a 30-, 11- and 20% increase in cell viability at 0.6:1 (w:w) PEI:DNA, compared to BM polyplexes at their optimal transfection ratio of 1.8 (w:w) PEI:DNA. MS polyplexes were also 60-77% smaller than BM polyplexes. The results suggest that diffusion-controlled polyplex assembly and separation of excess PEI results in relatively efficient gene delivery at low PEI/DNA ratios where cytotoxicity is reduced, potentially allowing administration of a higher dose of DNA. Additionally, this approach for separation in a microfluidic device

may be important in preparing a variety of nanoparticle drug delivery systems by removing potentially toxic components and enabling the fabrication of more complex delivery systems.

4.1 Introduction

Polymer-mediated gene delivery is of interest as a safer, more versatile alternative to viral vectors [45]. However, due to the relatively low delivery efficiency, instability in serum, and cytotoxicity associated with many gene delivery polymers, non-viral gene delivery vectors have had limited success in the clinic. Attempts to address the limitations of polymer-mediated gene delivery have largely focused on the chemistry of the materials. Strategies have included, for example, synthesizing biodegradable polymers with reduced cytotoxicity [101–105], conjugating cell-specific targeting moieties [93,106–108], designing copolymer hybrids [109–112] or other chemical modifications [7,113–115], and incorporating multiple polymers in a single vector [14,116–118].

The methods most often used for assembly of polymer/DNA complexes (polyplexes) represent another limitation of polymeric vectors. Conventionally, polyplexes are generated by simply mixing aqueous solutions of the constituents in a small volume followed by a short incubation period (15-30 min) during which spontaneous, entropically driven self-assembly occurs between the polycation and the nucleic acid (referred to as bulk mixing, BM). Although simple and easily implemented, polyplexes formed by BM are often large (200-500 nm) and exhibit strongly positive zeta potential (+25-50 mV) due to the presence of excess polycation. Polyplex sizes can be controlled to some extent by varying the polymer/DNA ratio and solution conditions, but

size distributions are commonly heterogeneous. In addition, excess free polymer usually remains in the resulting suspension, contributing to cytotoxicity [119–121]. Finally, this uncontrolled process provides poor reproducibility from batch to batch and, especially, lab to lab and would hinder large-scale manufacture required for clinical translation [122,123].

The use of microfluidic (MF) devices for the assembly of polyplexes offers a continuous and potentially more reproducible alternative to BM [16–18,78]. Typically, a plasmid DNA solution is passed through a central channel while the polycation is introduced from each side to hydrodynamically focus the DNA solution into a narrow stream. Because of the small channel dimensions (~200 μm), the flow is laminar and no mixing occurs between the parallel streams. The polymer, however, can diffuse into the DNA-containing stream. Thus, the rate of the polymer/DNA interaction is diffusion controlled (~$4D/L^2$; where D is polymer diffusivity and L is the width of the DNA-containing stream) and can be manipulated by varying the channel dimensions and relative DNA and polymer solution flow rates, which govern the width of the polymer and DNA streams within the channels. Compared to conventional polyplexes formed by BM, MF-assembled polyplexes are typically smaller, more uniform and exhibit higher gene delivery activity [16,17].

Several of the previously reported MF devices have employed channel lengths of <5 cm, cross sectional area of ~100x200 μm^2 and flow rates of ~100 μL/min, corresponding to a residence time of material within the device of <1 sec. Assuming polycation diffusivity on the order of 10^{-6} cm^2/sec and typical DNA-containing stream widths of 20-100 μm, the characteristic diffusion time (L^2/4D) is expected to be 1-25 sec

[124], suggesting that there is insufficient time for diffusion of polymer from the outer stream to the center of the channel within the device, and polyplex formation may continue in the bulk after exiting the microfluidic channels. Here we report the design of MF devices for polyplex assembly with significantly longer channel lengths. In addition, complete formation of polyplexes within the channels provides an opportunity to separate free polycation from the polyplexes, which remain confined to the center channel due to their much larger size and, therefore, lower diffusivity. Removal of free polymer may provide reduced cytotoxicity.

4.2 Materials and Methods

4.2.1 Materials

Branched PEI with an average molecular weight of 25 kDa was purchased from Sigma-Aldrich and dissolved in phosphate buffered saline (PBS). Lipofectamine 2000 transfection reagent was purchased from Thermo Fisher. Luciferase assay system and Cell Titer-Blue cell viability assay kit were purchased from Promega. Cellular lysis buffer was prepared as directed by the luciferase assay kit protocol. Luciferase plasmid (pGL3 control vector) was purchased from Elim Biopharmaceuticals.

4.2.2 Computational Fluid Dynamics

To aid in the design of the MF device, the flow and diffusion within the channels was modeled using COMSOL Multiphysics version 4.3b with the microfluidics module. The diffusivity of the PEI was estimated using the Stokes-Einstein relation and

approximated to be $1.0x10^{-7}$ cm^2/sec. Using the relation developed by Lukacs et al. the diffusivity of the plasmid DNA (5,217 bp, 2.98 MDa) was approximated to be $1.3x10^{-6}$ cm^2/sec [125].

4.2.3 Microfluidic Device Fabrication

Microfluidic devices were fabricated using well-established soft lithography techniques [126]. In short, channel designs were created in Autocad and printed onto a transparency to generate a photholithographic mask. A master mold was made using Microchem SU-8 3050 negative photoresist by adhering to the spin curves and processing suggested by Microchem. In short, glass slides were cleaned with acetone, ethanol and then water. The slides were then thoroughly dried with nitrogen and the photoresist was spincoated onto the slide and the depth was verified to be 100 μm with a profilometer. The slide and photoresist were then exposed to UV radiation in a mask aligner using the photolithographic mask. The slide and resist were then cured for an hour at 95 °C and then developed using Microchem SU-8 developer to yield the master mold. Dow Corning Sylgard 184 Silicone Encapsulant PDMS resin (Ellsworth Adhesives) was then applied to the master mold and cured in an oven at 100 °C for one hour. The PDMS containing the microchannels was then peeled from the mold and attached to a glass microscope slide using a Harrick Basic Plasma Cleaner PDC-32G-2. In all instances microfluidic channels are rectangular with a width of 200 μm and a depth of 100 μm. A microfluidic punch was used to create holes at the inlets and outlets of the device, and tubing was pressed directly into the holes. Tubes of equal length were used at all outlets to ensure that the resistance associated with each outlet was equal.

4.2.4 Flow Characterization

Flow characterization experiments were carried out by flowing 500 kDa fluorescein-conjugated dextran (Sigma-Aldrich) through the DNA inlet and 70 kDa rhodamine-conjugated dextran (Sigma-Aldrich) through the PEI inlet. Images were obtained with a Labsmith SVM340 synchronized video microscope with fluorescence capabilities.

4.2.5 Ninhydrin Assay

Ninhydrin reagent (Sigma-Aldrich) was used according to the protocol provided by the manufacturer with modifications to accommodate PEI rather than amine containing proteins. Specifically, Nin – Sol was mixed with lithium acetate buffer in a 3:1 volumetric ratio. Twenty microliters of both samples and standards were mixed with an equal volume of the reagent and incubated at 90 °C for 10 min. After the incubation period, samples and standard were diluted with 200 μL of ethanol and added to a clear 96–well plate. The absorbance was read at a wavelength of 572 nm on a Biotek Synergy II plate reader.

4.2.6 Polyethylenimine Labeling

Polymers were labeled with Alexa Fluor 594 by mixing 1 mg of an Alexa Fluor NHS-ester in 200 μL of anhydrous DMSO with 10 mg of PEI in 1.8 mL of 0.2 M sodium carbonate, pH 9.3. The reaction was allowed to run for 12 h with gentle mixing at room temperature and shielded from light to prevent photobleaching. The labeled polymer was

separated from unreacted dye by dialysis using a Spectra Por dialysis tubing with molecular weight cutoff of 10 kDa against 4 L pure water exchanged three times over a 24 h period. The resulting PEI-AF594 solution was lyophilized, weighed and then diluted into PBS to be used as a stock solution. Labeling density was determined to be 0.5 dyes per polymer chain.

4.2.7 Preparation of Polyplexes and Lipoplexes

BM polyplexes were generated using standard protocols. Briefly, DNA was diluted to 20 μg/mL in PBS at a pH of 6.8 and phosphate concentration of 0.0067 M. PEI was similarly diluted to appropriate concentrations to achieve the desired polymer:DNA ratio. Polyplexes were formed by pipetting 200 μL of PEI solution into a microcentrifuge tube containing an equal volume of DNA and mixed by briefly vortexing. Polyplexes were then incubated for 20 min at room temperature. Lipofectamine 2000/DNA complexes were formed according to the manufacturers protocol. Specifically 24 μL of Lipofectamine 2000 was diluted into 176 μL of Eagle's Minimum Essential Media (EMEM) . An equal volume of DNA (20 μg/mL in PBS) was added to the Lipofectamine 2000 solution and allowed to incubate for 5 min. For the production of polyplexes with MF devices, DNA was diluted to 15 μg/mL in PBS and PEI solutions were also prepared in PBS to provide the desired PEI:DNA ratios. The DNA and PEI solutions were pumped at a flow ratio of 0.2 (DNA flow rate/total flow rate) and at a total flow rate of 100 μL/min, to yield a product with the final DNA concentration of 10 μg/mL. The resulting polyplexes were used immediately for characterization or transfection as described below.

4.2.8 Agarose Gel Electrophoresis

The amount of free polymer in polyplex suspensions was determined by agarose gel electrophoresis. Polyplexes were prepared using PEI-AF594 either by BM or MF as described above. Samples of polyplexes and free PEI, each containing 50 µg PEI, were loaded into a 0.75% agarose gel and electrophoresed at 100 V for 30 min. The gel was imaged on a GE Typhoon FLA 7000 laser scanner and the amount of free polymer was determined by integration of the fluorescent bands.

4.2.9 Transfections

HeLa (human cervical carcinoma), U-87 MG (human glioblastoma) and MDA–MB–231 (human breast carcinoma) cell lines were obtained from ATCC and cultured in Eagle's minimum essential media (EMEM, ATCC) supplemented with 10% fetal bovine serum (VWR) at 37˚C and 5% CO_2 according to ATCC protocols. All transfections were carried out using protocols well established within the research group. Cells were seeded in 12-well plates at 100,000 cells per well 24 h prior to transfection. Growth media was removed from the cells and replaced with 1.5 mL of polyplex suspension containing 1 µg DNA per well. After 4 h, polyplexes were removed and replaced with growth media. Luciferase expression was quantified 24 h post-transfection using the Promega luciferase assay system. Luciferase activity was measured using a Biotek Synergy II plate reader. Results were normalized to total protein concentration in the lysate quantified using BCA assay (Pierce, Rockford, IL) following the manufacturers protocol.

4.2.10 Cytotoxicity

Cytotoxicity of BM and MF polyplexes was quantified using the Cell Titer-Blue viability assay (Promega). In short, cells were plated in 96-well tissue culture plates at 20,000 cells per well and transfected 24 h later following the same transfection procedure as above, substituting 10 μL of polyplex solution to accommodate the smaller wells. At 24 h post-transfection, 20 μL of the cell titer blue reagent was added to each well and incubated for 4 h. The fluorescence (ex 530 nm, em 590 nm) of each well was determined using a Biotek Synergy II plate reader.

4.2.11 Particle Characterization

Particle size, zeta potential and polydispersity were determined using a Malvern Zetasizer Nano ZS. Polplyexes were produced as described above. The resulting solution (400 μL) was then diluted by addition of 200 μL deionized water and immediately added to Malvern Folded Capillary Zeta Cell. Each measurement was performed in triplicate

4.3 Results and Discussion

4.3.1 Flow modeling and Channel Design

To predict the appropriate channel geometry for the device, an initial design was modeled in COMSOL (Fig. 4.1A) and the concentration of DNA was calculated as a function of position along the channel cross-section and channel length at varying flow ratios (FR), which we define here as the ratio of the flow rate of the center stream to the

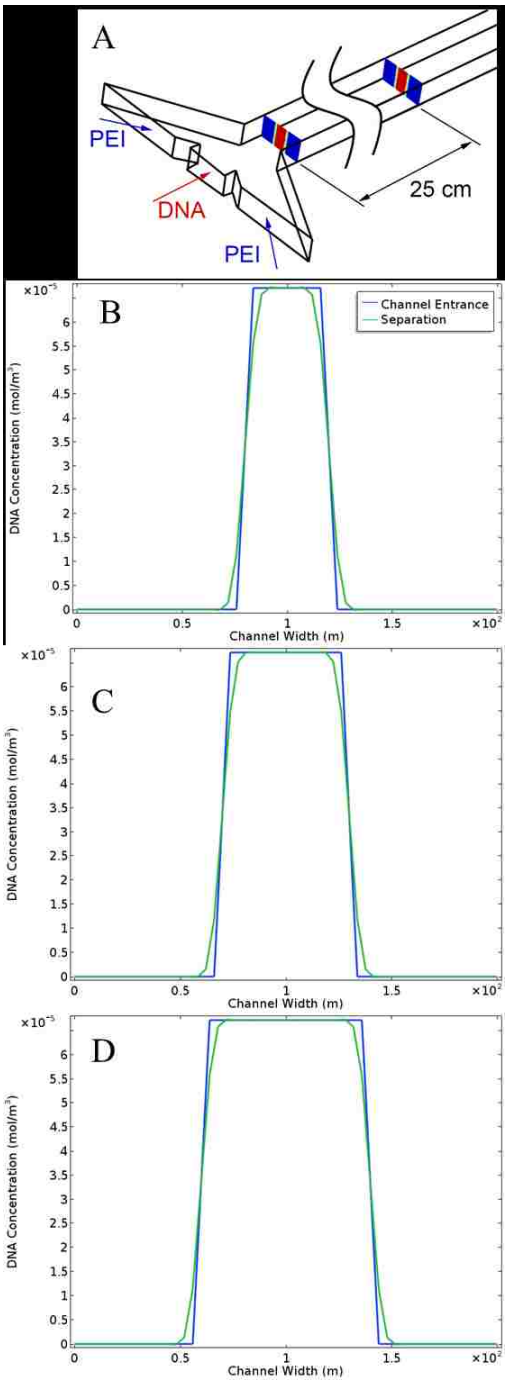

Figure 4.1: Initial channel design demonstrating the microfluidic channel geometry (A). DNA concentrations were determined computationally at various points along the channel and plotted as slices of the channel cross-section at those points. DNA cross-sectional concentration profiles are shown immediately after introduction of the outer streams (dark blue) and at 25 cm downstream (cyan) at FR = 0.2 (B), 0.3 (C) and 0.5 (D).

total flowrate (Fig. 4.1B – 4.1D). At the various flow ratios, the model shows similar DNA diffusion behavior with the DNA remaining mostly confined to the center portion of the channel. This result suggests that by sheering away the outer, DNA-free portions of the stream, the polyplexes may be separated from free PEI.

The concentration of PEI within the channels was also modeled at various values of FR. As expected due to the narrowing of the center DNA-containing stream, the PEI concentration in the center stream increased with decreasing FR (Fig. 4.2A). Lower flow ratios are more desirable in microfluidic nanoprecipitation as this leads to narrower DNA streams and often smaller average particle sizes [127]. It is also well known that there is a lower limit to the FR for a specific channel, below which flow of the center stream in the hydrodynamic focusing region is unstable due to the mechanics of the syringe pumps [128]. The lowest flow ratio that could provide stable flow in our device was found to be FR = 0.2 (data not shown). At this FR, the average concentration of PEI within the center stream is ~48% of the steady state concentration at 25 cm downstream (Fig. 4.2A) and is relatively uniform across the center stream (Fig. 2E). This information allows for the design of the separation mechanism as well as a good approximation of the appropriate inlet concentrations of DNA and PEI to achieve the desired polymer:DNA ratio in the polyplexes.

4.3.2 Flow Characterization and Model Validation

The microfluidic system for introduction of PEI and DNA, flow focusing, a serpentine diffusion region, and separation of free PEI is shown in Fig. 4.3A-E. Fluorescein-labeled dextran (500 kDa) was used to simulate the DNA center stream along

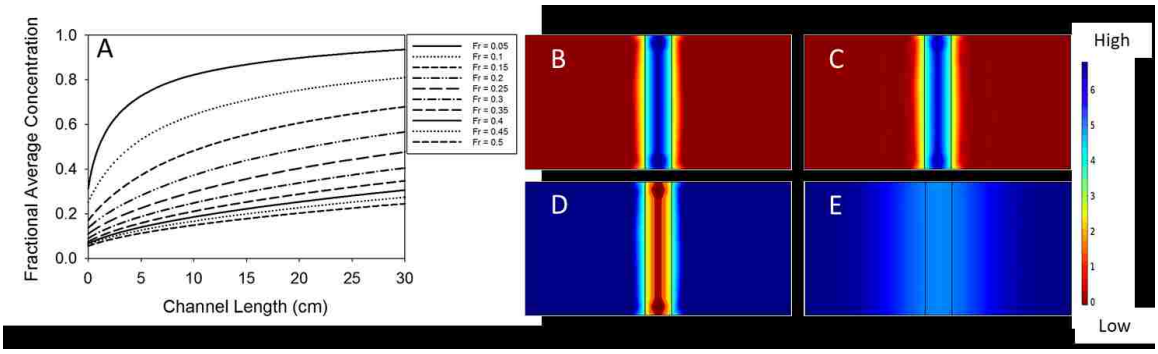

Figure 4.2: CFD analysis of microfluidic geometries. (a) Average fractional concentration of PEI within the product stream, calculated by integrating the concentration of PEI over the cross-sectional area of the channel representing the separation region at the relevant channel length of 25 cm. (b) Cross-sectional view of the channel, giving the initial concentration profile of DNA. (c) Cross-sectional view of the channel, giving the concentration profile of DNA at 25 cm. (d) Cross-sectional view of the channel, giving the initial concentration profile of PEI. (e) Cross-sectional view of the channel, giving the concentration profile of PEI at 25 cm.

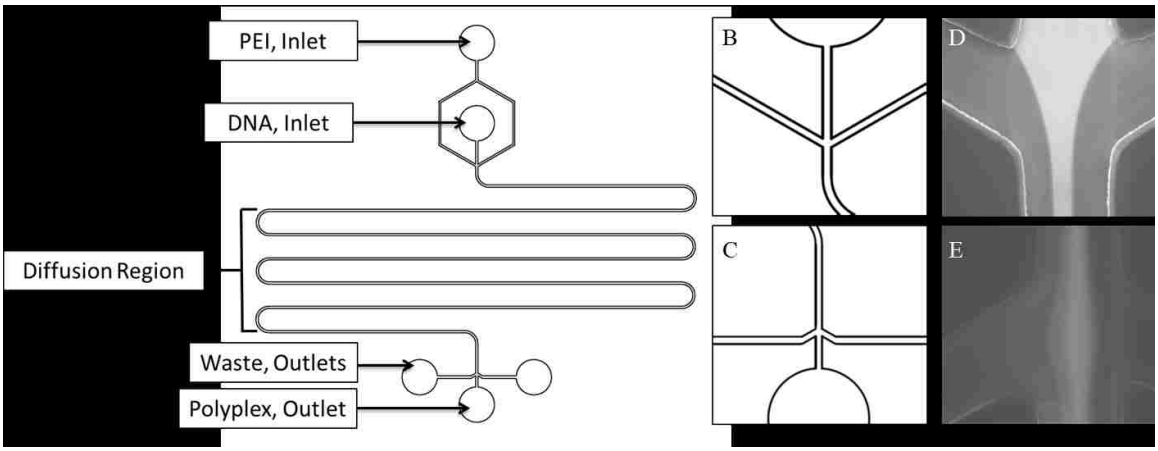

Figure 4.3: Separation device schematic and flow characterization. (A) The design and schematic of a microfluidic separator. (B) The hydrodynamic focusing region of the device. (C) The separation region of the microfluidic device. (D) Zoomed in fluorescence image of the hydrodynamic focusing region. (E) Zoomed in fluorescence image of the separation region.

with water in the outer channels for visualization of the flow focusing and separation regions of the microfluidic channels. Fluorescence microscopy of the flow focusing region reveals narrowing of the center stream from the inlet channel width of 200 μm to 40 μm, as expected at FR = 0.2 (Fig. 4.3D), creating two interfaces through which the PEI can diffuse into the center region of the channel. Fluorescence micrographs of the separation region show the center fluorescent portion of the stream continues on to the product outlet while the outer portions of the channel are separated to either side (Fig. 4.3E). It may appear that some of the outer stream continues to the center product stream after the separation. However, the intensity of the fluorescein emission decreases quickly as the fluorescein concentration decreases across the channel cross section, making it difficult to visualize the dextran at low concentrations at the edge of the center stream.

To validate the modeling results and evaluate the performance of the separation mechanism, PEI concentration in the outlet was quantified and compared to the inlet PEI concentration. PEI was pumped through the side channels of the MS device at concentrations ranging from 2 to 12 μg/mL, along with water through the center inlet at FR = 0.2. The concentration of PEI in the center stream after separation was 46.1% of the inlet concentration, which is in close agreement with the computational models described above [A.1]. This result suggests that only PEI that has diffused into the center channel is recovered in the product. In a separate experiment, DNA (15 μg/mL) was pumped through the center channel with water in the side channels at FR = 0.2. The outlet concentration of the DNA was determined to be 9.7 ± 0.57 μg/mL (n = 13), while the model predicts 10 μg/mL, further validating the model and indicating that the separation was achieved as expected.

4.3.3 Microfluidic Polyplex Formation and Characterization

Polyplexes were fabricated by conventional BM and the MS device, and the sizes of the resulting polyplexes were compared at PEI/DNA ratios of 0.6:1 to 3.0:1 (w:w) (Fig. 4.4A). The minimum size of BM polyplexes was ~200 nm at PEI/DNA ratio of 2.5:1 (w:w), while the smallest MS polyplexes were 170 nm at PEI/DNA ratio of 1.8:1 (w:w). At PEI/DNA ratio of 0.6:1 (w:w), BM polyplexes were >1 μm, likely due to aggregation, while MS polyplexes were only ~340 nm. Little difference in polydispersity of BM and MS polyplexes was observed at PEI/DNA ratios of 1.8:1 (w:w) or less, but the MS polyplexes were significantly less polydisperse at DNA/PEI 2.4:1 and 3.0:1 (w:w) (Fig. 4.4B). Finally, polyplex zeta potentials were ~10 mV at PEI/DNA 0.6:1 (w:w) and increased to ~15-20 mV at higher PEI/DNA ratios (Fig. 4.4C). The zeta potential of MS polyplexes was generally more positive than BM polyplexes, but the differences were not statistically significant.

4.3.4 Determination of Free PEI in Polyplex Suspensions

The amount of free polymer present in either BM or MS polyplex formulations may be important since free PEI is known to be cytotoxic [129]. We were interested in comparing the separation device with not only BM particles, but also polyplexes produced by a microfluidic device similar to those previously reported by other groups (with a 2 cm channel for diffusion, MF2) and another device that has the same 25-cm

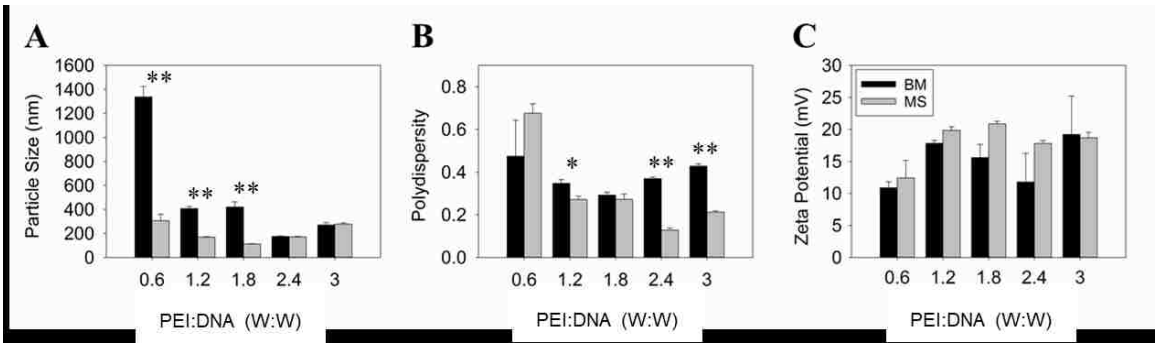

Figure 4.4: Comparison of physicochemical properties of polyplexes produced by different methods. Average particle size (A), size polydispersity (B), and zeta-potential (C) of PEI/DNA polyplexes produced either by BM or MS techniques over a range of W:W's. Error bars represent the mean ± S.E.M. (n=3). *P<0.05 and **P<0.01 for MS compared to BM polyplexes.

.

channel length as the MS device but no separation mechanism (MF25) [A.2A-A.2B] Comparing devices of different channel lengths demonstrates the role of mixing time in the production of polyplexes. The fraction of free PEI in BM, MS, MF25 and MF2 polyplex suspensions was determined by gel electrophoresis of polyplexes prepared with a fluorescently labeled PEI (PEI-AF594). This method allows for separation of the free PEI, free DNA and polyplexes. Free DNA migrates toward the cathode, polyplexes are likely too big to migrate and remain in the loading well, and the free polymer is positively charged and migrates toward the anode. By comparing the band intensities of free PEI-AF594 resulting from electrophoresis of PEI only and PEI/DNA polyplex suspensions, we can determine the amount of free polymer in the polyplexes (Fig. 4.5A).

Polyplex suspensions produced at PEI/DNA ratio of 1.8:1 (w:w) contained 57, 42, 34 and 25% free PEI for BM, MF2, MF25, and MS devices, respectively (Fig. 4.5B). Significantly less free PEI was observed in MS polyplexes compared to BM polyplexes, confirming that the separation mechanism allows for the separation of free polymer that is present in the side channels of the MS device. Additionally, MF2 polyplexes contained a larger amount of free PEI compared to MF25 polyplexes, further suggesting that the MF2 device and similar systems do not allow sufficient time for complete interaction of the PEI and DNA.

4.3.5 Transfection with BM and MS Polyplexes

Initial transfections were carried out over PEI/DNA ratios from 0.6:1 to 3.0:1 (w:w) for both BM and MS polyplexes in three model human cells lines: U-87 MG, glioblastoma; HeLa, cervical adenocarcinoma; and MDA–MB–231, breast

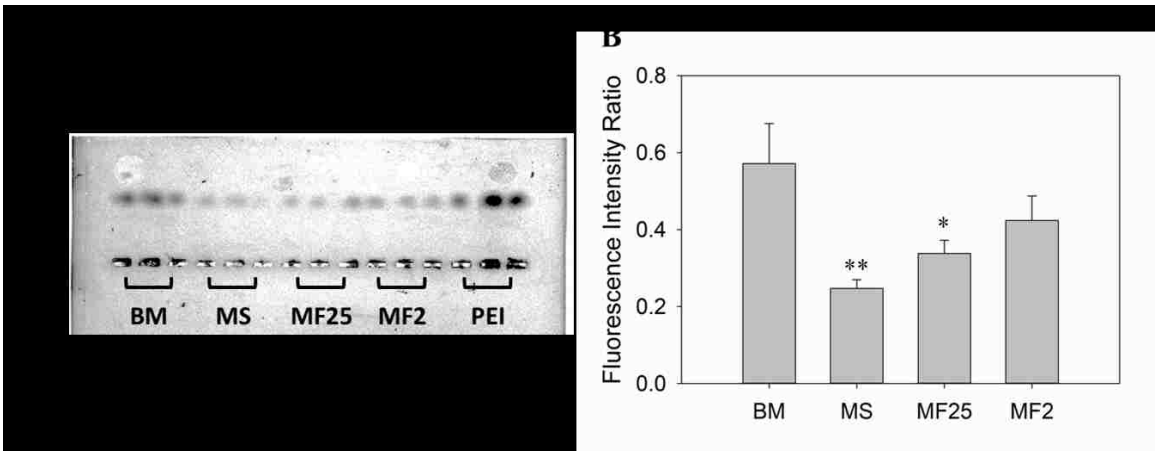

Figure 4.5: Determination of free PEI by agarose gel electrophoresis. (a) PEI-AF594 fluorescence in an agarose gel showing bands representing free PEI in samples of polyplexes (BM, MS, MF25 and MF2) and polymer only without DNA (PEI). (b) PEI-AF594 fluorescence intensities integrated over the area of the bands as a ratio to integrated band intensities of PEI only. Error bars represent the mean ± S.E.M. (n=3). *P<0.05 and **P<0.01 for sample compared to BM polyplexes

adenocarinoma. Upon transfection with BM polyplexes, the maximum transgene expression was observed at DNA/PEI ratio of 1.8:1 (w:w) for all three cell lines. For transfections with MS polyplexes, maxima were observed at PEI/DNA ratio of 1.8:1 (w:w) in U-87 MG and HeLa cells, and 1.2:1 (w:w) in MDA–MB–231 cells (Fig. 4.6). Although transfection activities of MS and BM polyplexes were similar at their respective maximal PEI/DNA ratios, with only transfections carried out in the HeLa cells exhibiting statistically significant increases in transfection efficiency, MS polyplexes exhibited slightly higher average transfection activity in most cases. Importantly, transfections with MS polyplexes were significantly more efficient than BM polyplexes at PEI/DNA = 0.6:1 (w:w), where MS polyplexes exhibited 325-, 1.5- and 6-fold increases in normalized transfection activity in comparison to BM polyplexes in U-87 MG, HeLa, and MDA–MD–231 cell lines, respectively. This result suggests that MS polyplexes at low PEI/DNA ratios may provide efficient transfection with less cytotoxicity, potentially allowing administration of a higher dose.

4.3.6 Cytotoxicity of BM and MS Polyplexes

To investigate the potential cytotoxicity of differing amounts of free PEI in BM and MS polyplexes, each of the three cell lines was transfected at various PEI/DNA ratios and cellular metabolic activity was assayed. Metabolic activity of all three cell lines decreased ~20-60% following transfections with no clear trend in cytotoxicity with PEI/DNA ratio. This may be due to the difference in amounts of free PEI at the varying PEI/DNA ratios. In general, cells transfected with MS polyplexes exhibited less cytotoxicity compared to those transfected with BM polyplexes, though the differences

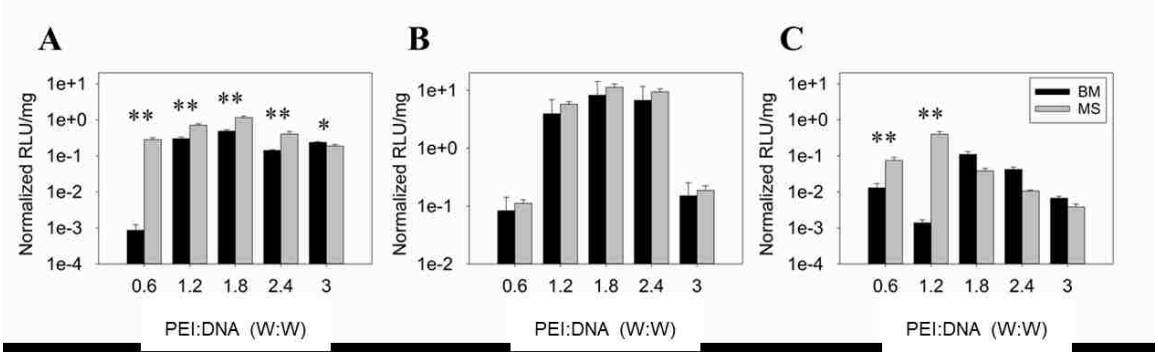

Figure 4.6: Gene expression in three cell lines. Transfection of (A) HeLa, (B) U-87 MG, and (C) MDA-MB-231 cells by PEI/DNA polyplexes assembled by bulk mixing (BM) and the microfluidic device with separation (MS). Transfection efficiency is expressed as luciferase activity mediated by polyplex transfection normalized to luciferase activity mediated by transfection mediated by Lipofectamine 2000 carried out at the same time. Error bars represent the mean ± S.E.M (n=3). *P<0.05 and **P<0.01 for MS compared to BM polyplexes at the same PEI/DNA ratio.

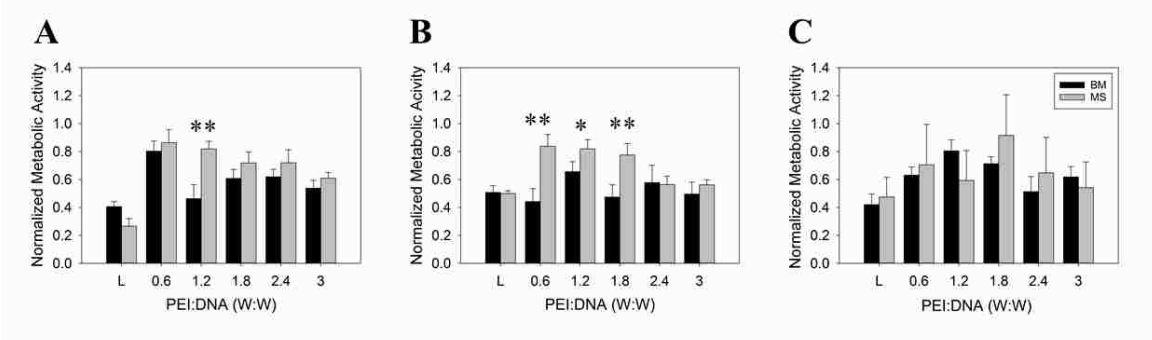

Figure 4.7: Cell viability of transfected cells. Metabolic acitivity of (A) HeLa, (B) U-87 MG, and (C) MDA-MB-231 cells following transfection with BM and MS PEI/DNA polyplexes and Lipofectamine 2000 (L) normalized to metabolic activity of untreated cells. Error bars represent the mean ± S.E.M (n=3). *P<0.05 and **P<0.01 for MS compared to BM polyplexes at the same PEI/DNA ratio

were not statistically significant in many instances (Figure 4.7). It appears likely that the reduced cytotoxicity of MS polyplexes is the result of significantly less free PEI in these formulations, as described above.

4.4 Conclusions

In summary, a microfluidic device employing a unique separation mechanism was used to fabricate PEI/DNA polyplexes for the delivery of nucleic acids. Mathematical modeling of the flow characteristics and diffusion of polymer in the device allowed prediction of fabrication parameters and inlet concentrations to produce polyplexes at desired PEI/DNA ratios and to effectively separate free PEI from the formed polyplexes. Our results indicate that the MS produced polyplexes not only have smaller particle sizes at lower PEI/DNA ratios, but additionally demonstrate enhanced transfection activity and lower cytotoxicity in comparison to polyplexes produced via BM. Additionally, the separation mechanism may allow for the production of more complex polyplex systems, such as layer-by-layer assembly of ternary polyanion/polycation/DNA polyplexes, which will be the subject of further investigation.

Chapter 5: Steps Towards Microfluidic Separation for the Production of Ternary Polyplexes

In this chapter, we will review experiments that demonstrate support for the use of the MS device for the production of ternary polyplexes. As throughout the manuscript, the primary focus of the research is the development of polymer-based non-viral gene delivery vectors that are clinically and commercially viable. Since in Chapter 4 we showed that MS-produced polyplexes demonstrated significant transfection efficiencies at lower PEI/DNA ratios, in this chapter we explore the effect of increasing the total dose of PEI/DNA polyplexes at these ratios in MS- and BM-produced polyplexes. After establishing the need for a more complex polymer system to advance towards clinical implementation, we will explore optimum molecular weights of PGA for use in transfections. As stated previously, it is unclear what molecular weights were used by Kurosaki et al [48].

5.1 Materials and Methods

5.1.1 Materials

Branched PEI with an average molecular weight of 25 kDa was purchased from Sigma-Aldrich and dissolved in phosphate buffered saline (PBS). PGA was purchased from Alamanda Polymers with molecular weights of 7.5, 15, and 30 kDa. Lipofectamine 2000 transfection reagent was purchased from Thermo Fisher. Luciferase assay system and Cell Titer-Blue cell viability assay kit were purchased from Promega. Cellular lysis

buffer was prepared as directed by the luciferase assay kit protocol. Luciferase plasmid (pGL3 control vector) was purchased from Elim Biopharmaceuticals.

5.1.2 Microfluidic Device Fabrication

Microfluidic devices were fabricated using well-established soft lithography techniques [126]. In short, channel designs were created in Autocad and printed onto a transparency to generate a photholithographic mask. A master mold was made using Microchem SU-8 3050 negative photoresist by adhering to the spin curves and processing suggested by Microchem. In short, glass slides were cleaned with acetone, ethanol and then water. The slides were then thoroughly dried with nitrogen and the photoresist was spincoated onto the slide. The depth was verified to be 100 μm with a profilometer. The slide and photoresist were then exposed to UV radiation in a mask aligner using the photolithographic mask. The slide and resist were cured for 1 h at 95 °C and then developed using Microchem SU-8 developer to yield the master mold. Dow Corning Sylgard 184 Silicone Encapsulant PDMS resin (Ellsworth Adhesives) was applied to the master mold and cured in an oven at 100 °C for 1 h. The PDMS containing the microchannels was peeled from the mold and attached to a glass microscope slide using a Harrick Basic Plasma Cleaner PDC-32G-2. In all instances microfluidic channels are rectangular with a width of 200 μm and a depth of 100 μm. A microfluidic punch was used to create holes at the inlets and outlets of the device, and tubing was pressed directly into the holes. Tubes of equal length were used at all outlets to ensure that the resistance associated with each outlet was equal.

5.1.3 Preparation of Polyplexes and Lipoplexes

BM polyplexes were generated using standard protocols. Briefly, DNA was diluted to 20 μg/mL in PBS at pH 6.8 and 0.0067 M phosphate. PEI was similarly diluted to appropriate concentrations to achieve the desired PEI:DNA ratio. Polyplexes were formed by pipetting 200 μL of PEI solution into a microcentrifuge tube containing an equal volume of DNA and mixed by briefly vortexing. Polyplexes were incubated for 20 min at room temperature. Lipofectamine 2000/DNA complexes were formed according to the manufacturers protocol. Specifically, 24 μL of Lipofectamine 2000 was diluted into 176 μL of Eagle's Minimum Essential Media (EMEM, ATCC). An equal volume of DNA (20 μg/mL in PBS) was added to the Lipofectamine 2000 solution and allowed to incubate for 5 min. For the production of binary polyplexes with MF devices, DNA was diluted to 50 μg/mL in PBS and PEI solutions were also prepared in PBS to provide the desired PEI:DNA ratios. The DNA and PEI solutions were pumped at a flow ratio of 0.2 (DNA flow rate/total flow rate) and at a total flow rate of 100 μL/min, to yield a product with the final DNA concentration of 10 μg/mL. For the production of ternary polyplexes with the MF device, a polyanionic solution of DNA and PGA was first created where the final concentration of DNA was 50 μg/mL and that of PGA was 60 μg/mL. The polyanionic and PEI solutions were pumped at a flow ratio of 0.2 (DNA flow rate/total flow rate) and at a total flow rate of 100 μL/min, to yield a product with the final DNA concentration of 10 μg/mL.

5.1.4 Transfections

HeLa (human cervical carcinoma) cells were obtained from ATCC and cultured in EMEM supplemented with 10% fetal bovine serum (VWR) at 37˚C and 5% CO_2 according to ATCC protocols. All transfections were carried out using protocols well established within the research group. Cells were seeded in 12-well plates at 100,000 cells per well 24 h prior to transfection. Growth media was removed from the cells and replaced with 1.5 mL of polyplex suspension containing 1 μg DNA per well. After 4 h, polyplexes were removed and replaced with growth media. Luciferase expression was quantified 24 h post-transfection using the Promega luciferase assay system. Luciferase activity was measured using a Biotek Synergy II plate reader. Results were normalized to total protein concentration in the lysate quantified using BCA assay (Pierce, Rockford, IL) following the manufacturers protocol.

5.1.5 Cytotoxicity

Cytotoxicity of BM and MF polyplexes was quantified using the Cell Titer-Blue viability assay (Promega). In short, cells were plated in 96-well tissue culture plates at 20,000 cells per well and transfected 24 h later following the same transfection procedure as above, substituting 10 μL of polyplex solution to accommodate the smaller wells. At 24 h post-transfection, 20 μL of the Cell Titer-Blue reagent was added to each well and incubated for 4 h. The fluorescence (ex 530 nm, em 590 nm) of each well was determined using a Biotek Synergy II plate reader.

5.2 Results

5.2.1 Dose Increase Experiments

To assess whether or not there would be an advantage in increasing the dose of binary polyplexes produced by microfluidics versus polyplexes produced by BM, we transfected HeLa cells produced by either method at a PEI/DNA weight ratio of 1.2 and at 1-, 3-, and 5-fold dose increases of DNA [Fig. 5.1]. Gene expression as assessed by luciferase assay indicated that there was more than a 10-fold increase in transgene expression for both BM and MS produced polyplexes at the highest dose in comparison to the standard dose of DNA. Cell viability experiments revealed that as the dose of DNA increased for either polyplex formulation method, cell viability also increased. In the case of BM-produced polyplexes, the viability increased from ~80% at the standard dose to ~98% at the 5X dose. For the case of MS-produced polyplexes, the viability increased from ~96% at the standard DNA dose to ~100% at the 5X dose.

5.2.2 Optimizing PGA Molecular Weight for Polyplex Formulations and Probing Premixed Polyanions for TP Production

To optimize for PGA molecular weight, a set of transfections was carried out in HeLa cells to determine the transgene expression mediated by TPs comprising PEI, DNA, and PGA of three molecular weights – 7.5, 15, and 30 kDa. TPs were formulated both by bulk mixing and MF mixing in the 2MF channel [4.3.4] [Fig. 5.2]. Importantly in the case of the 2MF device the DNA and PGA are premixed and then the mixture is pumped through the device where and the PEI is introduced. This experiment serves to

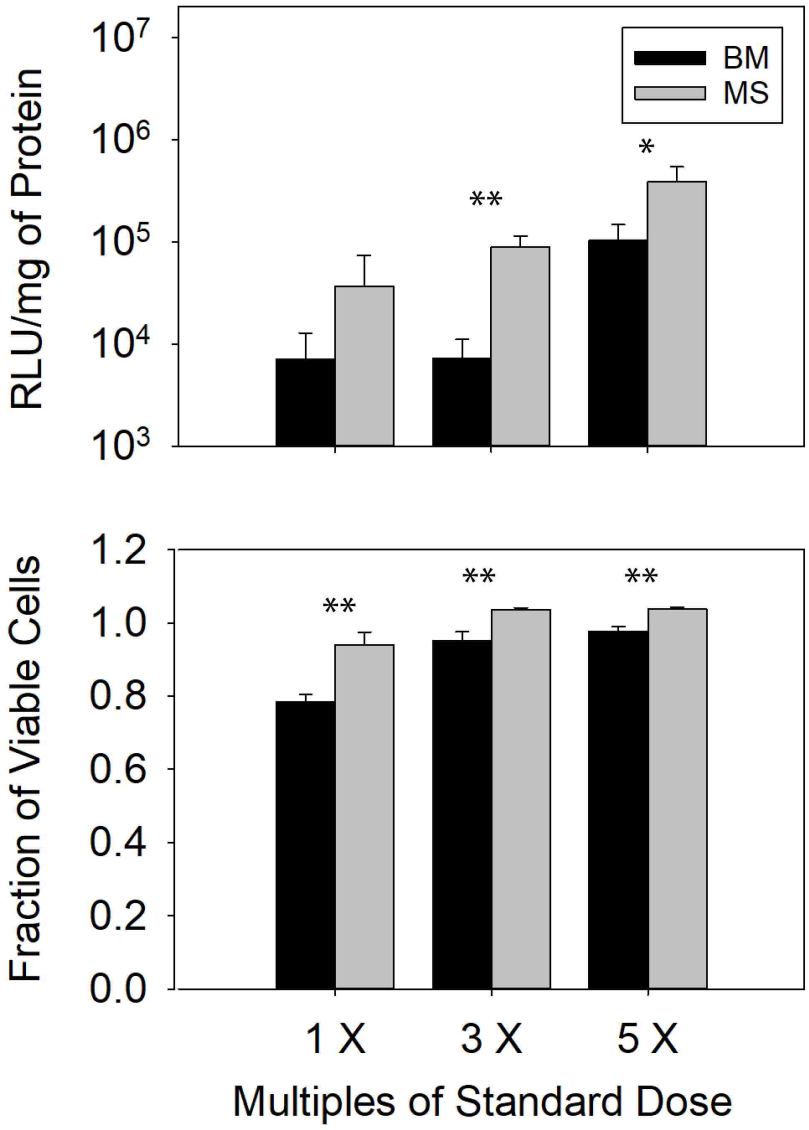

Figure 5.1: Transfections of HeLa cells carried out at 1-, 3-, and 5-times the standard dose of 1 μg of DNA with TPs produced either by BM or MS methods. The gene expression activity (A) and cell viability (B) of each transfection dose are reported. Error bars represent the mean ± S.E.M. (n=3). *P<0.05 and **P<0.01 for MS compared to BM polyplexes.

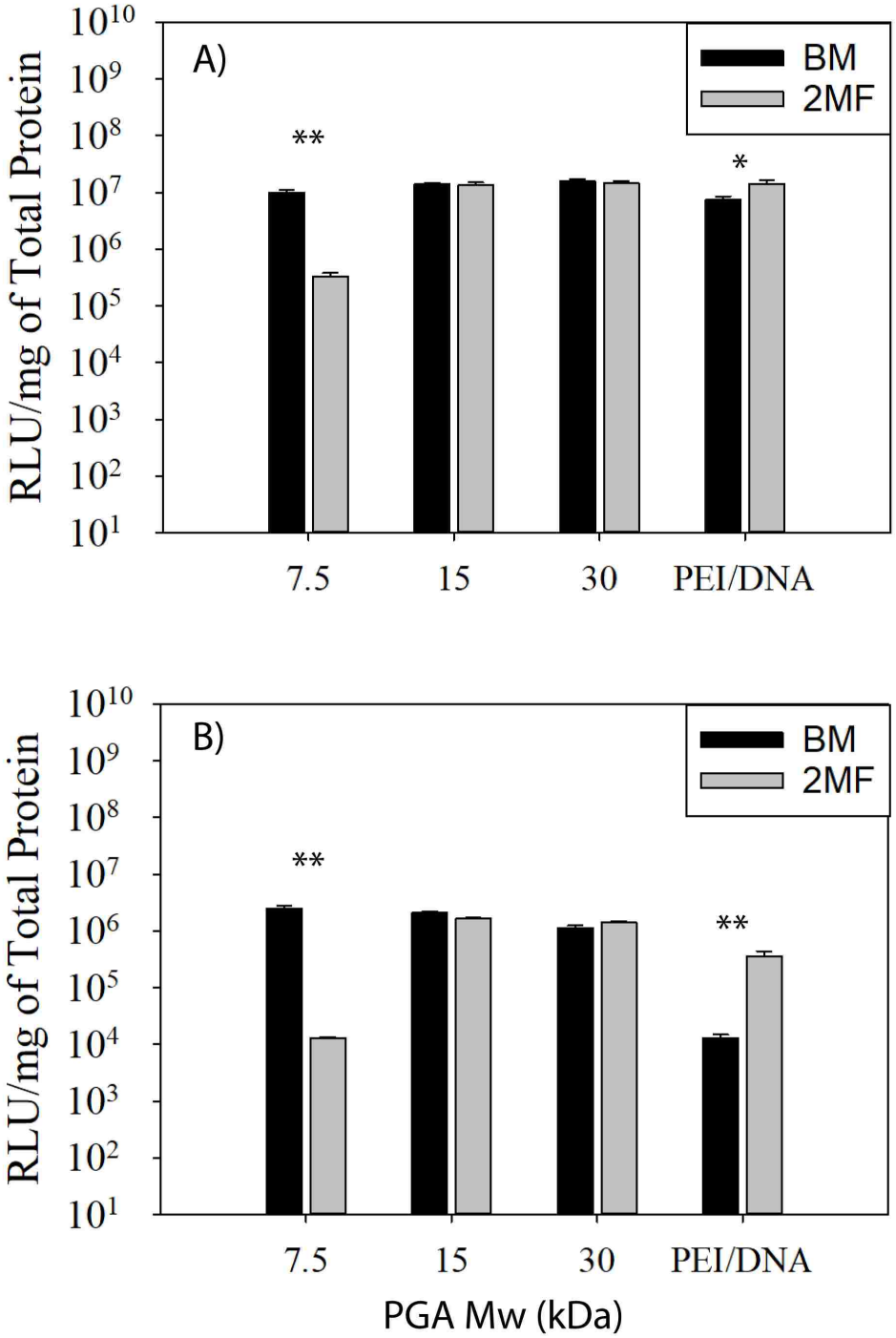

Figure 5.2: Comparing transfections of HeLa cells with TPs formed by BM and the 2MF device in serum free media (A) and media containing serum (B). PEI/DNA ratio is set to 1.8 throughout and the PGA/DNA ratio is set to 1.2 where applicable. Error bars represent the mean ± S.E.M. (n=3). *P<0.05 and **P<0.01 for 2MF compared to BM polyplexes.

demonstrate whether or not the Wang mixing method [Fig. 5.3], where PGA and DNA are premixed and PEI is then added to the resulting mixture, is advantageous for the microfluidic production of polyplexes in comparison to conventional BM polyplexes [13]. The experiments were carried out both in serum-free media and media containing serum at a PEI/DNA weight ratio of 1.8 and a PGA/DNA weight ratio of 1.2. In the case of the BM formulations, transfections carried out in serum-free media showed no significant difference in transgene expression between polyplexes containing PGA of different molecular weights [Fig. 5.2A]. For the MF formulation method, transfections carried out in serum-free media showed ~30-fold decrease in transfection efficiency for TPs comprised of 7.5 kDa PGA compared to 15 and 30 kDa PGA [Fig. 5.2A]. TPs comprised of the two larger molecular weight PGA demonstrated gene expression with no significant difference between the gene expression of the two formulation methods [Fig. 5.2A]. Similar results were noted in the case of transfections carried out in media containing serum, with BM formulations demonstrating no difference in gene expression levels over the range of PGA molecular weights and MF formulations exhibiting a 200-fold decrease in gene expression for 7.5 kDa PGA, and no significant difference between the other two PGA molecular weights [Fig. 5.2A].

5.3 Discussion

Previous reports of MF-produced polyplexes suggested that, since higher gene delivery efficiency was noted at lower polymer/DNA ratios and higher toxicity is associated with excess PEI, MF production of binary polyplexes followed by transfecting cells with a higher dose of the MF-produced polyplexes might provide an avenue to

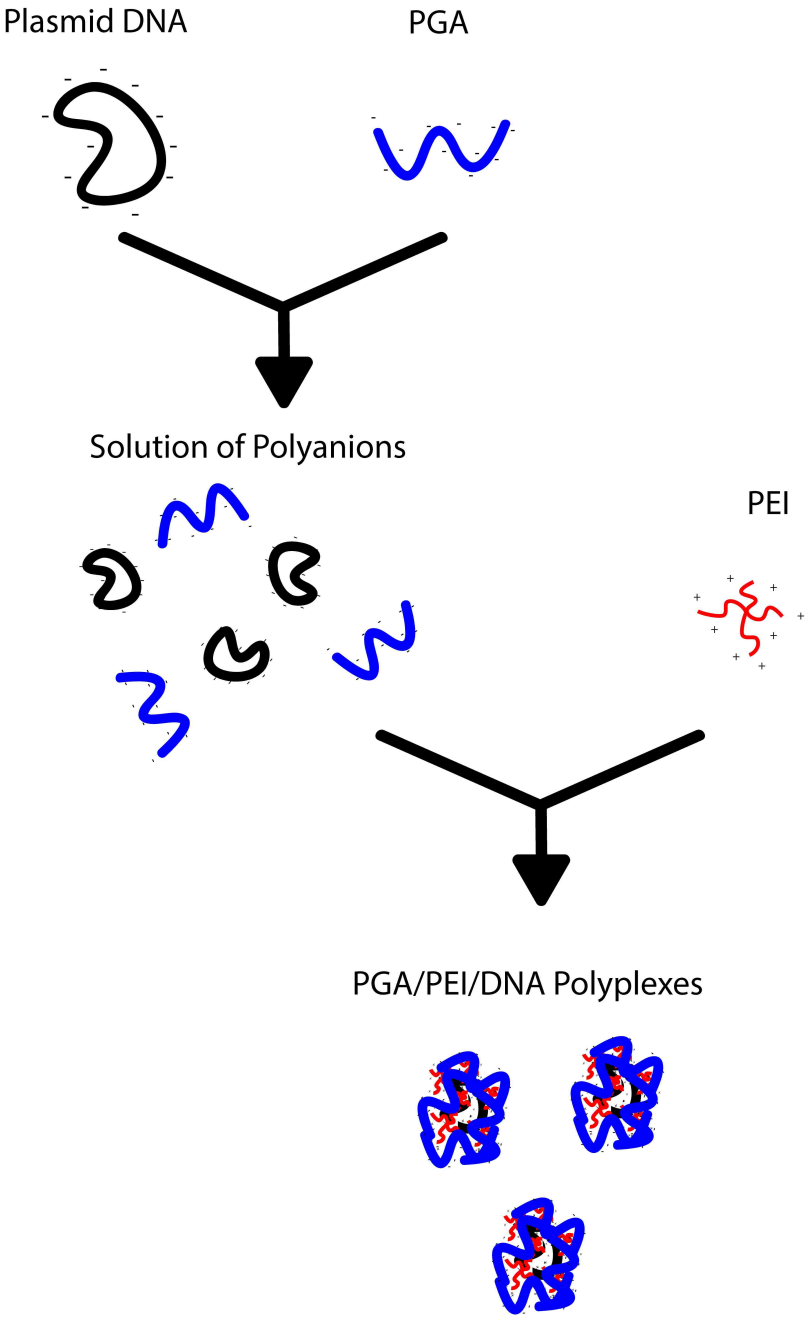

Figure 5.3: Schematic of the mixing method used by Wang et al. where DNA and PGA are premixed and the resulting anionic solution is mixed with PEI to produce TPs.

increase gene delivery efficiency while simultaneously mitigating cytotoxicity [16]. Our results confirm that MF-produced polyplexes tend to allow for significantly increased transfection at these low doses compared to BM-produced polyplexes. However, when comparing polyplexes produced by the two methods, there was no difference in cytotoxicity at the higher doses. This result suggests that while MF production of polyplexes does provide an enhancement to transfection at low doses, the additional advantage of decreased cytotoxicity is not present.

Seeking to shed light on the effect of PGA molecular weight on TP transfection activity, we optimized transfections for PGA molecular weight for two different mixing methods both in serum-free media and media containing serum. In this case it was noted that PGA molecular weight seemed to have no effect on polyplex transfection activity of BM polyplexes. However, in the case of MF mixing it was shown that lower molecular weight PGAs performed poorly, demonstrating decreased transfection activity. Due to these results, further experimentation with TPs produced by microfluidic systems will employ PGA with a molecular weight of 15 kDa. Additionally, it was shown that combining the Wang TP mixing method and fabricating the polyplexes in a device similar to that used by Koh et al. led to no enhancement of gene transfection activity, a result that suggests that further device development would be necessary for the MF production of TPs.

5.4 Conclusions

In this chapter, we explored the effect of dose increases on gene delivery levels in HeLa cells transfected with binary polyplexes produced by two different methods. It was

shown that while enhanced transgene expression was observed at standard doses of the polyplexes, increased dosing showed no advantage in terms of cellular toxicity. It was also shown that transfecting with TPs produced by PGAs of varying molecular weights had a minimal impact on transgene expression associated with TPs produced by BM. In the case of MF-produced TPs, however, we presented strong evidence suggesting that a PGA with molecular weights of 15 kDa or above would be better for increased transfection activity. Finally, while it is tempting to directly employ the Wang mixing method for TP production and Koh device for polyplex assembly, combining these two methods gave no advantage in terms of gene delivery efficiency.

Chapter 6: Assembly of Charge-Shielding Polyglutamic acid/Polyethylenimine/DNA Ternary Polyplexes in a Microfluidic Device

Ternary polyanion/polycation/DNA polyplexes provide advantages over more conventional binary polyplexes by allowing for increased stability of the polyplexes in serum through reduced interactions with proteins that are prevalent in the media. These vectors, however, are still limited by low gene delivery efficiency and batch to batch variation when the vectors are produced by conventional methods. To improve the effectiveness of non-viral gene delivery vectors, ternary polyplexes were fabricated through the use of microfluidic devices. Comprised of plasmid DNA (DNA), polyethyleneimine (PEI) and α-polyglutamic acid (PGA), the vectors have demonstrated charge shielding and cell-targeting properties enabling prolonged stability in serum containing media and thus enhanced transfection efficiencies in these environments. Here we have developed a microfluidic separator (MS) capable of separating free PEI from polyplexes and sequential microfluidic mixer (SMF) for introducing polymers of alternating charge in sequence. The use of a MS in the production of the polyplexes is shown here to increase transfection activity by 24- and 35-fold in comparison to either conventional bulk mixing (BM) or a sequential microfluidic mixer (SMF) methodologies in MDA-MB-231 cells at an optimized PGA/DNA weight ratio of 1.2. A key result is the removal of free PEI with the MS system and thus the removal PEI/PGA "ghost" particles from the mixture, which exhibit no transfection activity due to their lack of genetic material.

6.1 Introduction

By allowing for the production of therapeutic proteins at affected tissue sites and other relevant locations throughout the body, gene therapy shows considerable promise as a treatment for many diseases [130]. Researchers have explored a variety of gene delivery vectors in search of the ideal delivery method, which would exhibit high gene delivery efficiency while simultaneously being shown to be safe. By packaging genetic material with recombinant viruses [36], cationic polymers [45], lipids [43], metallic nanoparticles [62], and combinations of the above [131,132], a variety of vectors have been produced. Cationic polymers, such as PEI, form complexes with DNA, which have been shown to protect the DNA from enzymatic degradation, associate with cellular membrane, and allow for endosomal escape through the proton sponge effect [1].

Poor serum stability, however, is still a significant issue negatively impacting the clinical implementation of cationic non-viral vectors since it hinders systemic administration of the drugs. Aggregation due to association with negatively charged serum proteins leads to large particles, which demonstrate poor transfection ability in a wide variety of cell lines in vitro as well as mouse models in vivo [13]. Charge shielding, accomplished by coating a polyplex with a biocompatible polyanion, hinders binding of serum proteins and the resulting aggregation, thus maintaining transfection ability of polyplexes in serum-containing media as well as in vivo. In addition to charge shielding, ternary polyplexes (TPs) allow for the creation of more complex vectors that can overcome multiple barriers to cell delivery. Important mechanisms that enable the vectors to overcome cellular barriers to delivery that have been demonstrated include charge conversion [51,52], membrane disruption [14], cell-specific targeting [64,66], pH- and

light-induced chemical bond degradation [57,59] and some combinations of the above [55,67]. With broad applicability to enhance non-viral gene therapy, TPs present an opportunity to move non-viral vectors toward clinical viability.

A significant problem facing assembly of TPs and conventional polyplexes is the variability associated with mixing of the constituent materials. For example, Wang et al. [13] and Kurosaki et al. [48] report widely varying particle sizes for two PGA/PEI/DNA polyplex systems. Microfluidic hydrodynamic flow focusing has been demonstrated as potential method for standardizing vector formulation and allowing for consistent polyplexes from batch-to-batch and also between different labs [16,17]. In Chapter 3, I described the design, fabrication, and validation of a microfluidic system for the production of conventional PEI/DNA polyplexes and importantly the removal of free PEI from the product.

Here we report the first use, to our knowledge, of a microfluidic system for the production of ternary polyplexes. By comparing polyplexes produced by bulk mixing (BM), by a microfluidic device capable of separating free PEI from polyplexes (MS), and sequential microfluidic diffusive mixing (SMF) where PEI and PGA are hydrodynamically focused with DNA in sequence, we demonstrate the advantages of using MS in the production of PGA/PEI/DNA ternary polyplexes. We will compare the transfection efficiency, physicochemical properties, and toxicity of polyplexes produced by each method in serum free and serum-containing media. We will additionally probe cellular uptake and analyze the resulting ghost particle concentration for each method.

6.2 Materials and Methods

6.2.1 Materials

Branched PEI with an average molecular weight of 25 kDa was purchased from Sigma-Aldrich and dissolved in phosphate buffered saline (PBS). PGA with a molecular weight of 15 kDa was purchased from Alamanda Polymers. Lipofectamine 2000 transfection reagent was purchased from Thermo Fisher. Luciferase assay system and Cell Titer-Blue cell viability assay kit were purchased from Promega. Luciferase plasmid (pGL3 control vector) was purchased from Elim Biopharmaceuticals.

6.2.2 Microfluidic Device Fabrication

Microfluidic devices were fabricated using well-established soft lithography techniques [126]. In short, channel designs were created in Autocad and printed onto a transparency to generate a photholithographic mask. A master mold was made using Microchem SU-8 3050 negative photoresist by adhering to the spin curves and processing suggested by Microchem. In short, glass slides were cleaned with acetone, ethanol and then water. The slides were then thoroughly dried with nitrogen and the photoresist was spincoated onto the slide and the depth was verified to be 100 μm with a profilometer. The slide and photoresist were then exposed to UV radiation in a mask aligner using the photolithographic mask. The slide and resist were then cured for an hour at 95 °C and then developed using Microchem SU-8 developer to yield the master mold. Dow Corning Sylgard 184 Silicone Encapsulant PDMS resin (Ellsworth Adhesives) was then applied to the master mold and cured in an oven at 100 °C for one hour. The PDMS containing the

microchannels was then peeled from the mold and attached to a glass microscope slide using a Harrick Basic Plasma Cleaner PDC-32G-2. In all instances microfluidic channels are rectangular with a width of 200 μm and a depth of 100 μm. A microfluidic punch was used to create holes at the inlets and outlets of the device, and tubing was pressed directly into the holes. Tubes of equal length were used at all outlets to ensure that the resistance associated with each outlet was equal.

6.2.3 Preparation of Polyplexes and Lipoplexes

BM polyplexes were generated using standard protocols. Briefly, DNA was diluted to 30 μg/mL in PBS (6.7 mM phosphate, pH 6,8). PEI was diluted to 54 μg/mL to yield PEI/DNA polyplexes at a PEI/DNA ratio of 1.8 (w:w). PGA was similarly diluted to appropriate concentrations to achieve the desired polymer:DNA ratios. Polyplexes were formed by pipetting 200 μL of PEI solution into a microcentrifuge tube containing an equal volume of DNA and mixing briefly by vortexing. Polyplexes were then incubated for 20 min at room temperature. After the incubation period, 200 μL of PGA was added to the PEI/DNA polyplex solutions at appropriate concentrations to achieve the desired PGA/PEI/DNA ratios. Lipofectamine 2000/DNA lipoplexes were formed according to the manufacturer's protocol. Specifically, 24 μL of Lipofectamine 2000 was diluted into 176 μL of Eagle's Minimum Essential Media (EMEM). An equal volume of DNA (20 μg/mL in PBS) was added to the Lipofectamine 2000 solution and allowed to incubate for 5 min.

For the production of polyplexes with the MS device, DNA was diluted to 22.5 μg/mL in PBS and PEI solutions were also prepared in PBS at a concentration of 40.5

μg/mL. The DNA and PEI solutions were pumped at a flow ratio of 0.2 (DNA flow rate/total flow rate) and at a total flow rate of 100 μL/min, to yield a 400 μL of product with the final DNA concentration at 15 μg/mL. The resulting polyplexes were immediately mixed with 200 μL of PGA at the appropriate concentrations to achieve the desired PGA/PEI/DNA ratios, final DNA concentration of 10 μg/mL, and allowed to incubate for 20 min at room temperature. For the production of polyplexes with the SMF device, initial DNA dilutions were made in PBS at a concentration of 200 μg/mL and initial PEI dilutions were made at a concentration of 112.5 μg/mL. The DNA was pumped at a flow rate of 20 μL/min, the PEI solution was pumped at a rate of 80 μL/min and the PGA solution was pumped at a rate of 400 μL/min resulting in two hydrodynamic focusing regions both at FR = 0.2. The final DNA concentration in this case was also 10 μg/mL.

6.2.4 Transfections

HeLa (human cervical carcinoma), U-87 MG (human glioblastoma) and MDA–MB–231 (human breast carcinoma) cell lines were obtained from ATCC and cultured in Eagle's minimum essential media (EMEM, ATCC) supplemented with 10% fetal bovine serum (VWR) at 37 ˚C and 5% CO_2 according to ATCC protocols. All transfections were carried out using protocols well established within the research group. Cells were seeded in 24-well plates at 200,000 cells per well 24 h prior to transfection. Growth media was removed from the cells and replaced with 1.5 mL of polyplex suspension containing 1 μg DNA per well. After 4 h, polyplexes were removed and replaced with growth media. Luciferase expression was quantified 24 h post-transfection using the Promega luciferase

assay system. Luciferase activity was measured using a Biotek Synergy II plate reader. Results were normalized to total protein concentration in the lysate quantified using BCA assay (Pierce, Rockford, IL) following the manufacturers protocol. In the case of transfections carried out in media containing serum, the same procedure as above was followed but with serum containing media throughout.

6.2.5 Polyethylenimine Labeling

Polymers were labeled with Alexa Fluor 488 by mixing 1 mg of an Alexa Fluor NHS-ester in 200 μL of anhydrous DMSO with 10 mg of PEI in 1.8 mL of 0.2 M sodium carbonate, pH 9.3. The reaction was allowed to run for 12 h with gentle mixing at room temperature and shielded from light to prevent photobleaching. The labeled polymer was separated from unreacted dye by dialysis using a Spectra Por dialysis tubing with molecular weight cutoff of 10 kDa against 4 L pure water exchanged three times over a 24 h period. The resulting PEI-AF488 solution was lyophilized, weighed and then diluted into PBS to be used as a stock solution. Labeling density was determined to be 0.5 dyes per polymer chain.

6.2.6 Cytotoxicity

Cytotoxicity of BM and MF polyplexes was quantified using the Cell Titer-Blue viability assay (Promega). In short, cells were plated in 96-well tissue culture plates at 20,000 cells per well and transfected 24 h later following the same transfection procedure as above, substituting 10 μL of polyplex solution to accommodate the smaller wells. At 24 h post-transfection, 20 μL of the cell titer blue reagent was added to each well and

incubated for 4 h. The fluorescence (ex 530 nm, em 590 nm) of each well was determined using a Biotek Synergy II plate reader.

6.2.7 Particle Characterization

Particle size, zeta potential and polydispersity were determined using a Malvern Zetasizer Nano ZS. Polplyexes were produced as described above. The resulting solution (600 μL) was then diluted by addition of 300 μL deionized water and immediately added to Malvern Folded Capillary Zeta Cell. Each measurement was performed in triplicate.

6.2.8 Flow Cytometry

Plasmid DNA was first incubated with YOYO-1 at a volume/weight ratio of 15 nL YOYO-1 per 1 μg of DNA at 4 °C for 30 min. Ternary polyplexes were formed with both alexa-labeled and unlabeled PEI, unlabeled PGA, and YOYO-1 intercalated DNA using each of the three methods described above (BM, SMF, MS). Each of the three cell lines were cultured as described above and plated in 24-well plates at $7.5x10^4$ cells/well 24 h prior to transfection. 50 μL of polyplex solution was then added to vials containing 700 μL of either serum-free or serum-containing media and the resulting solution was then added to each well resulting in 0.5 μg plasmid/well. To remove surface-bound polyplexes, the cells were rinsed twice with 0.001% SDS in PBS and PBS two hours after transfection. 250 μL of 0.05% trypsin in PBS was then added to each well and the cells and trypsin were allowed to incubate for 5 min. After the cells were dislodged from the plate, 50 μL of FBS was added to each well and the cells were centrifuged at 6400 rpm for 5 min. The supernatant was aspirated and discarded, after which the resulting cell

pellet was resuspended in 1 mL of PBS. Each of the samples was then placed in a 15 mL centrifuge tube and ready for FACS analysis by an Attune flow cytometer and the data was processed using FloJo software.

6.2.9 Fluorescence Correlation Spectroscopy (FCS)

Employing a commercial dual-channel confocal spectrometer (ALBA FFS system, ISS, Champaign, IL), fluorescence intensity-fluctuation data was collected. A 488 nm laser diode was used as an excitation source and was passed through a 514 nm long pass edge filter before detection. A Nikon Ti-U microscope (60x/1.2 NA water immersion objective lens) was used to direct excitation light to the experimental samples, while two Hamamatsu H7422P-40 photomultiplier tubes assessed the emission signal. The dimensions of the confocal volume were determined by using rhodamine 110 (R110) as a standard at known concentrations with a diffusion coefficient of D = 440 ($\mu m^2 s^{-1}$). The results are reported as an average of 9 measurements in different positions within the sample to ensure solution homogeneity and sample times were 30 seconds in all cases. The FCS data was analyzed using Vista Vision Software (ISS Champagne, IL) to determine the diffusion coefficients. PEI was labeled with AlexaFlour 488 as described above and diluted to a final concentration of 100 μg/mL for the uncomplexed PEI samples. For BM, SMF, and MS samples the final concentration of DNA is the same as for transfections at 10 μg/mL and a PGA/PEI/DNA ratio of 1.2/1.8/1.0.

6.3 Results

6.3.1 Device Design

A previous device that was developed by our group, discussed in detail in Chapter 4, for the production of PEI/DNA polyplexes incorporating a unique separation mechanism for the removal of free PEI was employed as a first step in the production of ternary polyplexes. A problem commonly encountered in the assembly of ternary polyplexes is the formation of "ghost" particles, complexes of free PEI remaining the binary polyplex suspension and the polyanion, which contain no DNA [133]. Assembly of PEI/DNA polyplexes in a MS device, which removes free PEI, is expected to yield fewer ghost particles when the binary polyplexes are mixed with a polyanion. In addition, we compared TPs assembled in this fashion with TPs produced in a SMF device, which introduces PEI and DNA to form binary polyplexes similar to previously reported devices and subsequently introduces PGA on the same microfluidic device after the PEI and DNA polyplexes have come into contact [16,17] [Fig. A.3]. In this case the channel lengths in which diffusion can occur are much shorter than that of the MS device and comparable to previously reported devices. Fluorescence microscopy of the SMF device shows that two distinct diffusion interfaces are formed by the device [Fig: A.4].

6.3.2 Physicochemical Properties of Ternary Polyplexes

Particle size and zeta potential of polyplexes formed by each of the formulation methods at a PEI/DNA ratio of 1.2:1 (w:w) and over PGA/DNA ratios from 0.6:1 to 3.0:1 (w:w) are shown in Figure 6.1. Particle sizes measured upon formation of the

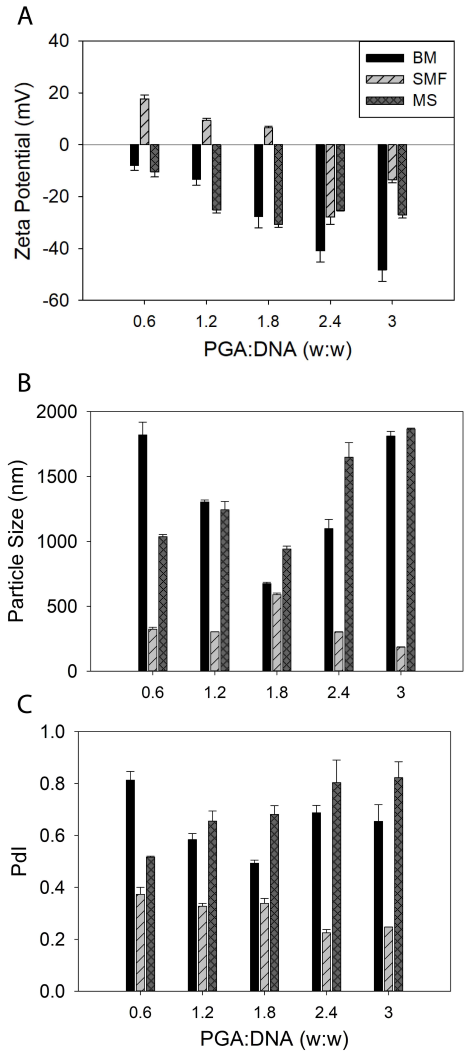

Figure 6.1: Comparison of physicochemical properties of TPs produced by different methods. average particle sizes (A), size polydispersity (B), and zeta-potential (C) of PGA/PEI/DNA polyplexes produced either by BM , SMF, or MS techniques over a range of W:W's. Error bars represent the mean ± S.E.M. (n=3). *P<0.05 and **P<0.01 for MS compared to BM polyplexes.

PGA/PEI/DNA polyplexes by the MS device were not significantly different from polyplexes produced by bulk mixing, ranging from 650 – 1800 nm. Particle sizes observed when PGA/PEI/DNA polyplexes were produced by the SMF device were smaller than those produced by either of the other mixing methods, ranging from 10 – 100 nm. The similarity in particle sizes between BM and MS polyplexes may be attributed to the subsequent bulk mixing of the MS polyplexes to create ternary polyplexes, since the polyanionic coating is added in a non-controlled manner. The smaller particle sizes observed with the SMF produced polyplexes is likely due to the presence of a significant amount of ghost particles produced by the interaction of PEI and PGA before the PEI can diffuse into the DNA-containing stream.

Zeta potentials of PGA/PEI/DNA TPs produced by BM ranged from -8 mV – -50 mV, becoming increasingly negative as the amount of PGA in the complexes increased (Figure 6.1C). The minimum zeta potential was -42 mV at PGA/DNA ratio 3:1 (w:w) as would be expected. Similarly, the zeta potential of the MS-produced polyplexes grew increasingly negative with increasing amounts of PGA. However, the minimum value in this case plateaued at approximately -30 mV at PGA/DNA ratio 1.2:1 (w:w). For TPs fabricated in the SMF device, the zeta potentials ranged from +15 to -30 mV, and negatively charged particles were not observed until PGA/DNA ratio of 2.4 (w:w).

6.3.3 Transfection with PGA/PEI/DNA Ternary Polyplexes

TPs produced by all three formulation methods were used to transfect HeLa, MDA-MB-231 and U-87 MG cell lines, in both the absence and presence of serum. The PGA/PEI/DNA ternary polyplexes were assembled at a fixed PEI/DNA ratio of 2:1

(w:w), while the PGA/DNA ratio was varied from 0:1 to 3:1 (w:w). In the absence of serum, the MS-produced polyplexes, at all PGA/DNA ratios, mediated significantly increased transgene expression compared to either of the other two methods in HeLa and MDA-MB-231 cells. Maximum differences in transgene expression mediated by TPs fabricated by the MS device, compared to BM and the SMF device, were observed at PGA/PEI/DNA ratio of 0.6:2:1 and 1.2:2:1 (w:w:w) in HeLa and MDA-MB-231 cells, respectively. MS-produced TPs exhibited 2.2- and 23-fold increases in transgene expression in comparison to BM TPs in HeLa and MDA-MB-231 cells, respectively at the optimum ratios. SMF-produced polyplexes showed significantly decreased transgene expression compared to TPs produced by either of the other two methods at all ratios for the HeLa and MDA-MB-231 cell lines. Significant drops in gene expression for the SMF-produced TPs was also noted for the case of U87-MG cells at PGA:DNA ratios above 0.6.

Similar results to the serum-free transfections were observed with those carried out in serum containing media, with the notable difference being the large increase in transfection activity for the TPs in comparison to PEI/DNA polyplexes. MS-produced polyplexes showed significantly greater transgene expression compared to both BM- and SMF-produced polyplexes in both HeLa and MDA-MB-231 cells, while no increases in transgene expression were observed in the U-87 MG cell line. In the case of transfections carried out in media containing serum, the highest gains in gene expression, when comparing BM to MS produced polyplexes, were observed at w/w's of 1.8 for both cell lines with a 3.3- and 12-fold increase for HeLa and MDA-MB-231 cell lines respectively.

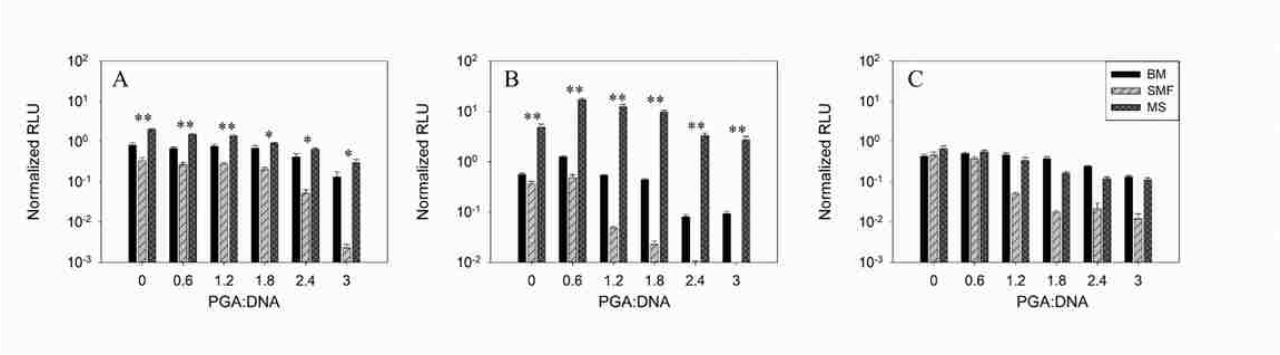

Figure 6.2: Serum-free transfections of three cell lines with TPs produced by different methods. Transfection of (A) HeLa, (B) MDA-MB-231, and (C) U-87 MG cells by PGA/PEI/DNA polyplexes assembled by BM, SMF, and MS techniques in serum-free media. Transfection efficiency is expressed as luciferase activity mediated by polyplex transfection normalized to luciferase activity mediated by transfection mediated by Lipofectamine 2000 carried out at the same time. Error bars represent the mean ± S.E.M (n=3). *P<0.05 and **P<0.01 for MS compared to BM polyplexes at the same PGA/DNA ratio.

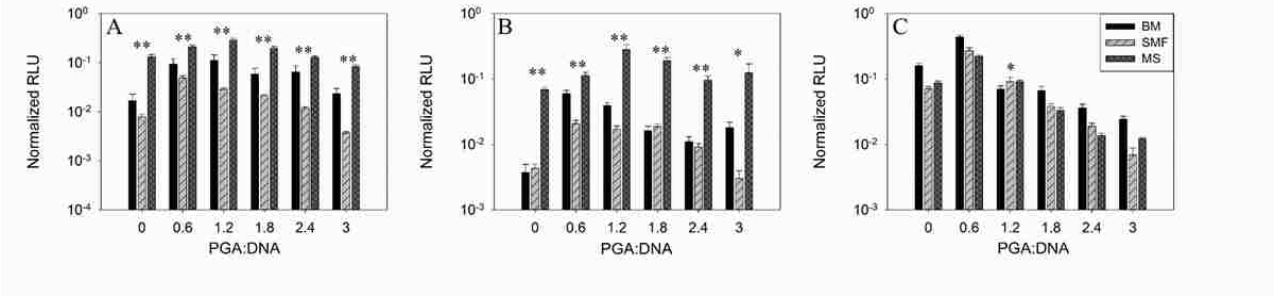

Figure 6.3: In serum transfections of three cell lines with TPs produced by different methods. Transfection of (A) HeLa, (B) MDA-MB-231, and (C) U-87 MG cells by PGA/PEI/DNA polyplexes assembled by BM, SMF, and MS techniques in media containing 10% FBS. Transfection efficiency is expressed as luciferase activity mediated by polyplex transfection normalized to luciferase activity mediated by transfection mediated by Lipofectamine 2000 carried out at the same time. Error bars represent the mean ± S.E.M (n=3). *P<0.05 and **P<0.01 for MS compared to BM polyplexes at the same PGA/DNA ratio.

6.3.4 Cellular Internalization of Ternary Polyplexes

To assess the relative amounts of TPs internalized by the cells, transfections were carried out in HeLa, MDA-MB-231 and U-87 MG cell lines with TPs containing fluorescently labeled DNA at their optimal PGA/PEI/DNA ratios, and fluorescence resulting from internalized TPs was quantified by flow cytometry. In this case only the optimum w/w's for gene expression were tested and the transfections were carried out in serum-free media. Interestingly, SMF-produced TPs exhibited the highest cellular uptake in the HeLa and U-87 MG cell lines, while in both cases these same polyplexes showed significantly reduced transfection efficiency in comparison to TPs fabricated using the other two methods. MS-produced TPs demonstrated significant increases in uptake in comparison to BM-produced polyplexes in both HeLa and MDA-MB-231 cell lines and no significant increase in the U-87 MG cell line. Uptake was 20% and 10% higher for the MS-produced TPs in comparison to the BM produced TPs in these two cell lines.

6.3.5 Cytotoxicity of Ternary Polyplexes

Cytotoxicity was as assessed by measuring cellular metabolic activity in all three cell lines after transfection with TPs produced by the three different methods at a PGA/PEI/DNA ratio of 1.2:2:1 (w:w:w) in media containing serum and serum-free media. In the absence of serum, MS-produced TPs demonstrated greater cell viability than both BM- and SMF-produced polyplexes in the HeLa and U87-MG cell lines.

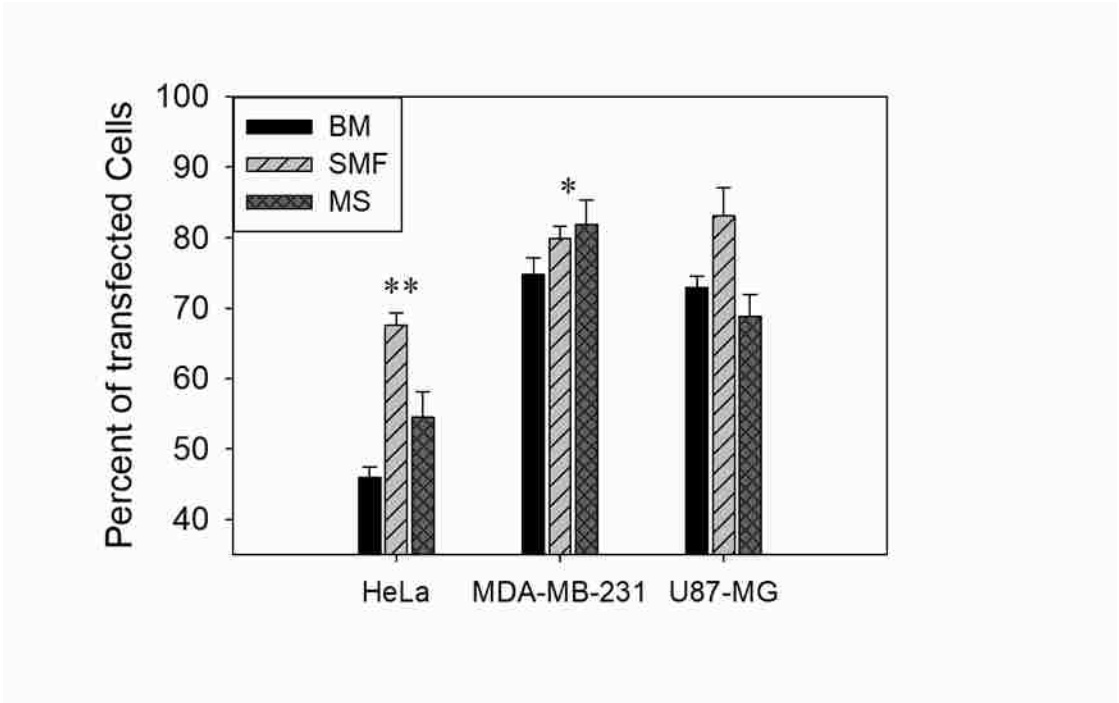

Figure 6.4: Cellular uptake analysis of TPs produced by different methods on HeLa cells. Flow cytometry data to probe cellular uptake of the TPs at PGA/PEI/DNA ratio of 1.2/1.8/1 for HeLa, MDA-MB-231 and U87-MG cell lines. Error bars represent the mean ± S.E.M (n=3). *P<0.05 and **P<0.01 for MS compared to BM polyplexes

.

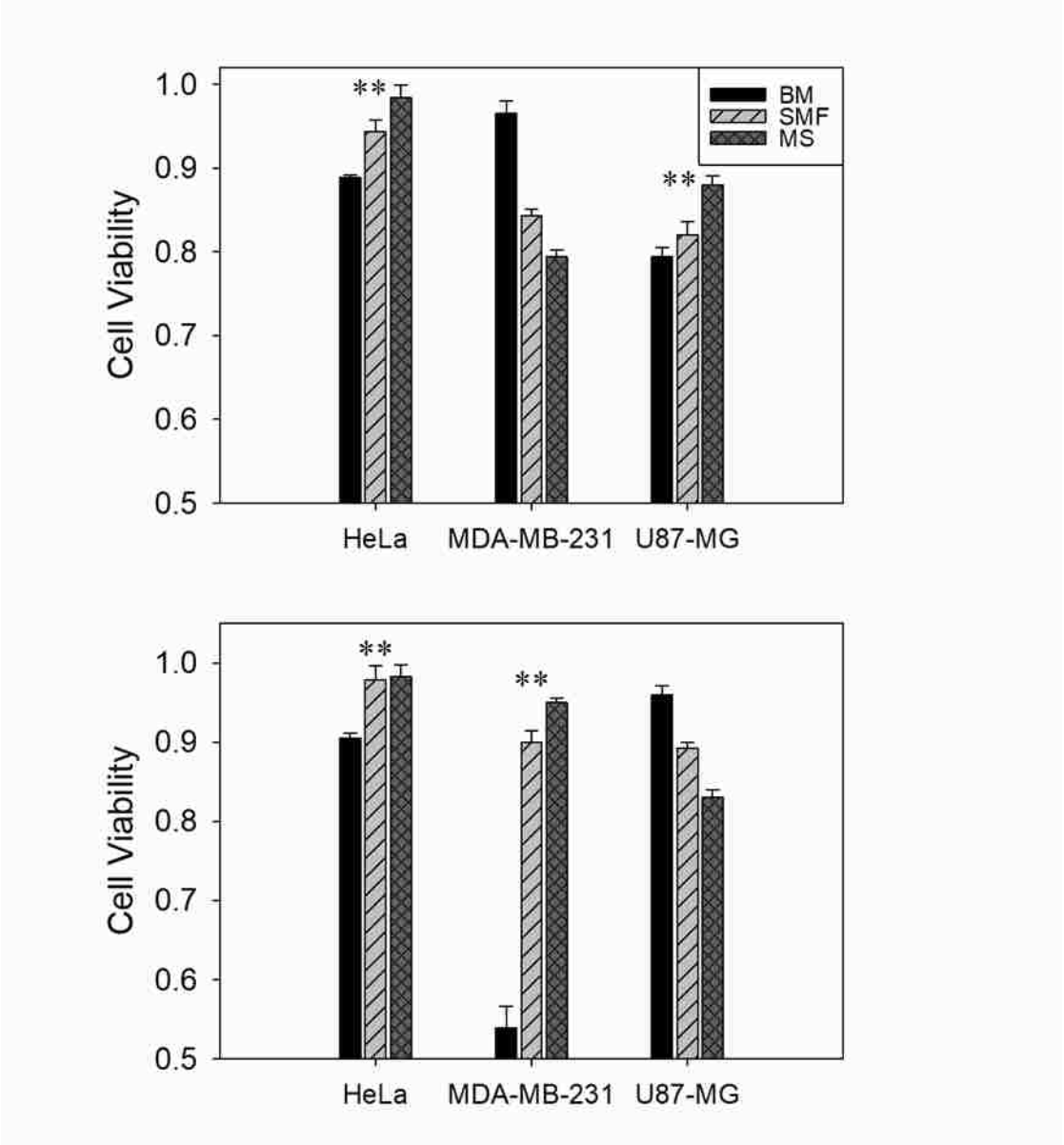

Figure 6.5: Cell viability as assessed by cell titer blue assay on HeLa, MDA-MB-231, and U87-MG cells both in serum-free (A) and Serum containing (B) media. Data expressed as percent of untreated control. Error bars represent the mean ± S.E.M (n=3). *P<0.05 and **P<0.01 for MS compared to BM polyplexes.

6.3.6 Determination of Free Polymer and Ghost Particles in Ternary Polyplex Suspensions

By measuring the fluorescence fluctuations emitted from labeled molecules moving in and out of the confocal volume, fluorescence correlation spectroscopy (FCS) allows for the determination of the diffusion coefficient of particle within a sample. The confocal detection optics, excitation volume of the focused laser beam, and characterizing the measurements against a standard of known diffusion constant (R110) gives a fixed effective illumination volume. The measured fluctuations are then compared after a lag time τ for similarity by calculating the normalized cross correlation G(τ):

$$G(\tau) = 1 + \frac{\langle \delta F(t) \delta F(t+\tau) \rangle}{\langle F(t) \rangle^2} \quad (1)$$

Here δF(t) is the deviation from the mean fluorescence, F(t), at a given time and δF(t+ τ) is the deviation from the mean fluorescence at the same time plus a lag time τ. A general time autocorrelation function for fluorescent particles that are uniformly distributed, and undergoing ideal Brownian motion, can be used to model the fluorescence fluctuations and give data about the sample, such as the diffusion coefficient. The general autocorrelation function is:

$$G(\tau) = 1 + \frac{1}{N} \sum_{i=0}^{n} \left(\frac{1}{1+\frac{\tau}{\tau_{D,i}}} \right) \cdot \frac{x_i}{\sqrt{1+\frac{\omega^2}{z^2} \cdot \frac{\tau}{\tau_{D,i}}}} \quad (2)$$

Here ω and z are constants specific to the instrument, τ is the lag time, and x_i is the fraction of particles with the translational diffusion time $\tau_{D,i}$. Therefore the diffusion coefficient, D, of the particles can be determined by the following equation:

$$\tau_{D,i} = \frac{\omega^2}{4D_i} \quad (3)$$

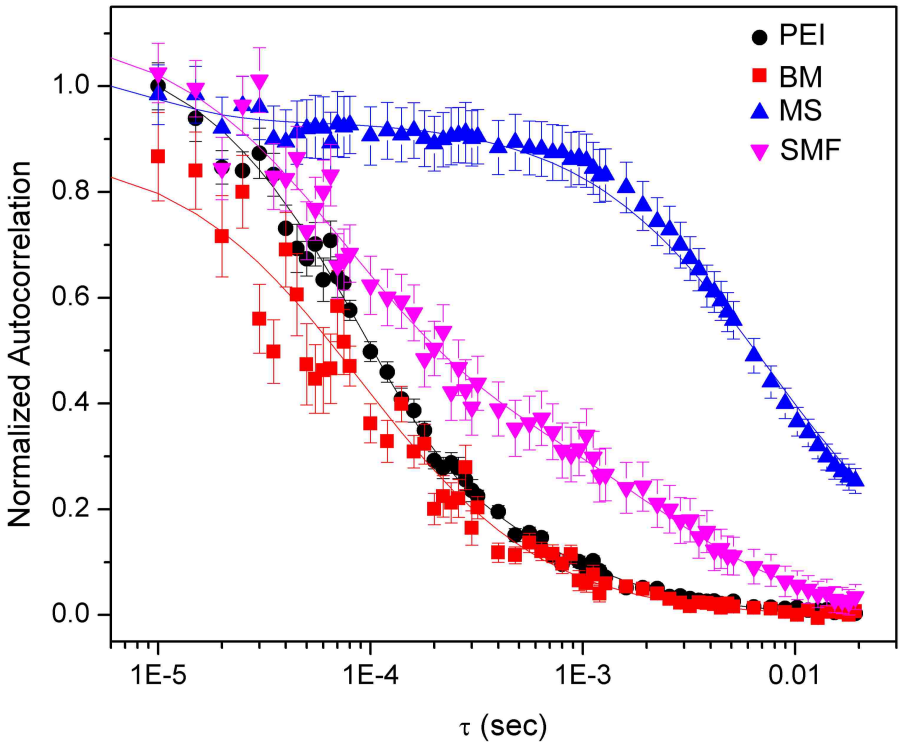

Figure 6.6: Determination of free polymer and ghost particles by FCS. Normalized autocorrelation curves for free PEI, BM, SMF, and MS methods. PGA/PEI/DNA weight ratios are all at 1.2/1.8/1.0 where applicable. Error bars represent the mean ± S.E.M (n=9).

For this set of experiments a two-component fit was employed to distinguish between TPs and free PEI or a combination of free PEI and ghost particles. FCS data show a distinct shift for MS-produced polyplexes to the right in comparison to free PEI, BM-produced TPs, or SMF-produced TPs [Fig. 6]. The BM-produced TP and free PEI samples yield autocorrelation curves that are very similar with the SMF-produced TP sample, having a curve that is slightly shifted in comparison to the BM sample curve. The fractions of free PEI determined by the autocorrelation function were determined to be 97.5, 80.0, and 0.0 for the BM-, SMF-, and MS-produced TPs, respectively.

6.4 Discussion

Polymeric gene delivery vectors offer the potential to circumvent many of the drawbacks associated with viral gene delivery vectors. Ternary polyplexes allow for enhancement of conventional two-component polyplexes by improving transfections in the presence of serum, reducing cytotoxicity, and potentially allowing for more flexibility in overcoming cellular barriers to delivery. Microfluidics can allow for the further advancement of polyplex formulations by allowing for the continuous production of polyplexes and the removal of excess components that are known to be toxic to cells.

Two microfluidic devices for assembly of TPs were designed and constructed, and the resulting vectors were compared to BM-produced TPs for their physicochemical characteristics and gene delivery activity. First, a novel sequential mixing device was created based on previous research that allows for the introduction of DNA and PEI to form a stream rich in PEI/DNA polyplexes, which is then hydrodynamically focused by a PGA stream. It was initially thought that the larger diffusivity of both PEI and PGA relative to DNA would lead to rapid mixing of PEI and PGA, which would then lead to

the formation of ghost particles possessing no transfection activity. A previous device, designed by our group, containing a separation mechanism, was also employed to first make PEI/DNA polyplexes that have been shown to have reduced amounts of free PEI and enhanced transfection activity, and then bulk mixed with PGA to produce TPs containing fewer ghost particles and thus enhanced transfection activity.

Physicochemical properties of TPs produced by the various mixing methods were first explored by DLS. It was shown that particle sizes of the MS-produced polyplexes were not significantly different than those of TPs produced by BM. The similarity in particle sizes in this case is most likely due to the bulk mixing of PGA, which occurs after the MS production of PEI/DNA polyplexes. SMF-produced TPs were the smallest at all PGA/DNA ratios. This may be due to the presence of a higher concentration of ghost particles, which are expected to be smaller than polyplexes [133]. This suggests that microfluidic production of the TPs on a single device would be ideal, but would require separation mechanisms within the chip, which will be the subject of future research.

Transfections mediated by TPs produced by the three different methods revealed that the removal of free PEI from the polyplex suspensions using the MS device led to enhanced transgene expression in the HeLa and MDA-MB-231 cell lines. The increases in transfection activity were observed both in serum-free media and media containing serum. Additionally, the MS-produced TPs perform about the same as BM TPs in the U-87 MG cell line, showing that, even in cell lines where separation may not provide gene expression enhancement, MS still may lead to a method for the continuous microfluidic production of TPs, which holds particular relevance for the processing and manufacturing of such drugs.

Quantitation of cellular internalization revealed that MS-produced TPs are taken up by a significantly greater percentage of HeLa cells than BM TPs, which may explain the increased gene expression seen in this cell line. HeLa cells show a significantly reduced cellular uptake than the other two cell lines, while simultaneously exhibiting the highest gene delivery activity. This may be due to a combination of cell surface receptors expressed by the cell line and generally lower metabolic activity associated with this specific cell line. It is interesting to note that while transgene expression was higher in most cases with the MS-produced polyplexes, cellular uptake was highest for the SMF-produced polyplexes in many instances. This may be due to membrane disruption associated with free PEI or ghost particles, allowing for more accessible entry into cells for the tagged DNA. The exact source of the combination of increased cellular uptake and reduced gene expression is unknown and needs to be further explored.

FCS data demonstrates further the ability of the MS device to separate free PEI from the polyplex sample. The two-component fit of the autocorrelation shows slower diffusion times for the sample and essentially no free PEI left in the resulting MS-produced polyplexes. In the case of the SMF device, the FCS data provides further evidence of the presence of a large amount of ghost particles when taking transfection data and particle size data into account as well. Since the FCS data indicate the sample has a similar amount of free PEI, while the transfection activity was very low and particle sizes were very small, these data seem to imply the presence of ghost particles.

6.6 Conclusions

Here we have described a method for the production of TPs using microfluidics and show that TPs produced by this method have higher transfection activity than those produced by BM in HeLa and MDA-MB-231 cell lines. Additionally, MS-produced polyplexes contained few ghost particles when compared to SMF-produced polyplexes, and also higher transfection activity in all cell lines explored. Lower cytotoxicity was also noted at optimal PGA/PEI/DNA ratios for the MS-produced polyplexes in comparison to BM-produced polyplexes.

Chapter 7: Conclusions and Future Perspectives

In this work, I explored the development of microfluidic devices for the production of non-viral polymeric-based gene delivery vectors. This dissertation demonstrated several key findings for this method of polyplex production. First in Chapter 4, it was shown that since polyethylenimine (PEI) and DNA diffuse at vastly different rates, it was feasible to separate free PEI from a product stream of a hydrodynamic focusing (HF) microfluidic device. Polyplexes produced by the microfluidic separator (MS) device were shown to be significantly smaller at some compositions. Transfections carried out over a range of PEI/DNA ratios showed that for some cell lines and at some compositions, MS-produced polyplexes demonstrated increased transfection efficiencies and decreased cellular toxicities. Importantly, through agarose gel electrophoresis, it was shown that MS-produced polyplexes yielded a product that contained ~40% less free PEI than BM-produced polyplexes. We then optimized mixing methods and PGA molecular weight for the production of ternary polyplexes in Chapter 5. It was shown that previous BM methods employed for the production of polyplexes may not have been ideal in the order in which polyplexes were mixed, and that for the production of ternary polyglutamic acid (PGA)/PEI/DNA polyplexes it was essential to first mix PEI with DNA and subsequently introduce PGA. This result paved the way for moving forward with the microfluidic production of ternary polyplexes discussed in Chapter 6. Additionally, in Chapter 5, it was shown that for the production of PGA/PEI/DNA polyplexes, 15-kDa PGA showed the most versatility for transfecting cells both in serum-free media and media containing serum. Chapter 6 explored strategies for the microfluidic production of ternary polyplexes. The design of a SMF device and

comparison of the polyplexes produced to both BM polyplexes and those produced by the MS device showed that separation of free PEI was beneficial for optimum transfection efficiencies and reduction of cytotoxicity in multiple cell lines in both serum-free and serum-containing media. Cellular uptake was shown to be enhanced by the separation of free PEI through flow cytometry studies carried out in multiple cell lines at the optimum transfection compositions.

Uniquely, we have demonstrated the development and utility of a microfluidic separation system for the production of both binary and ternary polymeric gene delivery vectors. Continuous production of pharmaceuticals can be difficult to accomplish due to the complex purification processes that are often necessary. In this case we have demonstrated a cheap and reliable method for the removal of toxic free PEI from the final drug product and simultaneous enhancements to the quality of the product. Although production volumes used throughout this research project have remained much smaller than those required for commercial production, this technique is easily scalable through the use of multiple parallel microfluidic systems.

7.1 Future Perspectives

The results presented in this dissertation suggest that MS is a promising advance for the continuous production of enhanced ternary polyplexes of high quality. However there are still steps to be taken to further advance this technique towards implementation on a commercial scale. The sections that follow give details about these challenges and the future goals of this research.

7.1.1 A Nested Device for the Production of Ternary Polyplexes

This work has demonstrated the utility of a microfluidic separation device for the production of purified binary polyplexes that can then be mixed with PGA to produce high-quality ternary polyplexes. However, one of the key end points for quality enhancement for this type of therapeutic is a controllable and consistent particle size. It was shown that in cases when all steps of polyplex production occurred within a microfluidic device, particle sizes were consistent and predictable. Moving forward we will continue this work by integrating the developed separation system into a nested microfluidic system that is capable of fabricating binary polyplexes, separating free PEI, and then introducing PGA, thus fabricating layer-by-layer ternary polyplexes all on one device [Fig 7.1]. A key point of emphasis for achieving this goal will be demonstrating the ability to control pressures at the various outlets to achieve the desired flow characteristics. We hypothesize that if the flow is manipulated by pressure controllers the desired flow rates will be achievable and, importantly, ternary polyplexes with predictable and consistent sizes can be produced. We believe that this will lead to polyplexes with enhanced properties such as lower cytotoxicity and increased transfection efficiency. Also, since this would be a more continuous approach to the production of ternary polyplexes, it would yield a more economically viable method for the production of the therapeutic. Taken together, these results would be a significant step towards clinically and commercially viable non-viral gene delivery vectors.

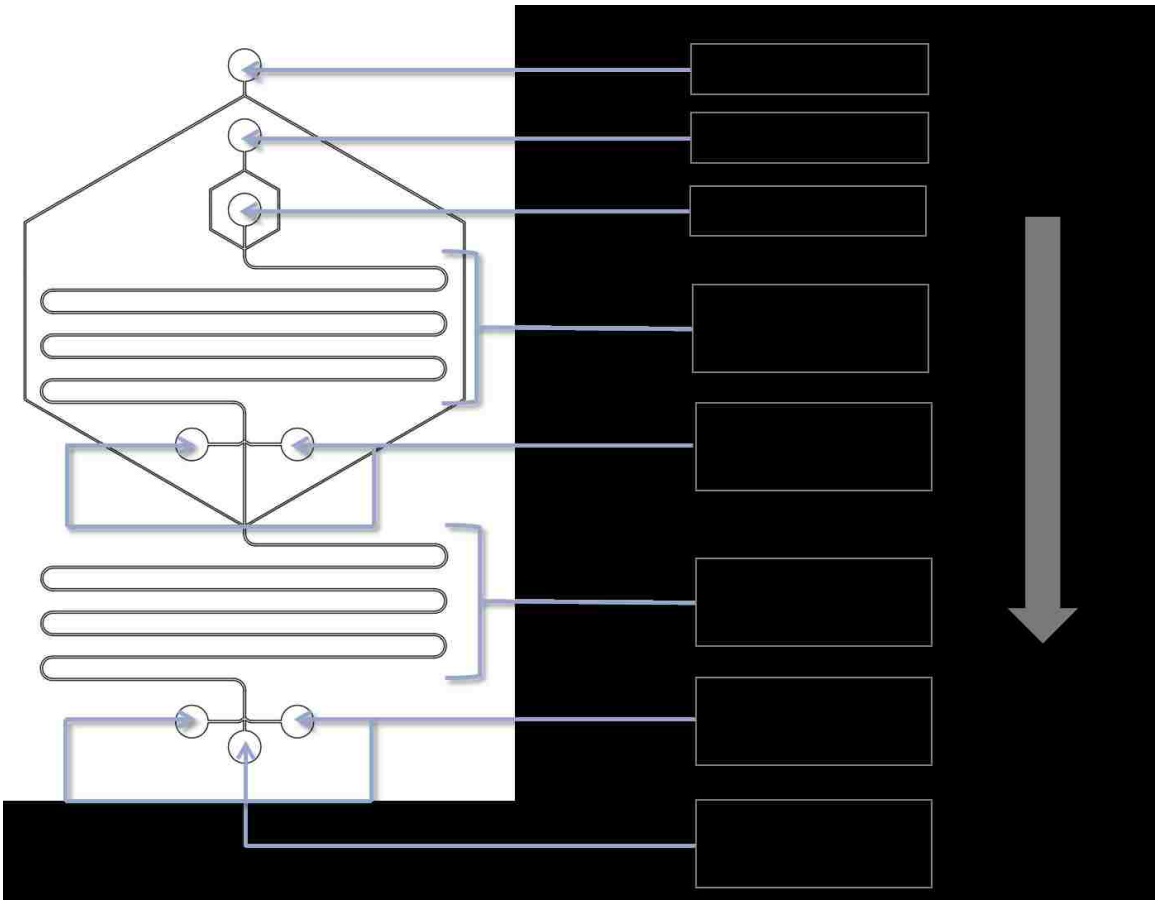

Figure 7.1: Nested microfluidic device design concept for the production of high quality ternary polyplexes.

7.1.2 Integrating More Complex Ternary Polyplex Systems

After the development of an all-in-one device for the production of ternary polyplexes, we believe the device could easily be adapted for the production of ternary polyplexes that include more advanced polymers such as the ones mentioned previously in the manuscript. Targeting polymers could easily be adapted to the system and implemented in second hydrodynamic focusing section on the device yielding TPs of consistent quality coated with targeting polymers. For example, FPP/PEI/DNA polyplexes might be well-suited for such a system yielding TPs that target folate receptors, which are over-expressed by many cancerous cells. The nested device mentioned above could lead to enhanced quality of TP systems such as this one. Additionally, it is clear that there are many such TP systems throughout this dissertation that address many of the cellular barriers to delivery that might be well-suited to such a system and be aided by the aforementioned benefits.

Addressing other challenges for clinical implementation of non-viral gene delivery vectors may also be possible by allowing for the continuous production of the TPs and freeze-dried storage. These very plausible improvements address two significant technical boundaries aiding in commercial success of non-viral vectors. Approaching the transfection efficiency of viral vectors, and thus competing with them as a viable alternative, is a significant challenge. However, we believe through implementation of microfluidic production and intelligent vector design, the ability of non-viral gene delivery vectors to address cellular barriers to delivery will be significantly enhanced. The high transfection efficiency of viral vectors is due to their highly evolved mechanisms to address cellular barriers to delivery. Thus, it is possible for the

transfection efficiency of polymeric-based vectors to approach that of viral vectors through these improvements. It is the opinion of the author that this research represents a significant advance towards commercially and clinically viable polymer-based gene delivery vectors.

Appendix

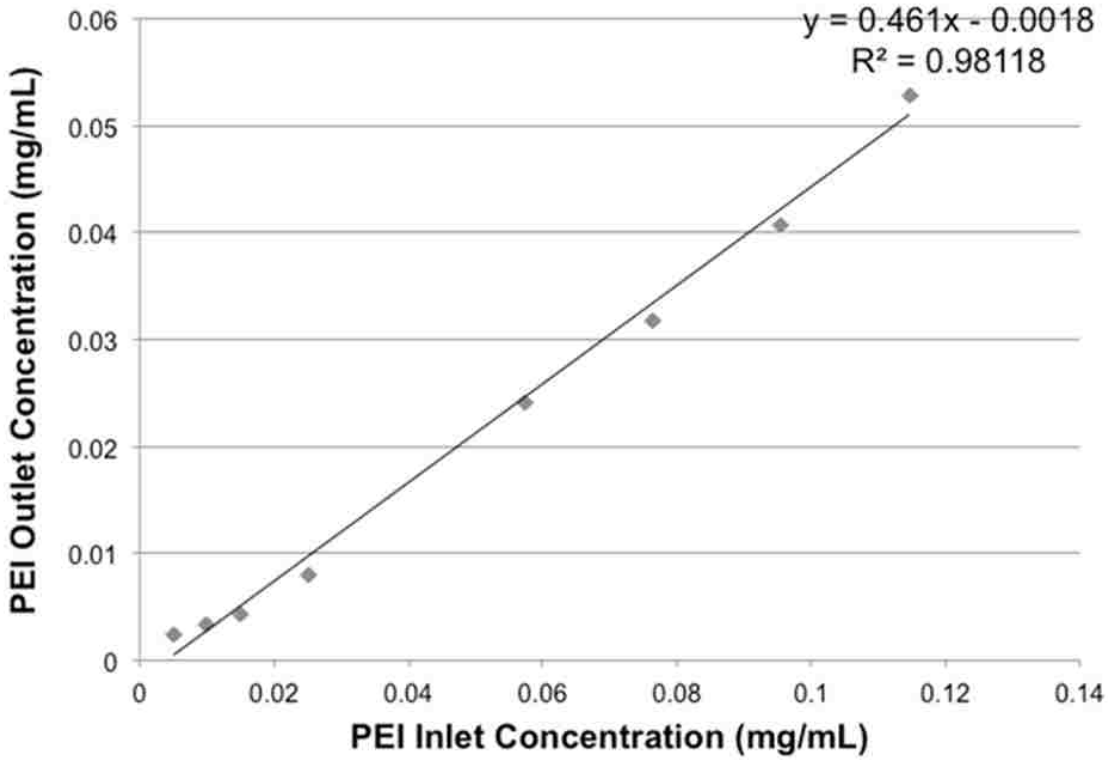

Figure A.1: PEI outlet concentrations for the MS device at different PEI inlet concentrations as assessed by ninhydrin assay.

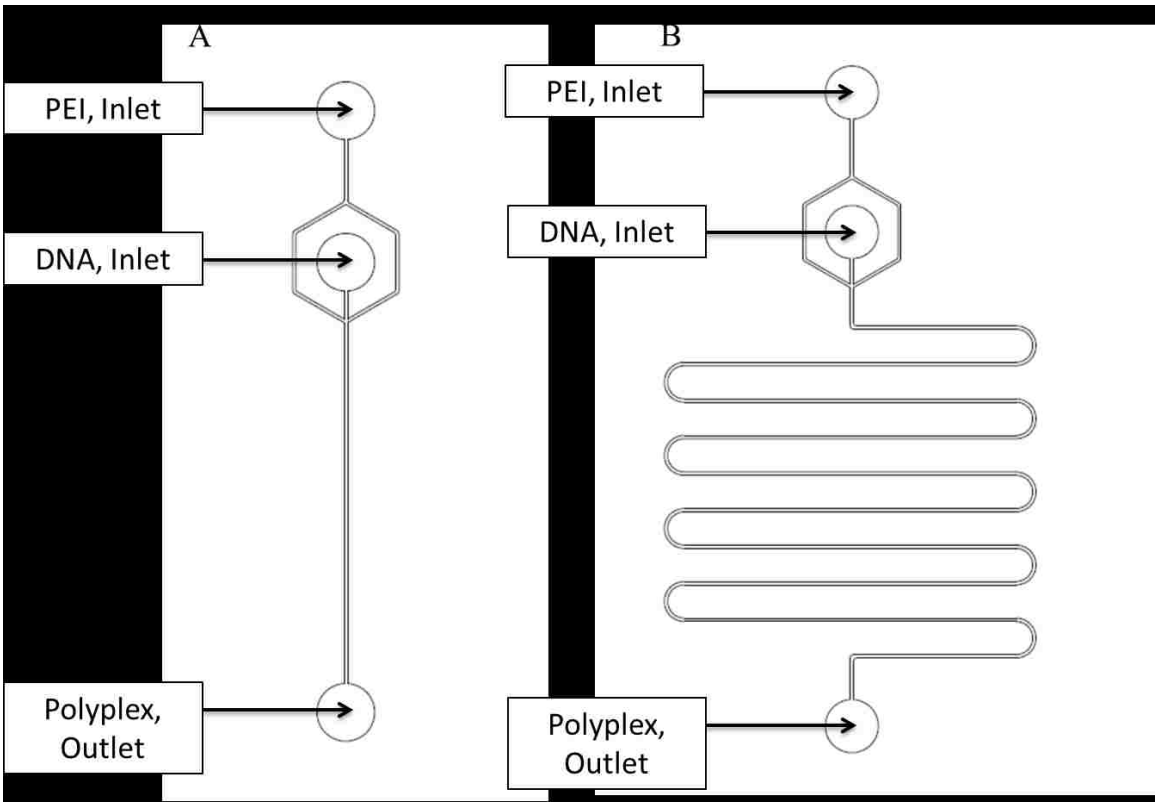

Figure A.2: Schematics for two different microfluidic devices with different diffusion lengths. A) 2 cm device, MF2. B) 25 cm device with 25 cm serpentine diffusion length, 25M

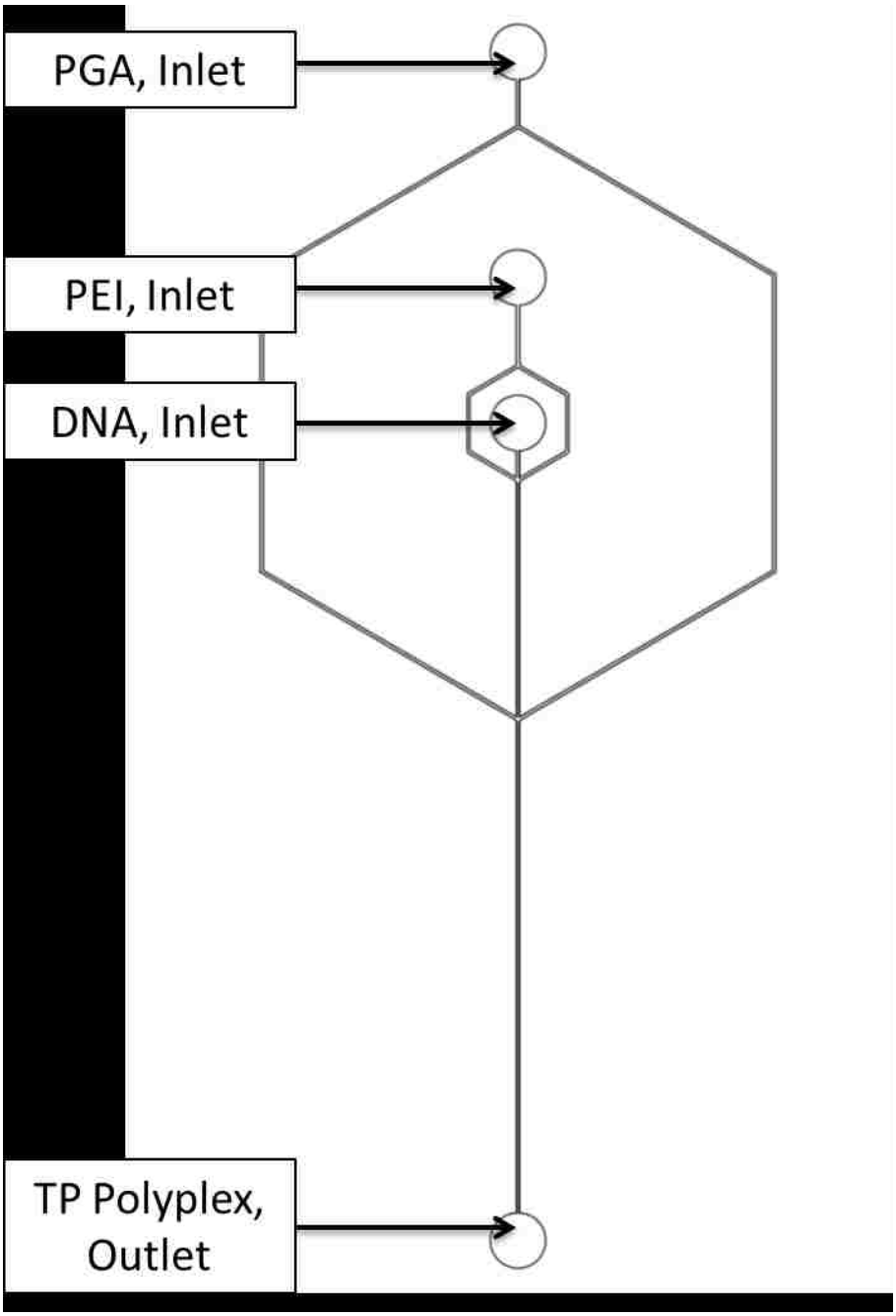

Figure A.3: Schematic of SMF device.

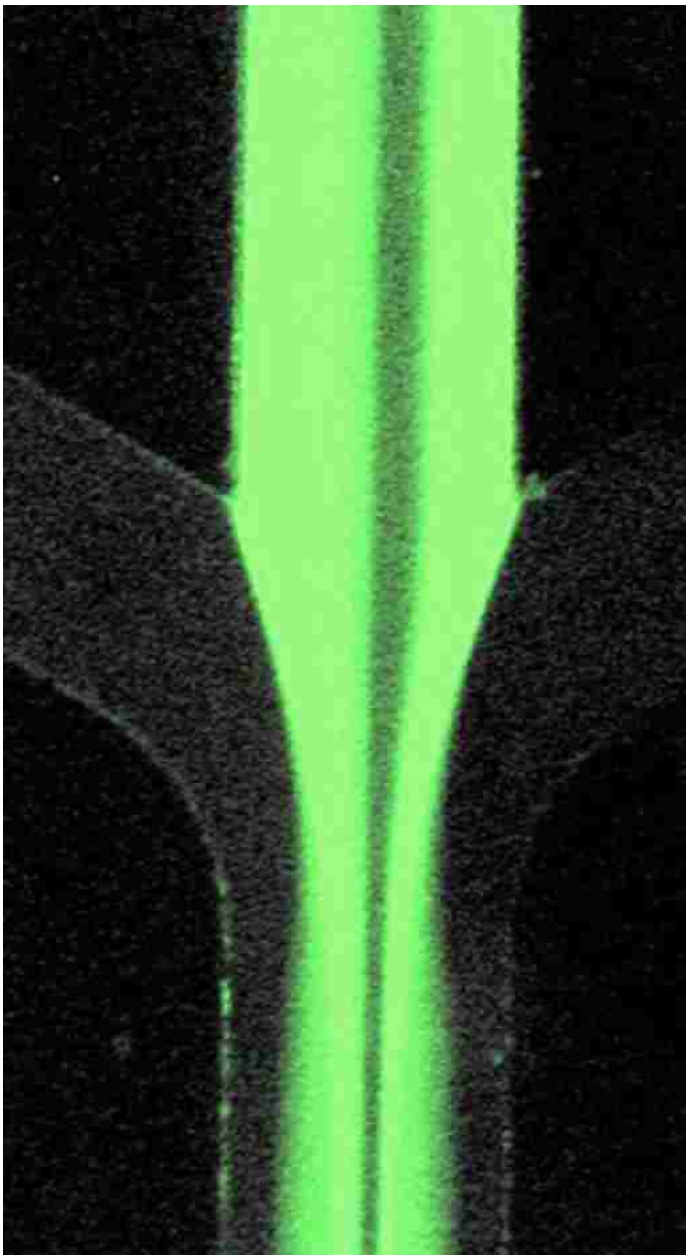

Figure A.4: Fluorescence microscopy image of the second HF region of the SMF device.

References

[1] O. Boussif, F. Lezoualc'h, M. Zanta, A versatile vector for gene and oligonucleotide transfer into cells in culture and in vivo: polyethylenimine, Proc. (1995). http://www.pnas.org/content/92/16/7297.short (accessed March 31, 2017).

[2] D.B. Rozema, D.L. Lewis, D.H. Wakefield, S.C. Wong, J.J. Klein, P.L. Roesch, S.L. Bertin, T.W. Reppen, Q. Chu, A. V. Blokhin, J.E. Hagstrom, J.A. Wolff, Dynamic PolyConjugates for targeted in vivo delivery of siRNA to hepatocytes, Proc. Natl. Acad. Sci. (2007). doi:10.1073/pnas.0703778104.

[3] P.M. and, M. Monsigny, Efficient Gene Transfer by Histidylated Polylysine/pDNA Complexes, (1999). doi:10.1021/BC9801070.

[4] D.M.L. and, R. Langer*, Degradable Poly(β-amino esters): Synthesis, Characterization, and Self-Assembly with Plasmid DNA, (2000). doi:10.1021/JA0015388.

[5] H. Gonzalez, S.J.S. Hwang, M.E. Davis, New class of polymers for the delivery of macromolecular therapeutics, Bioconjug. Chem. (1999). doi:10.1021/bc990072j.

[6] B. Abdallah, A. Hassan, C. Benoist, D. Goula, J.P. Behr, B. Demeneix, A Powerful Nonviral Vector for In Vivo Gene Transfer into the Adult Mammalian Brain: Polyethylenimine, Hum. Gene Ther. (1996). doi:10.1089/hum.1996.7.16-1947.

[7] D. Putnam, C. Gentry, D. Pack, Polymer-based gene delivery with low cytotoxicity by a unique balance of side-chain termini, Proc. (2001). doi:10.1073/pnas.031577698.

[8] N.P.G. and, †,‡ Daniel W. Pack*, Acetylation of Polyethylenimine Enhances Gene Delivery via Weakened Polymer/DNA Interactions, (2006). doi:10.1021/BM060300U.

[9] P. Xu, G.K. Quick, Y. Yeo, Gene delivery through the use of a hyaluronate-associated intracellularly degradable crosslinked polyethyleneimine, Biomaterials. (2009). doi:10.1016/j.biomaterials.2009.07.012.

[10] G. Jiang, S.H. Min, E.J. Oh, S.K. Hahn, DNA/PEI/Alginate polyplex as an efficient in vivo gene delivery system, Biotechnol. Bioprocess Eng. (2007). doi:10.1007/BF02931086.

[11] T. Ito, N. Iida-Tanaka, T. Niidome, T. Kawano, K. Kubo, K. Yoshikawa, T. Sato, Z. Yang, Y. Koyama, Hyaluronic acid and its derivative as a multi-functional gene expression enhancer: Protection from non-specific interactions, adhesion to targeted cells, and transcriptional activation, J. Control. Release. (2006). doi:10.1016/j.jconrel.2006.03.013.

[12] T. Ito, C. Yoshihara, K. Hamada, Y. Koyama, DNA/polyethyleneimine/hyaluronic acid small complex particles and tumor suppression in mice, Biomaterials. (2010). doi:10.1016/j.biomaterials.2009.12.032.

[13] C. Wang, X. Luo, Y. Zhao, L. Han, X. Zeng, M. Feng, S. Pan, H. Peng, C. Wu, Influence of the polyanion on the physico-chemical properties and biological activities of polyanion/DNA/polycation ternary polyplexes, Acta Biomater. 8 (2012) 3014–3026. doi:10.1016/j.actbio.2012.04.034.

[14] C. Wang, X. Bao, X. Ding, Y. Ding, S. Abbad, Y. Wang, M. Li, Y. Su, W. Wang, J. Zhou, A multifunctional self-dissociative polyethyleneimine derivative coating

polymer for enhancing the gene transfection efficiency of DNA/polyethyleneimine polyplexes in vitro and in vivo, 6 (2015) 780–796. doi:10.1039/C4PY01135J.
[15] T. Kurosaki, T. Kitahara, S. Kawakami, Y. Higuchi, A. Yamaguchi, H. Nakagawa, Y. Kodama, T. Hamamoto, M. Hashida, H. Sasaki, γ-Polyglutamic acid-coated vectors for effective and safe gene therapy, J. Control. Release. (2010). doi:10.1016/j.jconrel.2009.11.010.
[16] G.K. Chee, X. Kang, Y. Xie, Z. Fei, J. Guan, B. Yu, X. Zhang, L.J. Lee, Delivery of polyethylenimine/DNA complexes assembled in a microfluidics device, in: Mol. Pharm., 2009. doi:10.1021/mp900016q.
[17] H. Debus, M. Beck-Broichsitter, T. Kissel, Optimized preparation of pDNA/poly(ethylene imine) polyplexes using a microfluidic system., Lab Chip. (2012). doi:10.1039/c2lc40176b.
[18] Y.P. Ho, C.L. Grigsby, F. Zhao, K.W. Leong, Tuning physical properties of nanocomplexes through microfluidics-assisted confinement, Nano Lett. (2011). doi:10.1021/nl200862n.
[19] L.J. Scott, Alipogene Tiparvovec: A Review of Its Use in Adults with Familial Lipoprotein Lipase Deficiency, Drugs. 75 (2015) 175–182. doi:10.1007/s40265-014-0339-9.
[20] N. A.C., R. U.M., T. E.G.D., R. C., C. P., M. J., D.P. M., L. E., P. N., R. D., R. A., P. J., R. S., B. D., R. M., S. Y.-M., H. K.G., B.-T. E., M. F., H. K.A., A. J., K. M.A., N. C.Y.C., Z. J., C. M., M. C.L., G. J.T., S. D., N. A.W., D. A.M., Long-term safety and efficacy of factor IX gene therapy in hemophilia B, N. Engl. J. Med. (2014).
[21] A. Aiuti, B. Cassani, G. Andolfi, M. Mirolo, L. Biasco, A. Recchia, F. Urbinati, C. Valacca, S. Scaramuzza, M. Aker, S. Slavin, M. Cazzola, D. Sartori, A. Ambrosi, C. Di Serio, M.G. Roncarolo, F. Mavilio, C. Bordignon, Multilineage hematopoietic reconstitution without clonal selection in ADA-SCID patients treated with stem cell gene therapy, J. Clin. Invest. (2007). doi:10.1172/JCI31666.
[22] E. F.S., D. C., A. H., A.-B. R., B. A., D. C., D. J.-H., G. H.B., G. P., K. D.B., L. J., L. T.C., M. W.P., M. P.L., O. T., O. P.J., P. A.M., S. A.J., S. E., R. G.V., S. R., S. N.J.C., T. A.J., A. P., A phase 2/3 study of the efficacy and safety of ex vivo gene therapy with lenti-DTM lentiviral vector for the treatment of cerebral adrenoleukodystrophy, Mol. Ther. (2016).
[23] A. Georgiadis, Y. Duran, J. Ribeiro, L. Abelleira-Hervas, S.J. Robbie, B. Sünkel-Laing, S. Fourali, A. Gonzalez-Cordero, E. Cristante, M. Michaelides, J.W.B. Bainbridge, A.J. Smith, R.R. Ali, Development of an optimized AAV2/5 gene therapy vector for Leber congenital amaurosis owing to defects in RPE65, Gene Ther. 23 (2016) 857–862. doi:10.1038/gt.2016.66.
[24] S.S. De Ravin, A. Reik, P.-Q. Liu, L. Li, X. Wu, L. Su, C. Raley, N. Theobald, U. Choi, A.H. Song, A. Chan, J.R. Pearl, D.E. Paschon, J. Lee, H. Newcombe, S. Koontz, C. Sweeney, D.A. Shivak, K.A. Zarember, M. V Peshwa, P.D. Gregory, F.D. Urnov, H.L. Malech, Targeted gene addition in human CD34(+) hematopoietic cells for correction of X-linked chronic granulomatous disease., Nat. Biotechnol. (2016). doi:10.1038/nbt.3513.
[25] C. Long, J.R. McAnally, J.M. Shelton, A.A. Mireault, R. Bassel-Duby, E.N. Olson, Prevention of muscular dystrophy in mice by CRISPR/Cas9-mediated

editing of germline DNA, Science. (2014). doi:10.1126/science.1254445.
[26] A. Aiuti, L. Biasco, S. Scaramuzza, F. Ferrua, M.P. Cicalese, C. Baricordi, F. Dionisio, A. Calabria, S. Giannelli, M.C. Castiello, M. Bosticardo, C. Evangelio, A. Assanelli, M. Casiraghi, S. Di Nunzio, L. Callegaro, C. Benati, P. Rizzardi, D. Pellin, C. Di Serio, M. Schmidt, C. Von Kalle, J. Gardner, N. Mehta, V. Neduva, D.J. Dow, A. Galy, R. Miniero, A. Finocchi, A. Metin, P.P. Banerjee, J.S. Orange, S. Galimberti, M.G. Valsecchi, A. Biffi, E. Montini, A. Villa, F. Ciceri, M.G. Roncarolo, L. Naldini, A. Aiuti, L. Biasco, S. Scaramuzza, F. Ferrua, M.P. Cicalese, C. Baricordi, F. Dionisio, A. Calabria, S. Giannelli, M. Carmina, M. Bosticardo, C. Evangelio, A. Assanelli, M. Casiraghi, D. Nunzio, L. Callegaro, C. Benati, P. Rizzardi, D. Pellin, C. Di Serio, M. Schmidt, C. Von Kalle, J. Gardner, N. Mehta, V. Neduva, J. David, A. Galy, R. Miniero, A. Finocchi, A. Metin, P.P. Banerjee, S. Jordan, S. Galimberti, M.G. Valsecchi, A. Biffi, E. Montini, F. Ciceri, M.G. Roncarolo, L. Naldini, Lentiviral Hematopoietic Stem Cell Gene Therapy in Patients with Wiskott-Aldrich Syndrome., Science. (2013). doi:10.1126/science.1233151.
[27] S.L. Ginn, I.E. Alexander, M.L. Edelstein, M.R. Abedi, J. Wixon, Gene therapy clinical trials worldwide to 2012 - an update, J. Gene Med. (2013). doi:10.1002/jgm.2698.
[28] P. Zarogoulidis, K. Darwiche, A. Sakkas, L. Yarmus, H. Huang, Q. Li, L. Freitag, K. Zarogoulidis, M. Malecki, Suicide Gene Therapy for Cancer - Current Strategies., J. Genet. Syndr. Gene Ther. (2013). doi:10.4172/2157-7412.1000139.
[29] T.T. Smith, J.C. Roth, G.K. Friedman, G.Y. Gillespie, Oncolytic viral therapy: targeting cancer stem cells., Oncolytic Virotherapy. (2014). doi:10.2147/OV.S52749.
[30] H.L. Kong, R.G. Crystal, Gene therapy strategies for tumor antiangiogenesis, J. Natl. Cancer Inst. (1998). doi:10.1093/jnci/90.4.261-a.
[31] C.G. Drake, E.J. Lipson, J.R. Brahmer, Breathing new life into immunotherapy: Review of melanoma, lung and kidney cancer, Nat. Rev. Clin. Oncol. (2014). doi:10.1038/nrclinonc.2013.208.
[32] J. Tereshchenko, A. Maddalena, M. Bähr, S. Kügler, Pharmacologically controlled, discontinuous GDNF gene therapy restores motor function in a rat model of Parkinson's disease, Neurobiol. Dis. (2014). doi:10.1016/j.nbd.2014.01.009.
[33] N. Aronin, M. Difiglia, Huntingtin-lowering strategies in Huntington's disease: Antisense oligonucleotides, small RNAs, and gene editing, Mov. Disord. (2014). doi:10.1002/mds.26020.
[34] P. Tebas, D. Stein, W.W. Tang, I. Frank, S.Q. Wang, G. Lee, S.K. Spratt, R.T. Surosky, M.A. Giedlin, G. Nichol, M.C. Holmes, P.D. Gregory, D.G. Ando, M. Kalos, R.G. Collman, G. Binder-Scholl, G. Plesa, W.-T. Hwang, B.L. Levine, C.H. June, Gene Editing of CCR5 in Autologous CD4 T Cells of Persons Infected with HIV, N. Engl. J. Med. (2014). doi:10.1056/NEJMoa1300662.
[35] J.T. Schiffer, D.A. Swan, D. Stone, K.R. Jerome, Predictors of Hepatitis B Cure Using Gene Therapy to Deliver DNA Cleavage Enzymes: A Mathematical Modeling Approach, PLoS Comput. Biol. (2013). doi:10.1371/journal.pcbi.1003131.

[36] M.A. Kotterman, D. V Schaffer, Engineering adeno-associated viruses for clinical gene therapy., Nat. Rev. Genet. (2014). doi:10.1038/nrg3742.
[37] T. Kafri, H. Van Praag, F.H. Gage, I.M. Verma, Lentiviral Vectors: Regulated Gene Expression, Mol. Ther. (2000). doi:10.1006.
[38] M.N. Antoniou, K.A. Skipper, O. Anakok, Optimizing retroviral gene expression for effective therapies., Hum. Gene Ther. (2013). doi:10.1089/hum.2013.062.
[39] C. Baum, O. Kustikova, U. Modlich, Z. Li, B. Fehse, Mutagenesis and oncogenesis by chromosomal insertion of gene transfer vectors., Hum. Gene Ther. (2006). doi:10.1089/hum.2006.17.ft-190.
[40] N. Bessis, F.J. GarciaCozar, M.-C. Boissier, Immune responses to gene therapy vectors: influence on vector function and effector mechanisms., Gene Ther. (2004). doi:10.1038/sj.gt.3302364.
[41] R. Waehler, S.J. Russell, D.T. Curiel, Engineering targeted viral vectors for gene therapy., Nat. Rev. Genet. (2007). doi:10.1038/nrg2141.
[42] J.A. Allay, S. Sleep, S. Long, D.M. Tillman, R. Clark, G. Carney, P. Fagone, J.H. McIntosh, A.W. Nienhuis, A.M. Davidoff, A.C. Nathwani, J.T. Gray, Good manufacturing practice production of self-complementary serotype 8 adeno-associated viral vector for a hemophilia B clinical trial., Hum. Gene Ther. (2011). doi:10.1089/hum.2010.202.
[43] H. Yin, R.L. Kanasty, A.A. Eltoukhy, A.J. Vegas, R.J. Dorkin, D.G. Anderson, J.R. Dorkin, D.G. Anderson, Non-viral vectors for gene-based therapy, 2014. doi:10.1038/nrg3763.
[44] S.D. Li, L. Huang, Gene therapy progress and prospects: non-viral gene therapy by systemic delivery, Gene Ther. (2006). doi:10.1038/sj.gt.3302838.
[45] D. Pack, A. Hoffman, S. Pun, P. Stayton, Design and development of polymers for gene delivery, Nat. Rev. Drug. (2005). http://www.nature.com/nrd/journal/v4/n7/abs/nrd1775.html (accessed March 31, 2017).
[46] E. Junquera, E. Aicart, Cationic lipids as transfecting agents of DNA in gene therapy., Curr. Top. Med. Chem. (2014). doi:Doi 10.2174/1568026614666140118203128.
[47] J. Dobson, Gene therapy progress and prospects: magnetic nanoparticle-based gene delivery., Gene Ther. (2006). doi:10.1038/sj.gt.3302720.
[48] T. Kurosaki, T. Kitahara, S. Fumoto, K. Nishida, J. Nakamura, T. Niidome, Y. Kodama, H. Nakagawa, H. To, H. Sasaki, Ternary complexes of pDNA, polyethylenimine, and γ-polyglutamic acid for gene delivery systems, Biomaterials. (2009). doi:10.1016/j.biomaterials.2009.01.055.
[49] M. Hornof, M. de la Fuente, M. Hallikainen, R.H. Tammi, A. Urtti, Low molecular weight hyaluronan shielding of DNA/PEI polyplexes facilitates CD44 receptor mediated uptake in human corneal epithelial cells, J. Gene Med. 10 (2008) 70–80. doi:10.1002/jgm.1125.
[50] E. Nicolì, M.I. Syga, M. Bosetti, V.P. Shastri, Enhanced gene silencing through human serum albumin-mediated delivery of polyethylenimine-siRNA polyplexes, PLoS One. (2015). doi:10.1371/journal.pone.0122581.
[51] H. Tian, Z. Guo, L. Lin, Z. Jiao, J. Chen, S. Gao, X. Zhu, X. Chen, PH-responsive zwitterionic copolypeptides as charge conversional shielding system for gene

carriers, J. Control. Release. (2014). doi:10.1016/j.jconrel.2013.11.008.
[52] J. Chen, X. Dong, T. Feng, L. Lin, Z. Guo, J. Xia, H. Tian, X. Chen, Charge-conversional zwitterionic copolymer as pH-sensitive shielding system for effective tumor treatment, Acta Biomater. (2015). doi:10.1016/j.actbio.2015.08.018.
[53] Y.G. Fu, Y.J. Qu, K.C. Wu, H.H. Zhai, Z.G. Liu, D.M. Fan, Apoptosis-inducing effect of recombinant Caspase-3 expressed by constructed eukaryotic vector on gastric cancer cell line SGC7901, World J. Gastroenterol. (2003).
[54] S. Asayama, M. Sudo, H. Kawakami, Release of DNA binary complexes from the ternary complexes by carboxymethyl poly(L-histidine)., Nucleic Acids Symp. Ser. (Oxf). (2009). doi:10.1093/nass/nrp127.
[55] S. Asayama, M. Sudo, S. Nagaoka, H. Kawakami, Carboxymethyl poly(L-histidine) as a new pH-sensitive polypeptide to enhance polyplex gene delivery, Mol. Pharm. (2008). doi:10.1021/mp800094b.
[56] J. Li, Q. Chen, Z. Zha, H. Li, K. Toh, A. Dirisala, Y. Matsumoto, K. Osada, K. Kataoka, Z. Ge, Ternary polyplex micelles with PEG shells and intermediate barrier to complexed DNA cores for efficient systemic gene delivery, J. Control. Release. (2015). doi:10.1016/j.jconrel.2015.04.024.
[57] T. Nomoto, S. Fukushima, M. Kumagai, K. Machitani, Arnida, Y. Matsumoto, M. Oba, K. Miyata, K. Osada, N. Nishiyama, K. Kataoka, Three-layered polyplex micelle as a multifunctional nanocarrier platform for light-induced systemic gene transfer, Nat. Commun. (2014). doi:10.1038/ncomms4545.
[58] T.C. Lai, K. Kataoka, G.S. Kwon, Bioreducible polyether-based pDNA ternary polyplexes: Balancing particle stability and transfection efficiency, Colloids Surfaces B Biointerfaces. (2012). doi:10.1016/j.colsurfb.2011.09.026.
[59] M. Sanjoh, K. Miyata, R.J. Christie, T. Ishii, Y. Maeda, F. Pittella, S. Hiki, N. Nishiyama, K. Kataoka, Dual environment-responsive polyplex carriers for enhanced intracellular delivery of plasmid DNA, Biomacromolecules. (2012). doi:10.1021/bm301095a.
[60] M. Sanjoh, S. Hiki, Y. Lee, M. Oba, K. Miyata, T. Ishii, K. Kataoka, PDNA/poly(L-lysine) polyplexes functionalized with a pH-sensitive charge-conversional poly(aspartamide) derivative for controlled gene delivery to human umbilical vein endothelial cellsa, Macromol. Rapid Commun. (2010). doi:10.1002/marc.201000056.
[61] A. Elbakry, A. Zaky, R. Liebl, R. Rachel, A. Goepferich, M. Breunig, Layer-by-layer assembled gold nanoparticles for sirna delivery, Nano Lett. (2009). doi:10.1021/nl9003865.
[62] S. Guo, Y. Huang, Q. Jiang, Y. Sun, L. Deng, Z. Liang, Q. Du, J. Xing, Y. Zhao, P.C. Wang, A. Dong, X.-J. Liang, Enhanced Gene Delivery and siRNA Silencing by Gold Nanoparticles Coated with Charge-Reversal Polyelectrolyte, ASC Nano. (2010). doi:10.1021/nn101638u.Enhanced.
[63] K.C.-F. Leung, C.-H. Wong, X.-M. Zhu, S.-F. Lee, K.W.Y. Sham, J.M.Y. Lai, C.-P. Chak, Y.-X.J. Wang, C.H.K. Cheng, Ternary hybrid nanocomposites for gene delivery and magnetic resonance imaging of hepatocellular carcinoma cells, Quant. Imaging Med. Surg. (2013). doi:10.3978/j.issn.2223-4292.2013.12.05.
[64] C. Zhang, S. Gao, W. Jiang, S. Lin, F. Du, Z. Li, W. Huang, Targeted minicircle DNA delivery using folate-poly(ethylene glycol)-polyethylenimine as non-viral

carrier, Biomaterials. (2010). doi:10.1016/j.biomaterials.2010.04.042.
[65] G.L. Zwicke, G. Ali Mansoori, C.J. Jeffery, Utilizing the folate receptor for active targeting of cancer nanotherapeutics, Nano Rev. (2012). doi:10.3402/nano.v3i0.18496.
[66] Y.C. Chung, W.Y. Hsieh, T.H. Young, Polycation/DNA complexes coated with oligonucleotides for gene delivery, Biomaterials. (2010). doi:10.1016/j.biomaterials.2010.01.116.
[67] W. Zhang, W. Rödl, D. He, M. Döblinger, U. Lächelt, E. Wagner, Combination of sequence-defined oligoaminoamides with transferrin-polycation conjugates for receptor-targeted gene delivery, J. Gene Med. (2015). doi:10.1002/jgm.2838.
[68] H. Oliveira, R. Fernandez, L.R. Pires, M.C.L. Martins, S. Simões, M.A. Barbosa, A.P. Pêgo, Targeted gene delivery into peripheral sensorial neurons mediated by self-assembled vectors composed of poly(ethylene imine) and tetanus toxin fragment c, J. Control. Release. (2010). doi:10.1016/j.jconrel.2010.01.018.
[69] D. V. Schaffer, D.A. Lauffenburger, Optimization of cell surface binding enhances efficiency and specificity of molecular conjugate gene delivery, J. Biol. Chem. (1998). doi:10.1074/jbc.273.43.28004.
[70] A. Beyerle, M. Irmler, J. Beckers, T. Kissel, T. Stoeger, Toxicity pathway focused gene expression profiling of PEI-based polymers for pulmonary applications, Mol. Pharm. (2010). doi:10.1021/mp900278x.
[71] Q. Zhang, S. Chen, R.X. Zhuo, X.Z. Zhang, S.X. Cheng, Self-assembled terplexes for targeted gene delivery with improved transfection, Bioconjug. Chem. (2010). doi:10.1021/bc100309e.
[72] J. Gu, X. Chen, X. Ren, X. Zhang, X. Fang, X. Sha, CD44-Targeted Hyaluronic Acid-Coated Redox-Responsive Hyperbranched Poly(amido amine)/Plasmid DNA Ternary Nanoassemblies for Efficient Gene Delivery, Bioconjug. Chem. 27 (2016) 1723–1736. doi:10.1021/acs.bioconjchem.6b00240.
[73] G. Li, Y. Gao, Y. Cui, T. Zhang, R. Cui, Y. Jiang, J. Shi, Overexpression of CD44 is associated with the occurrence and migration of non-small cell lung cancer, Mol. Med. Rep. (2016). doi:10.3892/mmr.2016.5636.
[74] K. Liang, K.H. Bae, F. Lee, K. Xu, J.E. Chung, S.J. Gao, M. Kurisawa, Self-assembled ternary complexes stabilized with hyaluronic acid-green tea catechin conjugates for targeted gene delivery, J. Control. Release. 226 (2016) 205–216. doi:10.1016/j.jconrel.2016.02.004.
[75] T.T.H. Nguyen, Y.H. Moon, Y.B. Ryu, Y.M. Kim, S.H. Nam, M.S. Kim, A. Kimura, D. Kim, The influence of flavonoid compounds on the in vitro inhibition study of a human fibroblast collagenase catalytic domain expressed in E. coli, Enzyme Microb. Technol. (2013). doi:10.1016/j.enzmictec.2012.10.001.
[76] F. Lee, J. Lim, M.R. Reithofer, S.S. Lee, J.E. Chung, C.A.E. Hauser, M. Kurisawa, Synthesis and bioactivity of a conjugate composed of green tea catechins and hyaluronic acid, Polym. Chem. (2015). doi:10.1039/C5PY00495K.
[77] T. Kuzuhara, Y. Iwai, H. Takahashi, D. Hatakeyama, N. Echigo, Green tea catechins inhibit the endonuclease activity of influenza A virus RNA polymerase, PLoS Curr. (2009). doi:10.1371/currents.RRN1052.
[78] C.G. Koh, X. Zhang, S. Liu, S. Golan, B. Yu, X. Yang, J. Guan, Y. Jin, Y. Talmon, N. Muthusamy, K.K. Chan, J.C. Byrd, R.J. Lee, G. Marcucci, L.J. Lee,

Delivery of antisense oligodeoxyribonucleotide lipopolyplex nanoparticles assembled by microfluidic hydrodynamic focusing, J. Control. Release. (2010). doi:10.1016/j.jconrel.2009.08.019.
[79] S. Ding, N. Anton, T. Vandamme, Microfluidic nanoprecipitation systems for preparing pure drug or polymeric drug loaded nanoparticles: an overview, Expert Opin. Drug. (2016). http://www.tandfonline.com/doi/abs/10.1080/17425247.2016.1193151 (accessed March 31, 2017).
[80] C.A. Baker, C.T. Duong, A. Grimley, M.G. Roper, Recent advances in microfluidic detection systems, Bioanalysis. (2009). doi:10.4155/bio.09.86.
[81] E. Livak-Dahl, I. Sinn, M. Burns, Microfluidic Chemical Analysis Systems, Annu. Rev. Chem. Biomol. Eng. (2011). doi:10.1146/annurev-chembioeng-061010-114215.
[82] C. Wyatt Shields IV, C.D. Reyes, G.P. López, Microfluidic cell sorting: a review of the advances in the separation of cells from debulking to rare cell isolation, Lab Chip. (2015). doi:10.1039/C4LC01246A.
[83] H. Bi, C.M. Duarte, M. Brito, V. Vilas-Boas, S. Cardoso, P. Freitas, Performance enhanced UV/vis spectroscopic microfluidic sensor for ascorbic acid quantification in human blood, Biosens. Bioelectron. 85 (2016) 568–572. doi:10.1016/j.bios.2016.05.054.
[84] H. Yin, K. Killeen, R. Brennen, D. Sobek, M. Werlich, T. Van De Goor, Microfluidic chip for peptide analysis with an integrated HPLC column, sample enrichment column, and nanoelectrospray tip, Anal. Chem. (2005). doi:10.1021/ac049068d.
[85] M.-H. Fortier, E. Bonneil, P. Goodley, P. Thibault, Integrated Microfluidic Device for Mass Spectrometry-Based Proteomics and Its Application to Biomarker Discovery Programs, Anal. Chem. (2005). doi:10.1021/ac048506d.
[86] E.K. Sackmann, A.L. Fulton, D.J. Beebe, The present and future role of microfluidics in biomedical research, Nature. (2014). doi:10.1038/nature13118.
[87] R. Perry, D. Green, J. Maloney, Perry's chemical engineers' handbook, 1997. doi:10.10360071422943.
[88] Y. Zhang, S. Ge, J. Yu, Chemical and biochemical analysis on lab-on-a-chip devices fabricated using three-dimensional printing, TrAC - Trends Anal. Chem. (2016). doi:10.1016/j.trac.2016.09.008.
[89] C.X. Zhao, L. He, S.Z. Qiao, A.P.J. Middelberg, Nanoparticle synthesis in microreactors, Chem. Eng. Sci. (2011). doi:10.1016/j.ces.2010.08.039.
[90] Y. Won, F. Houshmand, D. Agonafer, M. Asheghi, K.E. Goodson, Microfluidic heat exchangers for high power density GaN on SiC, in: Tech. Dig. - IEEE Compd. Semicond. Integr. Circuit Symp. CSIC, 2014. doi:10.1109/CSICS.2014.6978568.
[91] M. Ramamoorth, A. Narvekar, Non viral vectors in gene therapy- an overview., J. Clin. Diagn. Res. (2015). doi:10.7860/JCDR/2015/10443.5394.
[92] Y.B. Lim, T. Kim, J.W. Lee, S.M. Kim, H.J. Kim, K. Kim, J.S. Park, Self-assembled ternary complex of cationic dendrimer, cucurbituril, and DNA: Noncovalent strategy in developing a gene delivery carrier, Bioconjug. Chem. (2002). doi:10.1021/bc025581r.

[93] J.. van Steenis, E.. van Maarseveen, F.. Verbaan, R. Verrijk, D.J.. Crommelin, G. Storm, W.. Hennink, Preparation and characterization of folate-targeted pEG-coated pDMAEMA-based polyplexes, J. Control. Release. 87 (2003) 167–176. doi:10.1016/S0168-3659(02)00361-9.
[94] Z. Wei, Z. Li, Continuous Cell Electroporation for Efficient DNA and siRNA Delivery Based on Laminar Microfluidic Chips, in: 2014: pp. 99–110. doi:10.1007/978-1-4614-9632-8_8.
[95] H.S. Shin, Shear Stress Effect on Transfection of Neurons Cultured in Microfluidic Devices, J. Nanosci. Nanotechnol. (2009). doi:10.1166/jnn.2009.1769.
[96] J. Kim, I. Hwang, D. Britain, T.D. Chung, Y. Sun, D.-H. Kim, Microfluidic approaches for gene delivery and gene therapy, Lab Chip. (2011). doi:10.1039/c1lc20766k.
[97] M. Lu, Y.P. Ho, C.L. Grigsby, A.A. Nawaz, K.W. Leong, T.J. Huang, Three-dimensional hydrodynamic focusing method for polyplex synthesis, ACS Nano. (2014). doi:10.1021/nn404193e.
[98] R.F. Ismagilov, A.D. Stroock, P.J.A. Kenis, G. Whitesides, H.A. Stone, Experimental and theoretical scaling laws for transverse diffusive broadening in two-phase laminar flows in microchannels, Appl. Phys. Lett. (2000). doi:10.1063/1.126351.
[99] D.R. Wilson, A. Mosenia, M.P. Suprenant, R. Upadhya, D. Routkevitch, R.A. Meyer, A. Quinones-Hinojosa, J.J. Green, Continuous microfluidic assembly of biodegradable poly(beta-amino ester)/DNA nanoparticles for enhanced gene delivery, J. Biomed. Mater. Res. Part A. 105 (2017) 1813–1825. doi:10.1002/jbm.a.36033.
[100] M.S. Croughan, K.B. Konstantinov, C. Cooney, The future of industrial bioprocessing: Batch or continuous?, Biotechnol. Bioeng. 112 (2015) 648–651. doi:10.1002/bit.25529.
[101] J. Piepmeier, Z. Jiang, W. Saltzman, Biodegradable poly (amine-co-ester) terpolymers for targeted gene delivery, (2012). https://www.researchgate.net/profile/Christopher_Cheng/publication/51850966_Biodegradable_polyamine-co-ester_terpolymers_for_targeted_gene_delivery/links/53eb68180cf23b8116a9bc77/Biodegradable-polyamine-co-ester-terpolymers-for-targeted-gene-delivery.pdf (accessed March 31, 2017).
[102] J. Zhou, J. Liu, C. Cheng, T. Patel, C. Weller, J. Piepmeier, Z. Jiang, W. Saltzman, Biodegradable poly (amine-co-ester) terpolymers for targeted gene delivery, Nat. Mater. (2012). https://www.researchgate.net/profile/Christopher_Cheng/publication/51850966_Biodegradable_polyamine-co-ester_terpolymers_for_targeted_gene_delivery/links/53eb68180cf23b8116a9bc77/Biodegradable-polyamine-co-ester-terpolymers-for-targeted-gene-delivery.pdf (accessed March 31, 2017).
[103] P.D. Petrov, N.I. Ivanova, M.D. Apostolova, C.B. Tsvetanov, C.B. Tsvetanov, S. Ikeda, R.J. Christie, K. Itaka, K. Kataoka, D. Crommelin, Biodegradable polymer network encapsulated polyplex for DNA delivery, RSC Adv. 3 (2013) 3508. doi:10.1039/c3ra21890b.

[104] K. Itaka, T. Ishii, Y. Hasegawa, K. Kataoka, Biodegradable polyamino acid-based polycations as safe and effective gene carrier minimizing cumulative toxicity, Biomaterials. 31 (2010) 3707–3714. doi:10.1016/j.biomaterials.2009.11.072.
[105] Y.-B. Lim, S.-O. Han, H.-U. Kong, Y. Lee, J.-S. Park, B. Jeong, S.W. Kim, Biodegradable Polyester, Poly[α-(4-Aminobutyl)-l-Glycolic Acid], as a Non-Toxic Gene Carrier, Pharm. Res. 17 (2000) 811–816. doi:10.1023/A:1007552007765.
[106] S.-J. Chiu, N.T. Ueno, R.J. Lee, Tumor-targeted gene delivery via anti-HER2 antibody (trastuzumab, Herceptin®) conjugated polyethylenimine, J. Control. Release. 97 (2004) 357–369. doi:10.1016/j.jconrel.2004.03.019.
[107] S. Boeckle, J. Fahrmeir, W. Roedl, M. Ogris, E. Wagner, Melittin analogs with high lytic activity at endosomal pH enhance transfection with purified targeted PEI polyplexes, J. Control. Release. 112 (2006) 240–248. doi:10.1016/j.jconrel.2006.02.002.
[108] W. Guo, R.J. Lee, Receptor-targeted gene delivery viafolate-conjugated polyethylenimine, AAPS PharmSci. 1 (1999) 20–26. doi:10.1208/ps010419.
[109] D. Ma, Q.-M. Lin, L.-M. Zhang, Y.-Y. Liang, W. Xue, A star-shaped porphyrin-arginine functionalized poly(l-lysine) copolymer for photo-enhanced drug and gene co-delivery, Biomaterials. 35 (2014) 4357–4367. doi:10.1016/j.biomaterials.2014.01.070.
[110] Y. Li, T. Liu, G. Zhang, Z. Ge, S. Liu, Tumor-Targeted Redox-Responsive Nonviral Gene Delivery Nanocarriers Based on Neutral-Cationic Brush Block Copolymers, Macromol. Rapid Commun. 35 (2014) 466–473. doi:10.1002/marc.201300719.
[111] X.J. Loh, Y.-L. Wu, S. Jiang, P.L. Chee, T.-C. Lee, X.J. Loh, Y. Mei, S. Park, S.H. Bhang, B.S. Kim, R. Langer, D.G. Anderson, J. Gauldie, F.L. Graham, Cationic star copolymers based on β-cyclodextrins for efficient gene delivery to mouse embryonic stem cell colonies, Chem. Commun. 51 (2015) 10815–10818. doi:10.1039/C5CC03686K.
[112] Y. Li, Y. Qian, T. Liu, G. Zhang, J. Hu, S. Liu, J.A. Wortman, H.T. Wolterbeek, J.A. Peters, I. Lukes, S. Roux, O. Tillement, V. Marsaud, P.N. Bories, L. Cynober, S. Gil, G. Ferey, P. Couvreur, R. Gref, Asymmetrically functionalized β-cyclodextrin-based star copolymers for integrated gene delivery and magnetic resonance imaging contrast enhancement, Polym. Chem. 5 (2014) 1743–1750. doi:10.1039/C3PY01278F.
[113] X. Zhao, Z. Li, H. Pan, W. Liu, M. Lv, F. Leung, W.W. Lu, Enhanced gene delivery by chitosan-disulfide-conjugated LMW-PEI for facilitating osteogenic differentiation, Acta Biomater. 9 (2013) 6694–6703. doi:10.1016/j.actbio.2013.01.039.
[114] Y. Lim, S. Kim, Y. Lee, W. Lee, T. Yang, Cationic hyperbranched poly (amino ester): a novel class of DNA condensing molecule with cationic surface, biodegradable three-dimensional structure, and, JOURNAL-. (2001). http://bionano.yonsei.ac.kr/bionano/Publication/06.1 (2001). jacs, h-pae.pdf (accessed March 31, 2017).
[115] W. Weecharangsan, O. Paecharoenchai, N. Niyomtham, P. Opanasopit, B. Yingyongnarongkul, R.J. Lee, Cholic Acid-Modified Polyethylenimine for Gene Delivery into Human Carcinoma Cells, Adv. Mater. Res. 1060 (2014) 3–6.

doi:10.4028/www.scientific.net/AMR.1060.3.
[116] Z. Yang, Z. Jiang, Z. Cao, C. Zhang, D. Gao, X. Luo, X. Zhang, H. Luo, Q. Jiang, J. Liu, A. Dong, A. Dong, Multifunctional non-viral gene vectors with enhanced stability, improved cellular and nuclear uptake capability, and increased transfection efficiency, Nanoscale. 6 (2014) 10193. doi:10.1039/C4NR02395A.
[117] Y. He, Y. Nie, G. Cheng, L. Xie, Y. Shen, Z. Gu, Viral Mimicking Ternary Polyplexes: A Reduction-Controlled Hierarchical Unpacking Vector for Gene Delivery, Adv. Mater. 26 (2014) 1534–1540. doi:10.1002/adma.201304592.
[118] S. Liu, T. Guo, Polycation-Based Ternary Gene Delivery System, (n.d.). http://www.ingentaconnect.com/content/ben/cdm/2015/00000016/00000002/art00007 (accessed March 31, 2017).
[119] R. V Benjaminsen, M.A. Mattebjerg, J.R. Henriksen, S.M. Moghimi, T.L. Andresen, The possible "proton sponge " effect of polyethylenimine (PEI) does not include change in lysosomal pH., Mol. Ther. 21 (2013) 149–57. doi:10.1038/mt.2012.185.
[120] Y. Fukumoto, Y. Obata, K. Ishibashi, N. Tamura, I. Kikuchi, K. Aoyama, Y. Hattori, K. Tsuda, Y. Nakayama, N. Yamaguchi, Cost-effective gene transfection by DNA compaction at pH 4.0 using acidified, long shelf-life polyethylenimine., Cytotechnology. 62 (2010) 73–82. doi:10.1007/s10616-010-9259-z.
[121] Q. Xie, G. Xinyong, C. Xianjin, W. Yayu, PEI/DNA formation affects transient gene expression in suspension Chinese hamster ovary cells via a one-step transfection process., Cytotechnology. 65 (2013) 263–71. doi:10.1007/s10616-012-9483-9.
[122] Y. Xu, S.W. Hui, P. Frederik, F.C. Szoka, Physicochemical characterization and purification of cationic lipoplexes., Biophys. J. (1999). doi:10.1016/S0006-3495(99)76894-3.
[123] V.K. Sharma, M. Thomas, A.M. Klibanov, Mechanistic studies on aggregation of polyethylenimine-DNA complexes and its prevention, Biotechnol. Bioeng. (2005). doi:10.1002/bit.20444.
[124] R. Rigler, Mets, J. Widengren, P. Kask, Fluorescence correlation spectroscopy with high count rate and low background: analysis of translational diffusion, Eur. Biophys. J. (1993). doi:10.1007/BF00185777.
[125] G. Lukacs, P. Haggie, O. Seksek, D. Lechardeur, Size-dependent DNA mobility in cytoplasm and nucleus, J. Biol. (2000). http://www.jbc.org/content/275/3/1625.short (accessed March 31, 2017).
[126] J.C. McDonald, G.M. Whitesides, Poly (dimethylsiloxane) as a Material for Fabricating Microfluidic Devices, Acc. Chem. Res. (2002). doi:10.1021/ac001132d.
[127] F. Bally, D.K. Garg, C.A. Serra, Y. Hoarau, N. Anton, C. Brochon, D. Parida, T. Vandamme, G. Hadziioannou, Improved size-tunable preparation of polymeric nanoparticles by microfluidic nanoprecipitation, Polymer (Guildf). 53 (2012) 5045–5051. doi:10.1016/j.polymer.2012.08.039.
[128] W. Zeng, I. Jacobi, D.J. Beck, S. Li, H. a Stone, Characterization of syringe-pump-driven induced pressure fluctuations in elastic microchannels, Lab Chip. (2015). doi:10.1039/c4lc01347f.
[129] V. Kafil, Y. Omidi, Cytotoxic impacts of linear and branched polyethylenimine

nanostructures in A431 cells, BioImpacts. (2011). doi:10.5681/bi.2011.004.
[130] C.E. Dunbar, K.A. High, J.K. Joung, D.B. Kohn, K. Ozawa, M. Sadelain, Gene therapy comes of age, Science (80-.). (2018). doi:10.1126/science.aan4672.
[131] J. Shi, Y. Xu, X. Xu, X. Zhu, E. Pridgen, J. Wu, A.R. Votruba, A. Swami, B.R. Zetter, O.C. Farokhzad, Hybrid lipid-polymer nanoparticles for sustained siRNA delivery and gene silencing, Nanomedicine Nanotechnology, Biol. Med. (2014). doi:10.1016/j.nano.2014.03.006.
[132] A. Paul, A. Hasan, H. Al Kindi, A.K. Gaharwar, V.T.S. Rao, M. Nikkhah, S.R. Shin, D. Krafft, M.R. Dokmeci, D. Shum-Tim, A. Khademhosseini, Injectable Graphene Oxide/Hydrogel-Based Angiogenic Gene Delivery System for Vasculogenesis and Cardiac Repair, ACS Nano. 8 (2014) 8050–8062. doi:10.1021/nn5020787.
[133] D. HÖnig, J. Derouchey, R. Jungmann, C. Koch, C. Plank, J.O. Rädler, Biophysical characterization of copolymer-protected gene vectors, Biomacromolecules. (2010). doi:10.1021/bm1002569.

Jason Matthew Absher Vita

Education:

B.S. Chemical Engineering, University of Louisville, May 2012

Research Experience:

University of Kentucky Chemical and Materials Engineering, Lexington, KY
Graduate Research Assistant, August 2012 – June 2018

Fellowships

NCI Cancer Nanotechnology Training Center Traineeship, 2015 – 2016

Publications and Presentations

Jason Absher, Daniel Pack, "Development of a Microfluidic Device for the Production of Ternary Polyplexes with Enhanced Properties." *Controlled Release Society Annual Meeting.* 2017 Boston

Jason Absher, Daniel Pack, "Microfluidic Production of Ternary Polyplexes for Non-Viral Gene Delivery." *AICHE Annual Meeting.* 2016 San Francisco

Jason Absher, Daniel Pack, "Microfluidic Production of High Efficiency PEI/DNA Polyplexes."
Controlled Release Society Annual Meeting. 2016 Seattle

Jason Absher, Daniel Pack, "Microfluidic Assembly of Multifunctional Polyplexes." *AICHE Annual Meeting.* 2015 Salt Lake City.

Franz G. Petzold, Jacek Jasinski, Ezra L. Clark, Jeong H. Kim, Jason Absher, Helge Toufar, Mahendra K. Sunkara, "Nickel supported on zinc oxide nanowires as advanced hydrodesulfurization catalysts", *Catalysis Today*, Available online 6 July 2012, ISSN 0920-5861, 10.1016/j.cattod.2012.05.030.

Vendra, V.K., Absher, J., Ellis, S., Druffel, T., Delaina, A., Sunkara, M.K, "Photoanode Area Dependent Efficiency and Recombination Effects in Dye-Sensitized Solar Cells", *Journal of the Electrochemical Society*, 159 (8) H728-H733 (2012)

Vendra, V.K., Absher, J., Ellis, S., Druffel, T., Delaina, A., Sunkara, M.K., "Photoanode area dependent efficiency and recombination in dye-sensitzed solar cells," *AICHE Annual Meeting* 2010, Minneapolis.